N7827079

WIND-TUNNEL INVESTIGATION OF EFFECTS OF TRAILING-EDGE GEOMETRY ON A NASA SUPERCRITICAL AIRFOIL SECTION

NATIONAL AERONAUTICS AND SPACE
ADMINISTRATION. LANGLEY RESEARCH CENTER
LANGLEY STATION, VA

SEP 1971

[redacted]

FACILITY FORM 602

[redacted]
(ACCESSION NUMBER) (THRU)

75 E 1
(PAGES) (CODE)

[redacted] 01
(NASA CR OR TMX OR AD NUMBER) (CATEGORY)

(NASA-TM-X-2336) WIND-TUNNEL INVESTIGATION
OF EFFECTS OF TRAILING-EDGE GEOMETRY ON A
NASA SUPERCRITICAL AIRFOIL SECTION (NASA)
78 p HC A05/MF A01
CSCL 01A

N78-27079

Unclas
H1/02 14899

ERRATA

NASA Technical Memorandum X-2336

WIND-TUNNEL INVESTIGATION OF EFFECTS OF TRAILING-EDGE GEOMETRY ON A NASA SUPERCRITICAL AIRFOIL SECTION

By Charles D. Harris
September 1971

Pages 37 to 49, pages 74 and 75: Section drag coefficients, c_d, in figures 9, 10, and 11 and the representative wake profiles, $\frac{\Delta p_t}{q}$, of figures 13 and 14 from which the section drag coefficients were derived are incorrect because of an erroneous instrumentation sensitivity constant. Correct drag levels are roughly 8 percent greater than indicated. Since only the absolute drag levels are affected, incremental drag effects are essentially unchanged and the discussion and conclusions pertaining to these figures are unaffected.

Issued August 1973

ORIGINAL PAGE IS
OF POOR QUALITY

~~CONFIDENTIAL~~ [redacted]

1. Report No.	2. Government Accession No.	3. Recipient's Catalog No.
NASA TM X-2336		

4. Title and Subtitle
WIND-TUNNEL INVESTIGATION OF EFFECTS OF TRAILING-EDGE GEOMETRY ON A NASA SUPERCRITICAL AIRFOIL SECTION

5. Report Date
September 1971

6. Performing Organization Code

7. Author(s)
Charles D. Harris

8. Performing Organization Report No.
L-7814

9. Performing Organization Name and Address
NASA Langley Research Center
Hampton, Va. 23365

10. Work Unit No.
136-13-01

11. Contract or Grant No.

12. Sponsoring Agency Name and Address
National Aeronautics and Space Administration
Washington, D.C. 20546

13. Type of Report and Period Covered
Technical Memorandum

14. Sponsoring Agency Code

15. Supplementary Notes

16. Abstract

Wind-tunnel tests have been conducted at Mach numbers from 0.60 to 0.81 to determine the effects of trailing-edge geometry on the aerodynamic characteristics of a NASA supercritical airfoil shape. Variations in trailing-edge thicknesses from 0 to 1.5 percent of the chord and a cavity in the trailing edge were investigated with airfoils with maximum thicknesses of 10 and 11 percent of the chord.

CLASSIFICATION CHANGE

To UNCLASSIFIED
By authority of NASA HQ Memo ADA-42 JH 6/10/76 Date 6/14/76
Changed by [illegible] Classified Document Master Control Station, NASA
Scientific and Technical Information Facility

~~CLASSIFIED BY [illegible]~~
~~SUBJECT TO [illegible] CLASSIFICATION~~
~~SCHEDULE OF [illegible] 11652.~~
~~AUTOMATICALLY [illegible] AT~~
~~TWO-YEAR [illegible]~~
~~DECLASSIFIED ON DECEMBER 31, 1977~~

17. Key Words (Suggested by Author(s))
Supercritical airfoil section
Trailing-edge geometry

18. Distribution Statement
[redacted]

19. Security Classif. (of this report)	20. Security Classif. (of this page)	21. No. of Pages	22. Price
[redacted]	Unclassified	75	

[redacted]

~~This material contains information affecting the national defense of the United States within the meaning of the espionage laws, Title 18, U.S.C., Secs. 793 and 794, the transmission or revelation of which in any manner to an unauthorized person is prohibited by law.~~

~~CONFIDENTIAL~~

WIND-TUNNEL INVESTIGATION OF EFFECTS OF TRAILING-EDGE GEOMETRY ON A NASA SUPERCRITICAL AIRFOIL SECTION*

By Charles D. Harris
Langley Research Center

SUMMARY

Wind-tunnel tests have been conducted at Mach numbers from 0.60 to 0.81 to determine the effects of trailing-edge geometry on the aerodynamic characteristics of a NASA supercritical airfoil shape. Variations in trailing-edge thicknesses from 0 to 1.5 percent of the chord and a cavity in the trailing edge were investigated with airfoils with maximum thicknesses of 10 and 11 percent of the chord.

Comparison of supercritical airfoils of slightly different maximum thicknesses at the design normal-force coefficient implied that increasing trailing-edge thickness yielded reductions in transonic drag levels with no apparent penalty at subcritical Mach numbers up to a trailing-edge thickness of about 0.7 percent. Increases in both subsonic and transonic drag levels appeared with further increases in trailing-edge thickness. The relationship between the optimum airfoil trailing-edge thickness and the upper-surface boundary-layer-displacement thickness at the trailing edge is recognized and discussed, and a general design criterion for trailing-edge thickness is offered. In addition, small drag improvements were realized when the airfoil with a trailing-edge thickness of 1.0 percent was modified to include a cavity in the trailing edge.

INTRODUCTION

Design philosophy of the NASA supercritical airfoil requires that the trailing-edge slopes of the upper and lower surfaces be equal. This requirement serves to retard flow separation by reducing the pressure-recovery gradient on the upper surface so that the pressure coefficients recover to only slightly positive values at the trailing edge. For an airfoil with a sharp trailing edge, such restrictions result in the airfoil being structurally thin over the aft region.

Because of this structural objection to sharp trailing edges and the potential aerodynamic advantages of thick trailing edges at transonic speeds (discussed, for example,

---

*

in refs. 1 and 2), an exploratory investigation was made during the early development phases of the supercritical airfoil to determine the effects on the aerodynamic characteristics of thickening the trailing edge. Increasing the trailing-edge thickness of an interim 11-percent-thick supercritical airfoil from 0 to 1.0 percent of the chord resulted in significant decreases in wave drag at transonic Mach numbers; however, these decreases were achieved at the expense of higher drag at subcritical Mach numbers.

Advantages of thick trailing edges at transonic Mach numbers were real and significant, but practical application would appear to depend on whether the drag penalty at subcritical Mach numbers could be reduced or eliminated. Two questions naturally arose: What would the optimum trailing-edge thickness be for the supercritical airfoil and could the drag penalty at the subcritical Mach numbers due to the thickened trailing edge be reduced by proper shaping of the trailing edge?

In order to investigate more comprehensively the effects of trailing-edge geometry, a refined 10-percent-thick supercritical airfoil was modified to permit variations in trailing-edge thickness and contour. Trailing-edge thicknesses of 0.7, 1.0, and 1.5 percent and a trailing-edge cavity were investigated.

Results of these trailing-edge variations and also the results of the investigation involving the interim 11-percent-thick airfoil are reported herein.

SYMBOLS

Values are given in both SI and U.S. Customary Units. The measurements and calculations were made in U.S. Customary Units.

C_p — pressure coefficient, $\dfrac{p_L - p_\infty}{q_\infty}$

$C_{p,sonic}$ — pressure coefficient corresponding to local Mach number of 1.0

c — chord of airfoil, cm (inches)

c_d — section drag coefficient, $\sum c_d' \dfrac{\Delta z}{c}$

c_d' — point drag coefficient (ref. 3), $2\left(\dfrac{\rho_1}{\rho_2}\right)^{1/2}\left(\dfrac{q_1}{q_\infty}\right)^{1/2}\left[\left(\dfrac{\rho_2}{\rho_\infty}\right)^{1/2} - \left(\dfrac{q_2}{q_\infty}\right)^{1/2}\right]$

c_m — section pitching-moment coefficient,

$$\sum_l C_p \frac{\Delta x}{c}\left(0.25 - \frac{x}{c}\right) - \sum_u C_p \frac{\Delta x}{c}\left(0.25 - \frac{x}{c}\right)$$

c_n	section normal-force coefficient, $\sum_{l} C_p \frac{\Delta x}{c} - \sum_{u} C_p \frac{\Delta x}{c}$
M	Mach number
m	slope of airfoil surface, dy/dx
p	static pressure, N/m^2 (lb/ft^2)
Δp_t	total-pressure loss, N/m^2 (lb/ft^2)
q	dynamic pressure, N/m^2 (lb/ft^2)
R	Reynolds number based on airfoil chord
t	airfoil thickness, cm (inches)
x	ordinate along airfoil reference line measured from airfoil leading edge, cm (inches)
y	ordinate vertical to airfoil reference line, cm (inches)
z	vertical distance in wake profile, cm (inches)
α	angle of attack of airfoil reference line, degrees
ρ	density, kg/m^3 (slugs/ft^3)

Subscripts:

L	local point on airfoil
l	lower surface
max	maximum
te	trailing edge
u	upper surface

∞ undisturbed stream conditions

1,2 flow stations designated in figure 1

APPARATUS AND TECHNIQUES

Much of the apparatus and many of the testing techniques used during the present investigation are similar or identical to those described in reference 4. The descriptions, when applicable, are repeated herein for completeness and convenience.

Wind Tunnel

The investigation was performed in the Langley 8-foot transonic pressure tunnel. This tunnel is a single-return, rectangular wind tunnel with controls that allow for the independent variation of Mach number, stagnation pressure, temperature, and humidity. The upper and lower test-section walls are axially slotted to permit testing through the transonic-speed range with minimum effects of choking. The slot width at the position of the model, designed on the basis of reference 5, to minimize solid-blockage interference, averaged about 5 percent of the width of the upper and lower walls. A more complete description of the Langley 8-foot transonic pressure tunnel may be found in reference 6.

The solid side walls and slotted upper and lower walls make this tunnel well suited to the investigation of two-dimensional models since the side walls act as end plates while the slots permit development of the flow field in the vertical direction.

Model

Airfoil shape.- Recent research in aeronautics has led to the development of an air foil shape which delays, at the usual cruise lift conditions, the subsonic drag rise well beyond the critical Mach number. This unique airfoil concept, known as the supercritical airfoil, has demonstrated in three-dimensional wind-tunnel-model application potential for substantially improved performance and significant economic advantage over present-day subsonic commercial jet transports. While it is not the primary purpose of this paper to report the characteristics of the supercritical airfoil itself, a brief discussion of some of its fundamental features may prove helpful in understanding the pressure distributions presented herein and in explaining the effects of the various trailing-edge modifications.

This airfoil, developed on the basis of intuitive reasoning and substantiating wind-tunnel experimentation and shaped to reduce the drag associated with energy losses due to shock waves and flow separation, is characterized by a large leading-edge radius, flattened upper surface, and highly cambered trailing edge. Early design philosophy which led to the development of the supercritical airfoil included a slotted trailing edge and is discussed in references 4 and 7. The slotted trailing edge permitted high-energy flow from the cambered lower surface to mix with the lower energy flow across the top of the airfoil. The slot, structurally complicated and sensitive to small deformities in shape, was eliminated when, in later unpublished developmental testing, it was shown that a highly cambered, properly shaped, unslotted trailing edge did not significantly degrade performance potential.

When the flow over an airfoil exceeds a local Mach number of 1, a region of supersonic flow extends vertically over the airfoil and usually terminates in a shock wave. The shock wave on conventional airfoils becomes increasingly stronger with associated increases in drag as the free-stream Mach number is increased. In addition, the strong, adverse-pressure gradient associated with the growth of the shock wave is likely to give rise to boundary-layer separation which results in an abrupt drag rise.

The supercritical airfoil, in contrast, is shaped so the expansion waves from the leading edge are reflected from the sonic line as a series of compression waves; thus, isentropic recompression in the supersonic flow downstream is encouraged and the strength of the shock wave is minimized. The essential geometric feature of such upper-surface shaping is an abrupt change from relatively high curvature at the leading edge to relatively low curvature downstream and can be achieved with a large leading-edge radius.

Another feature of the upper surface of the supercritical airfoil is the shaping of the aft portion to produce a short region of near-sonic velocity immediately behind the shock wave at design conditions. Such a plateau has been found desirable to permit the flow to stabilize before going through its final compression at the trailing edge and also to prevent disturbances from propagating forward and strengthening the shock wave. Care must be exercised, however, that the curvature required to produce such a near-sonic plateau does not generate such an expansion at off-design conditions that a second shock wave is formed which would tend to separate the flow over the rear portion of the airfoil.

The lower surface is generally shaped to prevent supercritical velocities on the lower surface which would lead to shock-wave formation and boundary-layer separation and also to provide a highly cambered trailing edge to compensate for the reduced lifting capacity of the relatively lightly cambered fore and mid region of the airfoil.

Because of the substantial lift generated over the rear portion of the airfoil, section pitching moments are relatively high compared with those of conventional airfoils. Unpublished wind-tunnel tests of three-dimensional swept-wing models incorporating the supercritical airfoil concept have shown that with the wing twist necessary to achieve the proper span load distribution, the overall wing pitching moments do not differ significantly from those of conventional airplanes. Trim-drag problems would therefore not be anticipated.

Wind-tunnel models.- Airfoil number designations used in the following discussion are those assigned as part of the overall supercritical-airfoil development-program numbering system and are noted for identification purposes only.

For the exploratory investigation mentioned in the introduction, the lower surface of an interim supercritical airfoil with a maximum thickness of 11 percent and sharp trailing edge (designated as supercritical airfoil 4) was rotated downward about the 64-percent chord line so that the trailing-edge thickness was 1.0 percent (referred to as a 1.0-percent-thick blunt trailing edge). Changing the trailing-edge thickness in this manner increased the aft camber of the airfoil without disturbing the shape of the upper surface. The resultant airfoil was designated as airfoil 5. Sketches of both airfoils are shown in figure 2, and coordinates are presented in table I. Figure 2(a) also illustrates the structural depth advantages of the thicker trailing edge on the supercritical airfoil.

In order to further define the effects of trailing-edge geometry, a refined supercritical airfoil with a maximum thickness of 10 percent, a blunt trailing-edge thickness of about 1.0 percent, and trailing-edge slopes of -0.37 (designated as supercritical airfoil 9 and described in table II) was modified to permit variations in trailing-edge thickness. The airfoil with a maximum thickness of 10 percent was felt to be more representative of the midsemispan region of present-day transports. For convenience, the lower surface of the airfoil was hinged along the 69.2-percent chord line to permit variations in trailing-edge thickness and resulted in an open cavity between the upper and lower surfaces. Changing trailing-edge thickness in this manner minimized surface discontinuities since the center of rotation was near the lower-surface inflection point. Trailing-edge thickness was maintained by spacers placed at intervals along the span and the cavity filled with wooden inserts shaped to the desired trailing-edge contours. The contour of the trailing edge was chosen somewhat arbitrarily but bears strong resemblance to the cusp-cavity described by Ringleb (snow cornice geometry) in reference 8.

Four trailing-edge geometries were investigated: a blunt trailing edge with $(t/c)_{te} = 1.0$ percent (airfoil 9); and a trailing edge with a cavity with $(t/c)_{te} = 1.0$, 1.5, and 0.7 percent (airfoils 9a, 10, and 11, respectively). Sketches of these airfoils are shown in figure 2(b).

The models, mounted in an inverted position, completely spanned the width of the tunnel except for small clearances at each wall. This clearance permitted the angle of attack to be changed manually by rotating the model about pivots in the tunnel side walls. Sketches of an airfoil mounted in the tunnel and the profile-drag rake are shown in figure 3, and a photograph of the airfoil and profile-drag rake mounted in the tunnel is shown in figure 4.

Boundary-layer transition.- Transition was fixed in an attempt to simulate full-scale Reynolds number boundary-layer and shock-wave characteristics. From consideration of the techniques discussed in references 9 to 11, 0.25-cm-wide (0.10-inch) bands of distributed roughness (No. 90 carborundum grains) were applied along the 28-percent-chord line on both the upper and lower surfaces to simulate the full-scale Reynolds numbers shown in figure 5. The simulation is limited on the upper surface to those conditions in which the shock wave occurs behind the transition location, that is, to the higher test Mach numbers. Full-scale simulation on the lower surface would be valid through the Mach number range of the investigation since the lower surface of the airfoil is shock free. Because the techniques on which this grit arrangement was based require that laminar flow be maintained ahead of the trip, the airfoil was painted and then sanded until it was extremely smooth.

Caution should be exercised when comparing the present results to results from earlier supercritical airfoil investigations since transition grit size and location used during earlier phases of the supercritical development program differed from that described above.

Measurements

Surface-pressure measurements.- The lift and pitching moments acting on the airfoils were determined from surface-pressure measurements. The wing was instrumented with flush-surface static-pressure orifices distributed in streamwise rows on the upper and lower surfaces approximately 0.32c from the center line of the tunnel. The orifices were concentrated near the leading and trailing edges of the airfoil to better define the severe pressure gradients in these regions. In addition, a rearward-facing pressure orifice was included in the trailing edge of the airfoil (identified at an upper-surface x/c location of 100 percent). Pressures were measured with the use of electronically actuated differential pressure-scanning-valve units. The maximum ranges of the transducers in the valves were ± 68.9 kN/m^2 (10 lb/in^2) for the upper surface and ± 51.7 kN/m^2 (7.5 lb/in^2) for the lower surface.

Wake measurements.- The drag forces acting on the airfoil, as measured by the momentum deficiency within the wake, were derived from vertical variations of the total and static pressures measured across the wake with the rake shown in figure 3(b). The rake was positioned in the vertical center-line plane of the tunnel approximately 1 chord length rearward of the trailing edge of the airfoil. The total-pressure tubes were flattened horizontally and closely spaced vertically (0.36 percent of airfoil chord) in the region of the wake associated with skin-friction and boundary-layer losses. Outside this region, the tube vertical spacing progressively widened until in the region above the wing where only shock losses were anticipated, the total-pressure tubes were spaced approximately 7.2 percent of the chord apart. The static pressure tubes were distributed as shown in figure 3(b). The rake was attached to the conventional sting mount of the tunnel, which permitted it to be moved vertically during the investigation to center the close concentration of tubes on the boundary-layer wake.

The total-head and static pressures were also measured with the use of electronically actuated differential-pressure scanning valves. The range of the transducer in the valve connected to total-head tubes intended to measure losses in the boundary-layer wake was $\pm 17.2\ kN/m^2$ (2.5 lb/in^2); the corresponding range for measuring shock and static pressure losses was $\pm 6.89\ kN/m^2$ (1 lb/in^2).

Reduction of Data and Corrections

Pressure measurements.- Airfoil-section normal-force and pitching-moment coefficients were obtained by machine integration of the local-pressure coefficients.

Wake measurements.- To obtain section drag coefficients from the total and static pressures behind the model, point drag coefficients for each of the total-pressure measurements were computed by using the procedure of reference 3 and then summed by machine integration across the wake. Because of the special spacing of the total-pressure tubes, the errors of the results obtained by this procedure are estimated to be less than 1 percent.

Corrections for wind-tunnel-wall effects.- The major interference effect of the wind-tunnel walls was an upflow at the position of the inverted model. This upflow, proportioned to the normal-force coefficient, would cause the aerodynamic angle of attack to be significantly less than the geometric angle of attack at the higher normal-force coefficients with attendant increases in the slope of the curve for normal force as a function of angle of attack. The mean value of this upflow at the midchord of the model, in degrees, may be estimated by the theory of reference 5 to be approximately 3.0 times the section normal-force coefficient. Based on experience in other two-dimensional tests in the 8-foot transonic pressure tunnel, however, such a correction is believed to be unrealistically large. Because of this uncertainty and since the forces and moments were obtained by surface-pressure and wake measurements which would be unaffected by angular corrections, the angles of attack used in the results presented herein have not been corrected for such effects.

The upflow at the inverted model would vary slightly from the leading edge to the trailing edge of the airfoil, as discussed in reference 12. No corrections have been applied to account for this variation since it would be quite small compared with the curvature of the induced streamlines and, therefore, probably have only secondary effects on the characteristics of the model.

The theory of reference 5 also indicates that tunnel-wall-blockage effects would be small; consequently, no corrections have been applied to the data to account for blockage effects.

TEST CONDITIONS

Tests were conducted at Mach numbers from 0.60 to 0.81 for stagnation pressures of 0.1013 MN/m^2 (1 atm) with resultant wind-tunnel Reynolds numbers based on the airfoil chord, as shown in figure 5. The stagnation temperature of the tunnel air was automatically controlled at approximately 322° K (120° F) and dried until the dewpoint temperature in the test section was reduced sufficiently to avoid condensation effects.

PRESENTATION OF RESULTS

The comparison of the aerodynamic force and moment characteristics of the interim supercritical airfoil with trailing-edge thicknesses of 0 and 1.0 percent is presented in figure 6, with the drag-rise characteristics summarized in figure 7 for the design normal-force coefficient of 0.7. The normal-force coefficient of 0.7 was chosen as the design goal since, when account is taken of the sweep effect, it is representative of lift coefficients at which advanced technology transports utilizing the supercritical airfoil concept are expected to cruise. Representative effects of trailing-edge thickness on airfoil pressure distributions and wake profiles are presented in figure 8.

Aerodynamic force and moment coefficients of the refined 10-percent-thick airfoil with a 1.0-percent-thick trailing edge with cavity (airfoil 9a) are presented over an extensive angle-of-attack range in figure 9. The aerodynamic characteristics of the refined airfoil with the various trailing-edge geometries investigated are compared in figure 10 over an abbreviated angle-of-attack range near the design normal-force coefficient of 0.7, with the drag-rise characteristics for the various trailing-edge geometries summarized in figure 11. Airfoil chordwise pressure distributions are compared in figure 12 and representative wake-profile measurements are presented in figures 13 and 14.

DISCUSSION

Increasing the trailing-edge thickness of an interim 11-percent-thick airfoil from 0 to 1.0 percent produced significant decreases in wave drag at transonic Mach numbers for the design normal-force coefficient; however these decreases were achieved at the expense of higher drag at subcritical Mach numbers. These results focused attention on the geometry of the trailing edge, and the following sections discuss results of an investigation which further defined the effects of trailing-edge thickness and shape.

Variations in Trailing-Edge Thickness

The incremental decrease in the drag level at $M = 0.60$ resulting from decreasing the trailing-edge thickness of the 10-percent-thick airfoil from 1.0 percent to 0.7 percent (fig. 11) approximately equals the increase in drag due to increasing the trailing-edge thickness of the 11-percent-thick airfoil from 0 to 1.0 percent (fig. 7). Although neither the drag levels nor the drag increments can be directly compared because of the difference in maximum thicknesses, the implication is that the trailing-edge thickness may be increased from 0 to approximately 0.7 percent, with significant improvements in the development of wave losses at transonic speeds, without incurring profile-drag penalties at subsonic Mach numbers. Further increases in trailing-edge thickness beyond approximately 0.7 percent adversely affect both the subsonic and transonic drag levels. The pressure distributions of figure 12 generally show a rearward movement of the upper-surface shock position and increases in the magnitude of the off-design second velocity peak with increases in trailing-edge thickness beyond 0.7 percent. In addition, the upper-surface pressure coefficients near the trailing edge become increasingly negative as the trailing-edge thickness increases, indicative of increased separation in this region.

The peak in the drag-rise curve at $M = 0.78$ (fig. 11) was due to the second region of supersonic flow on the upper surface of the airfoil developing to such an extent that a second shock wave was required to reduce the supersonic flow to subsonic flow downstream. (Compare the airfoil pressure distribution and wake-shock losses for $M = 0.76$ to those for $M = 0.78$ in figs. 12 to 14.) Local Mach numbers in this second region of supersonic flow were on the order of those near the leading edge for $M = 0.78$. These effects may be related to the increased aft camber resulting from the manner in which the trailing-edge thickness was increased. It is probable that the peak at $M = 0.78$ could be reduced by slightly reducing the aft camber of the airfoil while maintaining the same trailing-edge thicknesses. Such a reduction in camber could be accomplished by reducing the value of the trailing-edge slope in the as yet unpublished equations defining the NASA supercritical airfoil.

As the Mach number was increased to 0.79, the forward shock moved rearward (see fig. 12); thus, the magnitude of the second peak was reduced. Wave losses associated with the second peak are consequently reduced, as shown in figure 13 and as reflected in the dip in the drag-rise curve of figure 11.

A limited analysis (not presented) of the growth of the boundary-layer displacement thickness over the upper surface was made by using methods based on equations described in references 13 and 14 with the experimental pressure distributions for representative Mach numbers of 0.60 and 0.78 and an angle of attack of 1.5^{o}. The analysis indicated that at constant angle of attack the upper-surface boundary-layer displacement thickness at the trailing edge did not vary appreciably and remained greater than the trailing-edge thickness of the airfoil as it was increased from 0 to around 0.7 percent. The analysis further indicated that the upper-surface boundary-layer displacement thickness at the trailing edge equals the trailing-edge thickness of the airfoil at $(t/c)_{te}$ slightly greater than 0.7 percent at $M = 0.78$ and slightly less than 0.7 percent at $M = 0.60$. The 0.7-percent-thick trailing edge appears to be an acceptable compromise through the Mach number range for the simulated Reynolds numbers of this investigation.

The trend, therefore, was that of decreasing transonic drag levels with increases in trailing-edge thickness until the trailing-edge thickness of the airfoil exceeds that of the upper-surface boundary-layer displacement thickness at the trailing edge, after which, increases in both subsonic and transonic drag levels appear. Such variations in drag and boundary-layer characteristics suggest some relationship between the optimum trailing-edge thickness and the displacement thickness of the upper-surface boundary layer at the trailing edge. It is felt that in order to realize the full aerodynamic advantage, the design criterion for trailing-edge thickness should be such that the upper-surface pressure coefficients recover to approximately zero at the trailing edge with the trailing-edge thickness of the airfoil equal to or slightly less than the local upper-surface boundary-layer displacement thickness.

The lower-surface boundary layer need not be considered since the upper surface is more sensitive to conditions at the trailing edge because of the adverse pressure gradient on the upper surface in contrast to the favorable gradient on the lower surface.

There exists evidence from unpublished wind-tunnel tests, wherein satisfactory results were obtained for three-dimensional applications of the supercritical airfoil with $(t/c)_{te}$ of approximately 1.0 percent, that $(t/c)_{te}$ slightly larger than 0.7 percent would be acceptable in swept-wing three-dimensional applications. Although the reasons for this are not completely understood, it is believed to be in some way related to the three-dimensional relieving effect of the spanwise flow near the trailing edge.

Trailing-Edge Cavity

The potential reduction in subsonic drag associated with some sort of cavity in the trailing edge of airfoils has been discussed in numerous reports. (See refs. 1, 2, and 15 to 17, for example.) Such reductions in drag are generally attributable to two primary sources: reduction in base drag through changes in the pressure acting over the base area, and improvements in wake stability resulting in decreases in momentum losses associated with concentrations of vorticity in the wake. In addition to its influence on base drag and wake stability, the cavity was thought to hold potential for delaying separation when considered from the viewpoint of a mixing region where there would be an interchange between the high-energy air passing over the upper-surface trailing edge and the lower energy air in the cavity itself.

The results of the present investigation show a small, but consistently measurable, reduction in drag (fig. 11) for the 1.0-percent-thick trailing-edge cavity when compared with the 1.0-percent-thick blunt trailing edge for the 10-percent-thick airfoil. For the most part the pressure distributions of figure 12 indicate slightly more negative pressure coefficients over the base (upper-surface pressure orifice at $x/c = 1.00$ was located in the rearward face of the cavity) so the drag improvement due to the cavity must be attributed to improvements in the general flow over the airfoil itself or to the influence of the cavity on the wake rather than to an improvement in base drag. The influence of the cavity on the stability of the wake may only be conjectured in the absence of detailed measurements of velocity fluctuations in the wake.

No attempt was made to achieve an optimum cavity size or shape since the drag reductions reported in reference 15 for a cavity with contour approximating one theoretically derived by Ringleb was very nearly the same as that given by a simple rectangular trailing-edge cavity in reference 16.

CONCLUSIONS

Wind-tunnel tests have been conducted at Mach numbers from 0.60 to 0.81 to determine the effects of trailing-edge geometry on the aerodynamic characteristics of a NASA supercritical airfoil shape. Variations in trailing-edge thicknesses from 0 to 1.5 percent of the chord and a cavity in the trailing edge were investigated with airfoils with maximum thicknesses of 10 and 11 percent of the chord.

Results indicate the following general conclusions for the design normal-force coefficient of 0.7:

1. Comparison of supercritical airfoils of slightly different maximum thicknesses implied that increasing trailing-edge thickness yielded reductions in transonic drag levels with no apparent penalty at subcritical Mach numbers up to a trailing-edge thickness of about 0.7 percent. Increases in both subsonic and transonic drag levels appeared with increases in trailing-edge thickness beyond approximately 0.7 percent.

2. Small drag reductions through the Mach number range resulted when the 10-percent-thick airfoil with 1.0-percent-thick trailing edge was modified to include a cavity in the trailing edge.

3. There appears to exist some relationship between the optimum airfoil trailing-edge thickness and the boundary-layer displacement thickness over the upper surface of the airfoil. Calculations suggest that the reversal of the favorable effect of increasing trailing-edge thickness occurs when the airfoil trailing-edge thickness exceeds the displacement thickness of the upper-surface boundary layer at the trailing edge.

4. The general design criterion to realize the full aerodynamic advantage of trailing-edge thickness appears to be such that the pressure coefficients over the upper surface of

the airfoil recover to approximately zero at the trailing edge with the trailing-edge thickness of the airfoil equal to or slightly less than the local upper-surface boundary-layer displacement thickness.

Langley Research Center,
National Aeronautics and Space Administration,
Hampton, Va., July 6, 1971.

REFERENCES

1. Holder, D. W.: The Transonic Flow Past Two-Dimensional Aerofoils. J. Roy. Aeronaut. Soc., vol. 68, no. 644, Aug. 1964, pp. 501-516.

2. Pollock, N.: Two Dimensional Aerofoils at Transonic Speeds. Note ARL/A. 314, Dep. Supply, Aust. Def. Sci. Serv., Apr. 1969.

3. Baals, Donald D.; and Mourhess, Mary J.: Numerical Evaluation of the Wake-Survey Equations for Subsonic Flow Including the Effect of Energy Addition. NACA WR L-5, 1945. (Formerly NACA ARR L5H27.)

4. Whitcomb, Richard T.; and Clark, Larry R.: An Airfoil Shape for Efficient Flight at Supercritical Mach Numbers. NASA TM X-1109, 1965.

5. Davis, Don D., Jr.; and Moore, Dewey: Analytical Study of Blockage- and Lift-Interference Corrections for Slotted Tunnels Obtained by the Substitution of an Equivalent Homogeneous Boundary for the Discrete Slots. NACA RM L53E07b, 1953.

6. Schaefer, William T., Jr.: Characteristics of Major Active Wind Tunnels at the Langley Research Center. NASA TM X-1130, 1965.

7. Whitcomb, Richard T.; and Blackwell, James A., Jr.: Status of Research on a Supercritical Wing. Conference on Aircraft Aerodynamics, NASA SP-124, 1966, pp. 367-381.

8. Ringleb, Friedrich O.: Separation Control by Trapped Vortices. Boundary Layer and Flow Control. Vol. I, G. V. Lachmann, ed., Pergamon Press, Inc., 1961, pp. 265-294.

9. Loving, Donald L.: Wind-Tunnel—Flight Correlation of Shock-Induced Separated Flow. NASA TN D-3580, 1966.

10. Blackwell, James A., Jr.: Preliminary Study of Effects of Reynolds Number and Boundary-Layer Transition Location on Shock-Induced Separation. NASA TN D-5003, 1969.

11. Braslow, Albert L.; and Knox, Eugene C.: Simplified Method for Determination of Critical Height of Distributed Roughness Particles for Boundary-Layer Transition at Mach Numbers From 0 to 5. NACA TN 4363, 1958.

12. Katzoff, S.; and Barger, Raymond L.: Boundary-Induced Downwash Due to Lift in a Two-Dimensional Slotted Wind Tunnel. NASA TR R-25, 1959. (Supersedes NACA TN 4289.)

13. Schlichting, Hermann (J. Kestin, transl.): Boundary-Layer Theory. Sixth ed., McGraw-Hill Book Co., 1968.

14. Nash, J. F.; and MacDonald, A. G. J.: The Calculation of Momentum Thickness in a Turbulent Boundary Layer at Mach Numbers up to Unity. C.P. No. 963, Brit. A.R.C., 1967.

15. Pollock, N.: Some Effects of Base Geometry on Two Dimensional Base Drag at Subsonic and Transonic Speeds. Note ARL/Aero. 316, Dep. Supply, Aust. Def. Sci. Serv., Oct. 1969.

16. Nash, J. F.; Quincey, V. G.; and Callinan, J.: Experiments on Two-Dimensional Base Flow at Subsonic and Transonic Speeds. R. & M. No. 3427, Brit. A.R.C., 1966.

17. Nash, J. F.: A Discussion of Two-Dimensional Turbulent Base Flows. R. & M. No. 3468, Brit. A.R.C., 1967.

TABLE I.- SECTION COORDINATES FOR 11-PERCENT-THICK INTERIM SUPERCRITICAL AIRFOIL[a]

[c = 63.0 cm (24.8 inches)]

x/c	y/c for –			
	Airfoil 4 with sharp trailing edge		Airfoil 5 with 1-percent-thick blunt trailing edge	
	Upper	Lower	Upper	Lower
0.0065	0.0159	-0.0157	0.0159	-0.0157
.0125	.0203	-.0206	.0203	-.0206
.0250	.0267	-.0271	.0267	-.0271
.0375	.0302	-.0316	.0302	-.0316
.050	.0334	-.0351	.0334	-.0351
.075	.0381	-.0403	.0381	-.0403
.100	.0416	-.0440	.0416	-.0440
.125	.0444	-.0469	.0444	-.0469
.150	.0466	-.0491	.0466	-.0491
.175	.0484	-.0508	.0484	-.0508
.200	.0499	-.0521	.0499	-.0521
.250	.0521	-.0539	.0521	-.0539
.300	.0536	-.0548	.0536	-.0548
.350	.0545	-.0549	.0545	-.0549
.400	.0548	-.0541	.0548	-.0541
.450	.0549	-.0524	.0549	-.0524
.500	.0544	-.0497	.0544	-.0497
.550	.0535	-.0455	.0535	-.0455
.575	.0529	-.0426	.0529	-.0426
.600	.0519	-.0389	.0519	-.0389
.625	.0512	-.0342	.0512	-.0342
.650	.0502	-.0282	.0502	-.0285
.675	.0490	-.0215	.0490	-.0224
.700	.0477	-.0149	.0477	-.0165
.725	.0461	-.0090	.0461	-.0112
.750	.0443	-.0036	.0443	-.0065
.775	.0422	.0012	.0422	-.0024
.800	.0398	.0053	.0398	.0011
.825	.0370	.0088	.0370	.0039
.850	.0338	.011[illegible]	.0338	.0059
.875	.0300	.0132	.0300	.0070
.900	.0256	.0138	.0256	.0069
.925	.0204	.0131	.0204	.0056
.950	.0144	.0106	.0144	.0024
.975	.0074	.0060	.0074	-.0028
1.000	-.0008	-.0013	-.0008	-.0108

[a]Leading-edge radius, 0.0223c.

TABLE II.- SECTION COORDINATES OF 10-PERCENT-THICK SUPERCRITICAL AIRFOILS[a] 9 AND 9a WITH 1-PERCENT-THICK TRAILING EDGE

[c = 63.5 cm (25 inches)]

x/c	Calculated				Experimental (airfoil 9a)	
	y/c		m		y/c	
	Upper	Lower	Upper	Lower	Upper	Lower
0.0075	0.0162	-0.0162	0.850	-0.874	0.0160	-0.0165
.0125	.0196	-.0198	.570	-.810	.0196	-.0201
.0250	.0250	-.0257	.345	-.374	.0250	-.0259
.0375	.0287	-.0297	.255	-.276	.0286	-.0299
.050	.0316	-.0328	.204	-.219	.0314	-.0329
.075	.0359	-.0373	.145	-.153	.0358	-.0374
.100	.0390	-.0406	.110	-.114	.0389	-.0407
.125	.0414	-.0431	.086	-.087	.0415	-.0432
.150	.0434	-.0450	.069	-.067	.0433	-.0451
.175	.0449	-.0465	.056	-.052	.0448	-.0465
.200	.0462	-.0476	.045	-.040	.0461	-.0476
.250	.0480	-.0492	.029	-.021	.0479	-.0491
.300	.0492	-.0499	.017	-.008	.0491	-.0498
.350	.0498	-.0500	.008	.003	.0498	-.0500
.400	.0500	-.0495	.000	.014	.0500	-.0494
.450	.0498	-.0486	-.007	.025	.0499	-.0485
.500	.0493	-.0469	-.013	.042	.0494	-.0468
.550	.0485	-.0442	-.021	.070	.0485	-.0440
.575	.0479	-.0422	-.025	.091	.0480	-.0420
.600	.0472	-.0396	-.029	.120	.0474	-.0393
.625	.0465	-.0362	-.034	.157	.0465	-.0357
.650	.0456	-.0316	-.039	.206	.0456	-.0316
.675	.0445	-.0259	-.046	.239	.0445	-.0255
.700	.0433	-.0202	-.053	.216	.0433	-.0200
.725	.0418	-.0151	-.062	.193	.0419	-.0152
.750	.0402	-.0105	-.073	.169	.0401	-.0109
.775	.0382	-.0066	-.085	.145	.0382	-.0072
.800	.0359	-.0033	-.100	.118	.0359	-.0041
.825	.0332	-.0007	-.118	.089	.0332	-.0014
.850	.0299	.0011	-.140	.056	.0300	.0005
.875	.0261	.0020	-.165	.017	.0264	.0016
.900	.0217	.0019	-.194	-.031	.0220	.0016
.925	.0164	.0004	-.229	-.090	.0167	.0004
.950	.0102	-.0027	-.269	-.164	.0103	-.0026
.975	.0028	-.0079	-.316	-.256	.0035	-.0073
.990	-.0021	-.0123	-.348	-.321	-.0016	-.0120
1.000	-.0057	-.0157	-.370	-.370	-----	-.0157

[a]Leading-edge radius, 0.0212c.

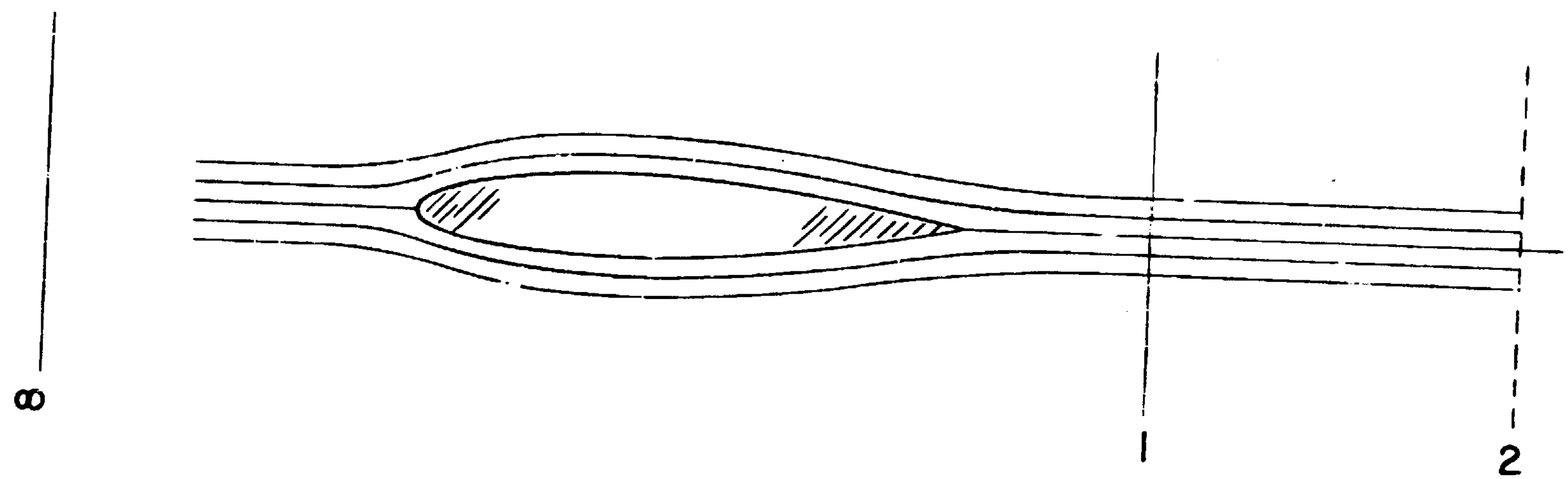

Figure 1.- Station designations for measurement of profile drag (ref. 3).

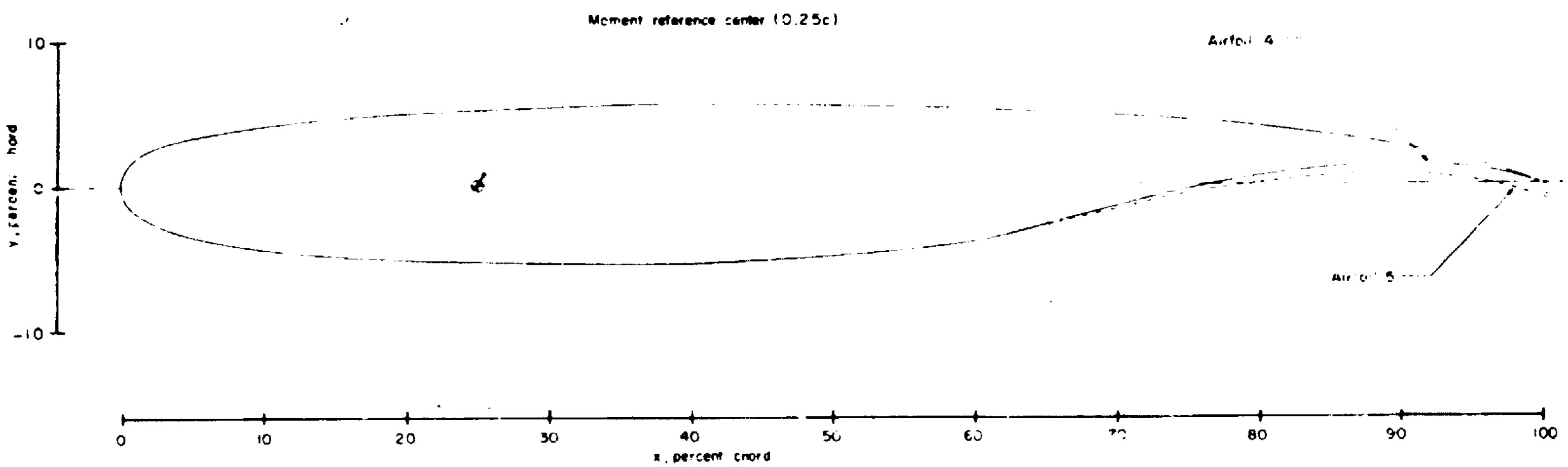

(a) Supercritical airfoils; $(t/c)_{max} = 0.11$.

Figure 2.- Model sketches.

ORIGINAL PAGE IS
OF POOR QUALITY

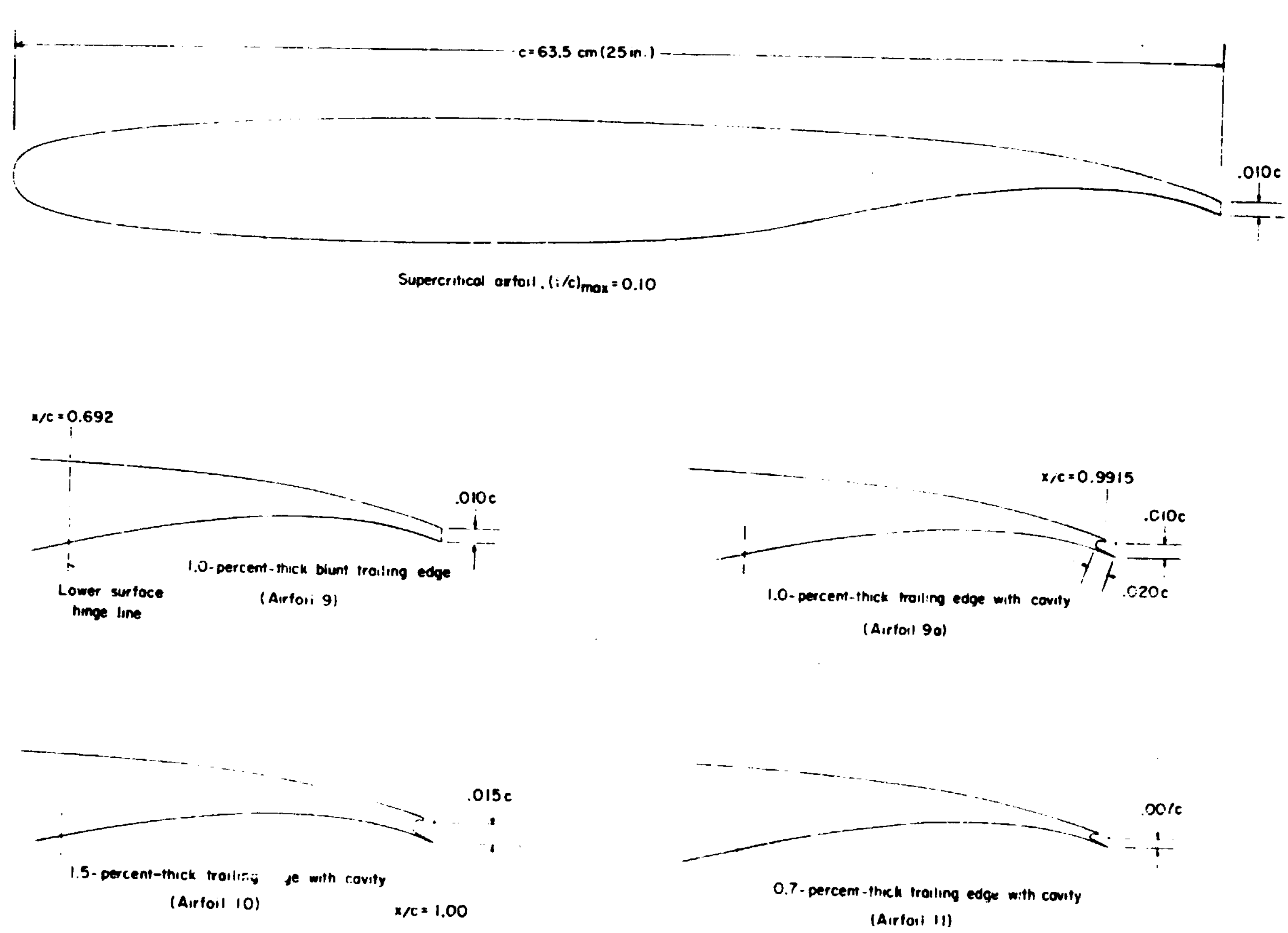

(b) Trailing-edge geometry.

Figure 2.- Concluded.

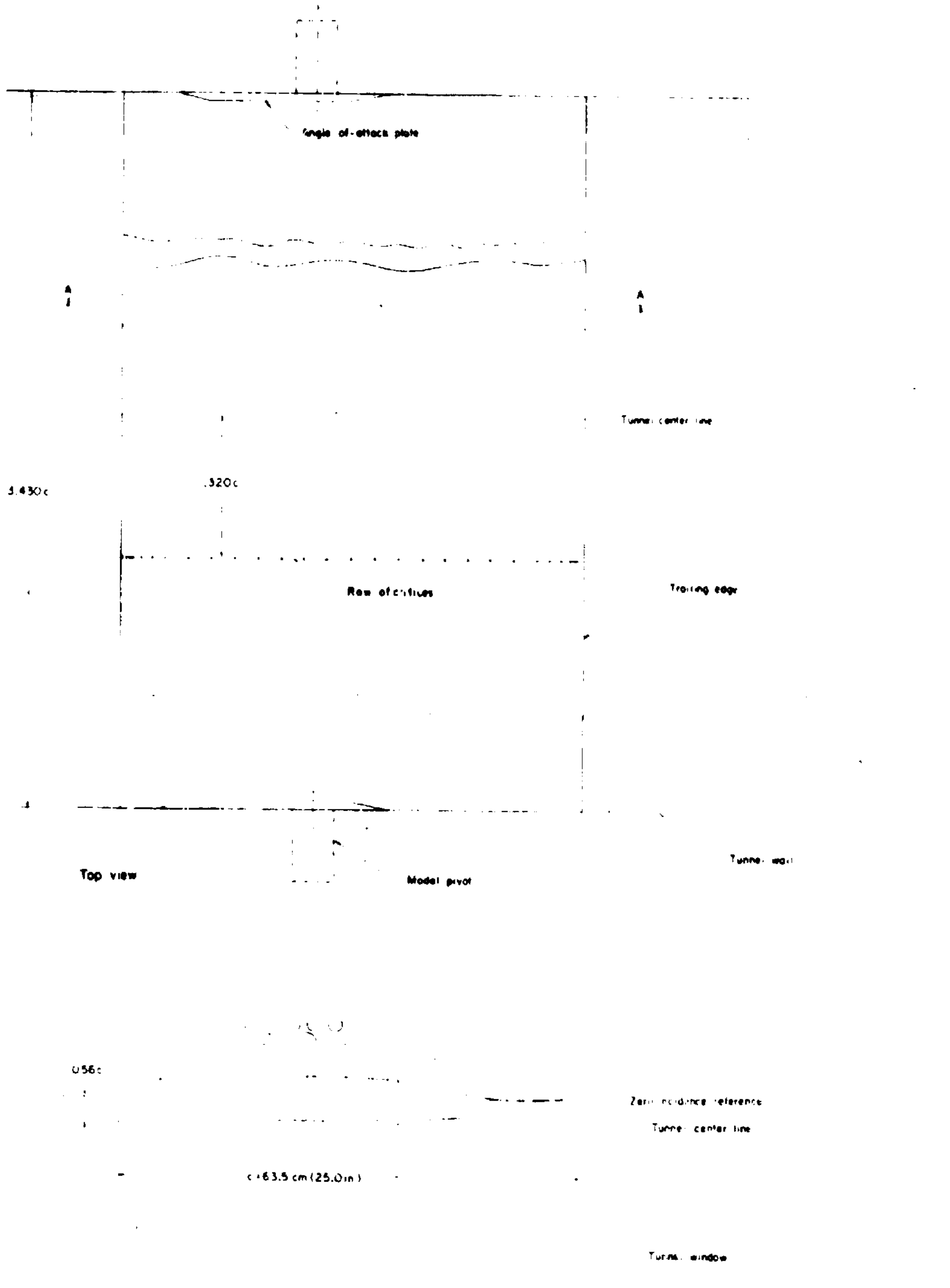

(a) Airfoil mounted in tunnel.

Figure 3.- Apparatus.

ORIGINAL PAGE IS
OF POOR QUALITY

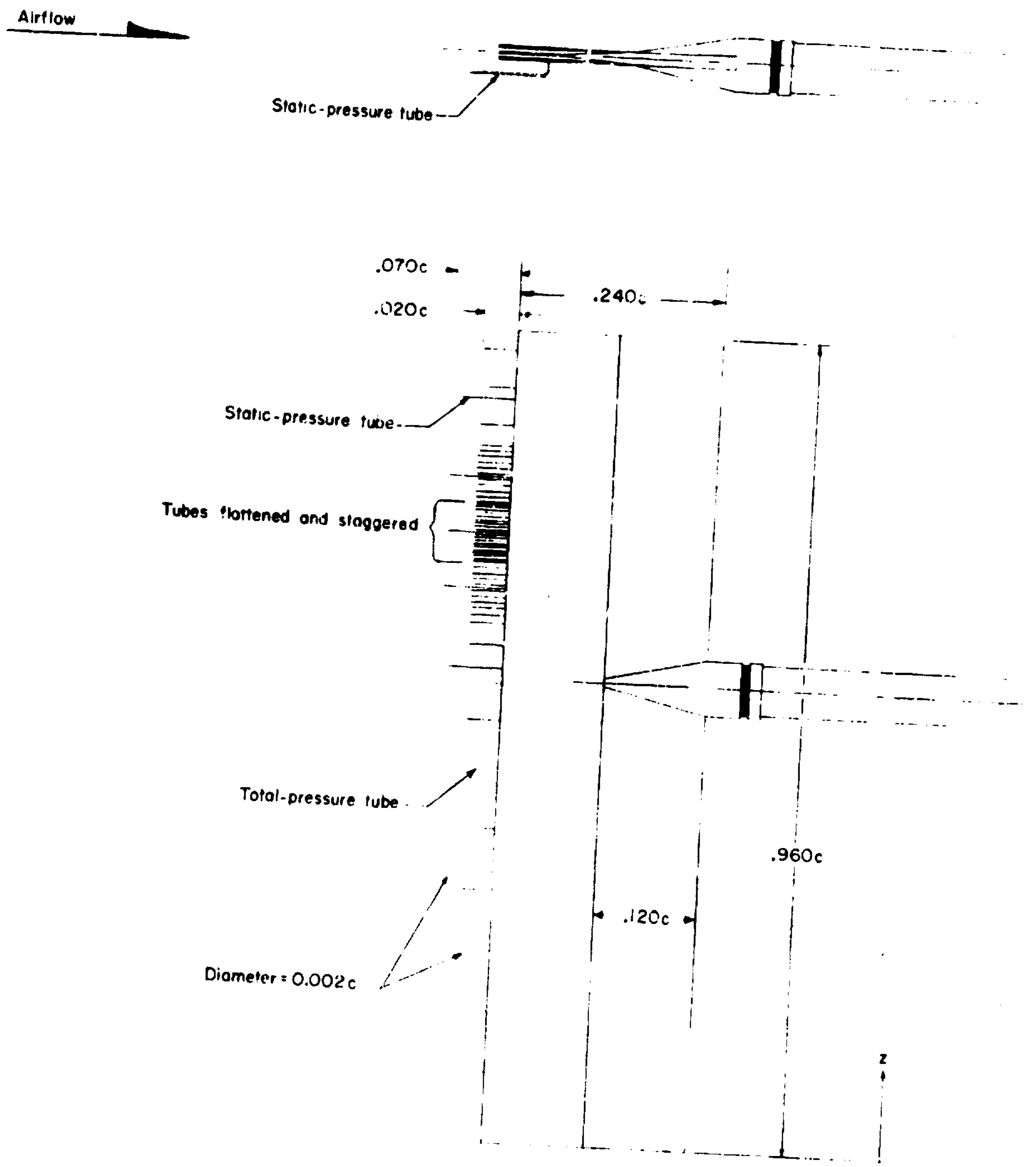

(b) Profile-drag rake.

Figure 3.- Concluded.

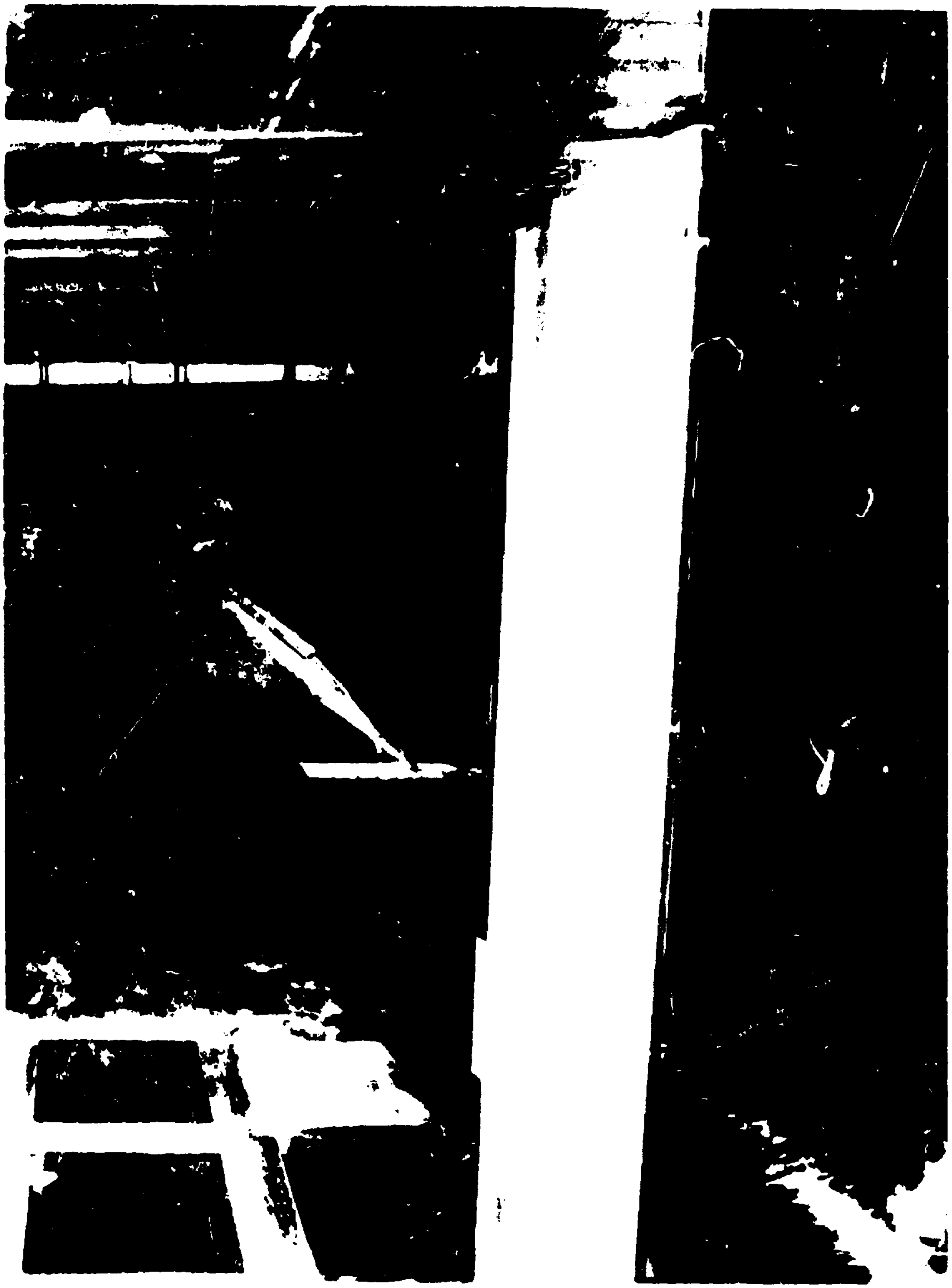

L-77-[illegible]

Figure [illegible].- Photograph of [illegible] airfoil in the wind tunnel.

[redacted]

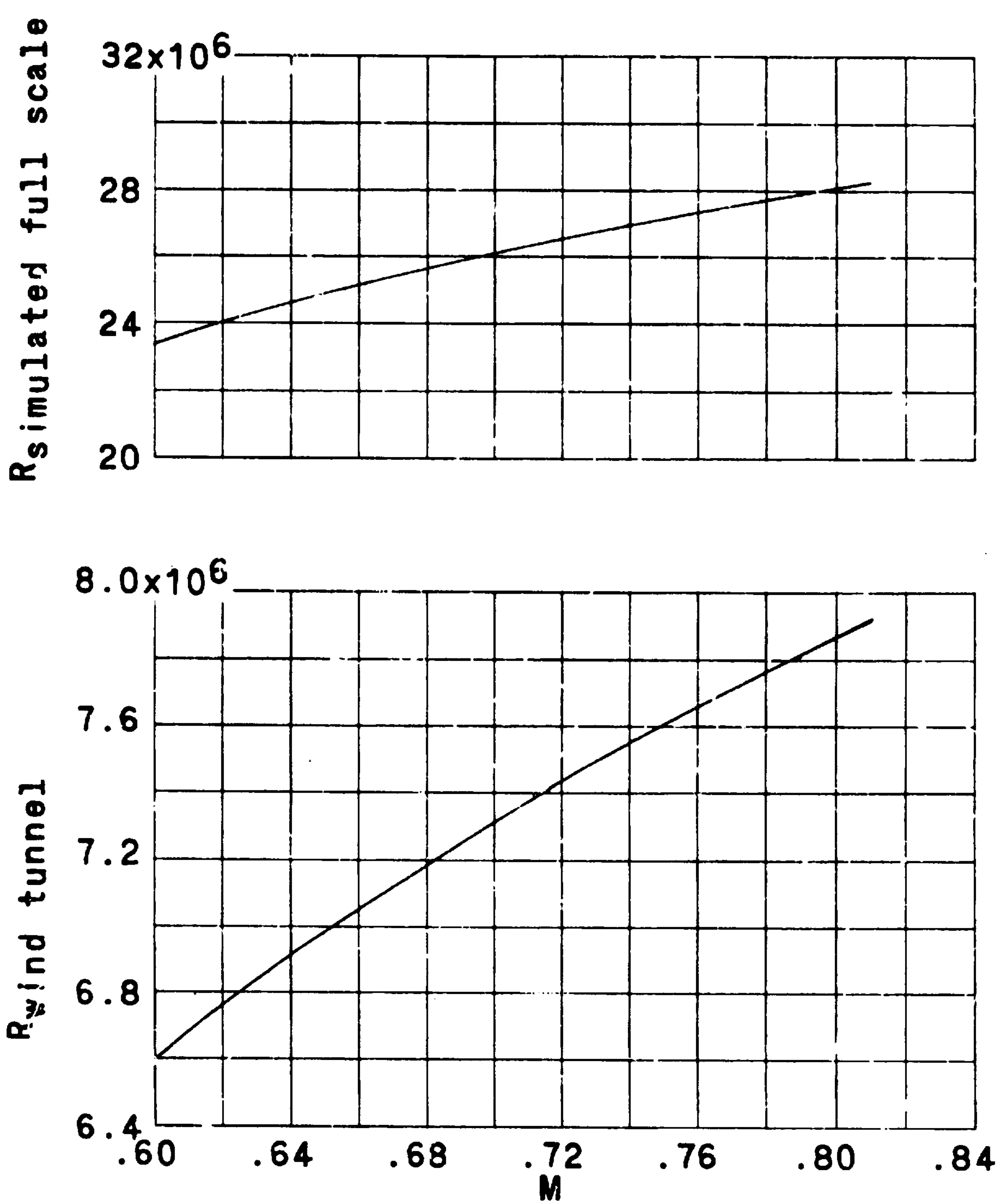

Figure [illegible].- Variation with Mach number of test wind-tunnel Reynolds number and simulated full-scale Reynolds number.

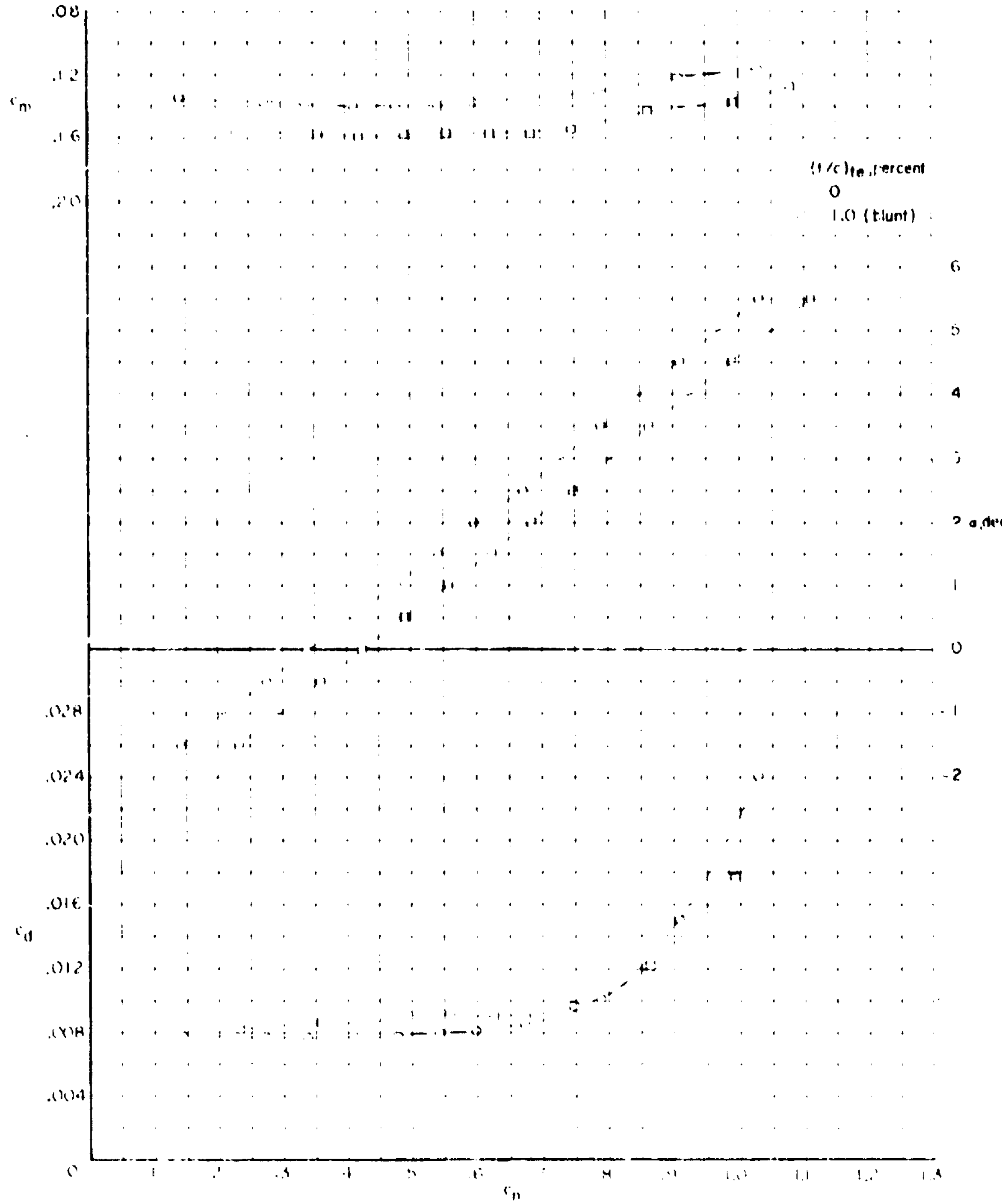

(a) M = 0.60.

Figure 6.- Comparison of 11-percent-thick interim supercritical airfoil with sharp and blunt trailing edge.

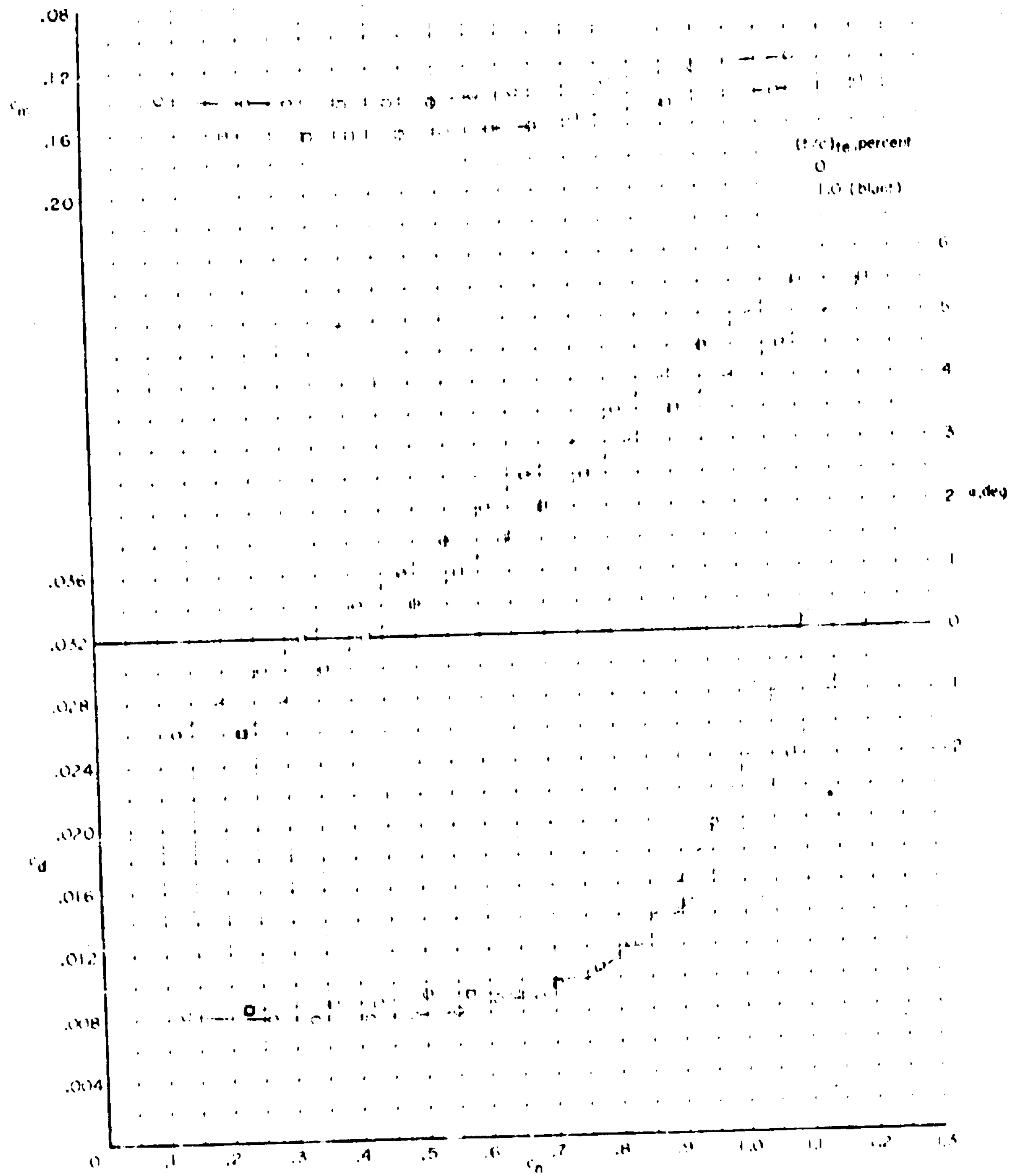

(b) M 0.65.

Figure 6.- Continued.

ORIGINAL PAGE IS OF POOR QUALITY

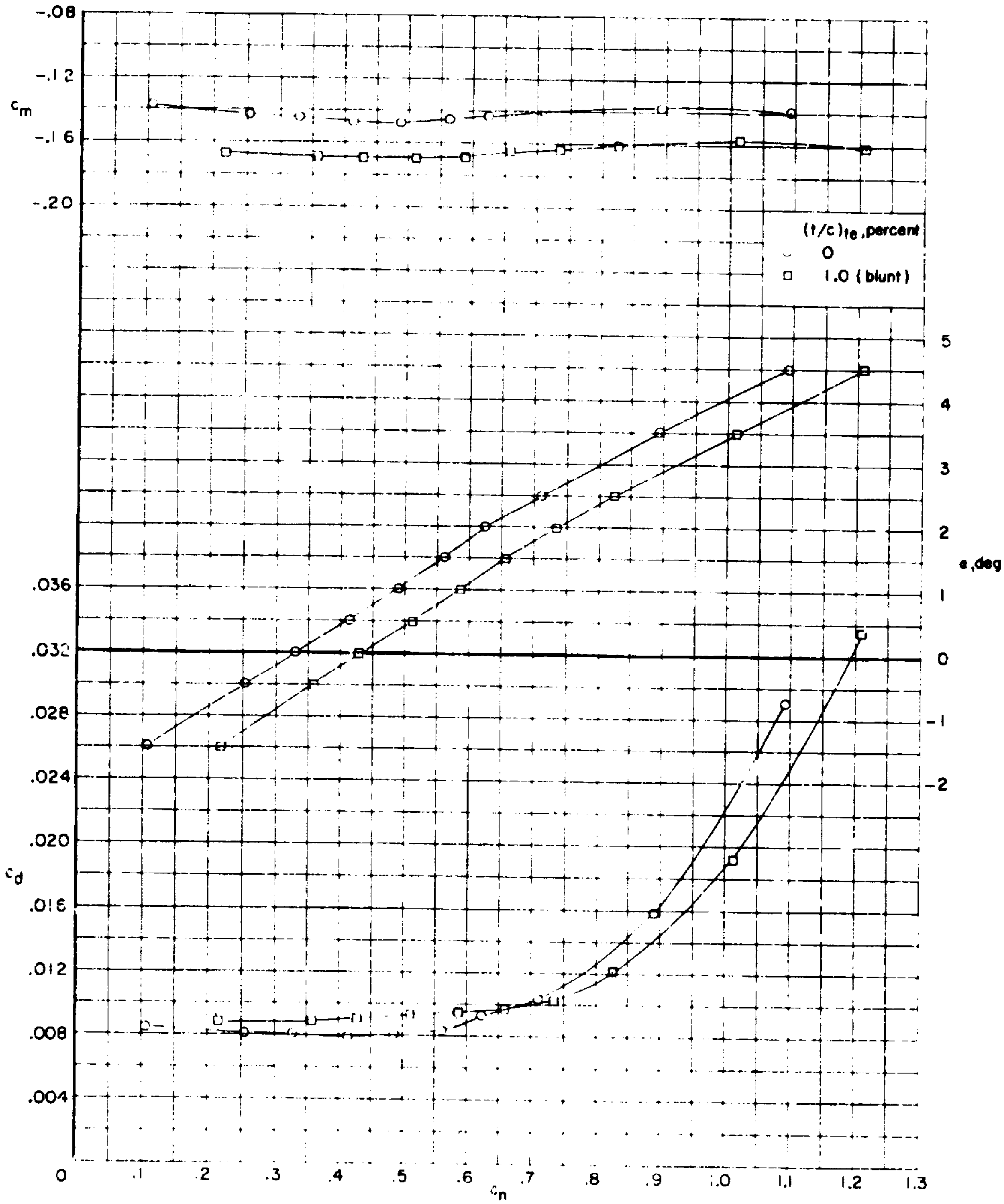

(c) M = 0.70.

Figure 6.- Continued.

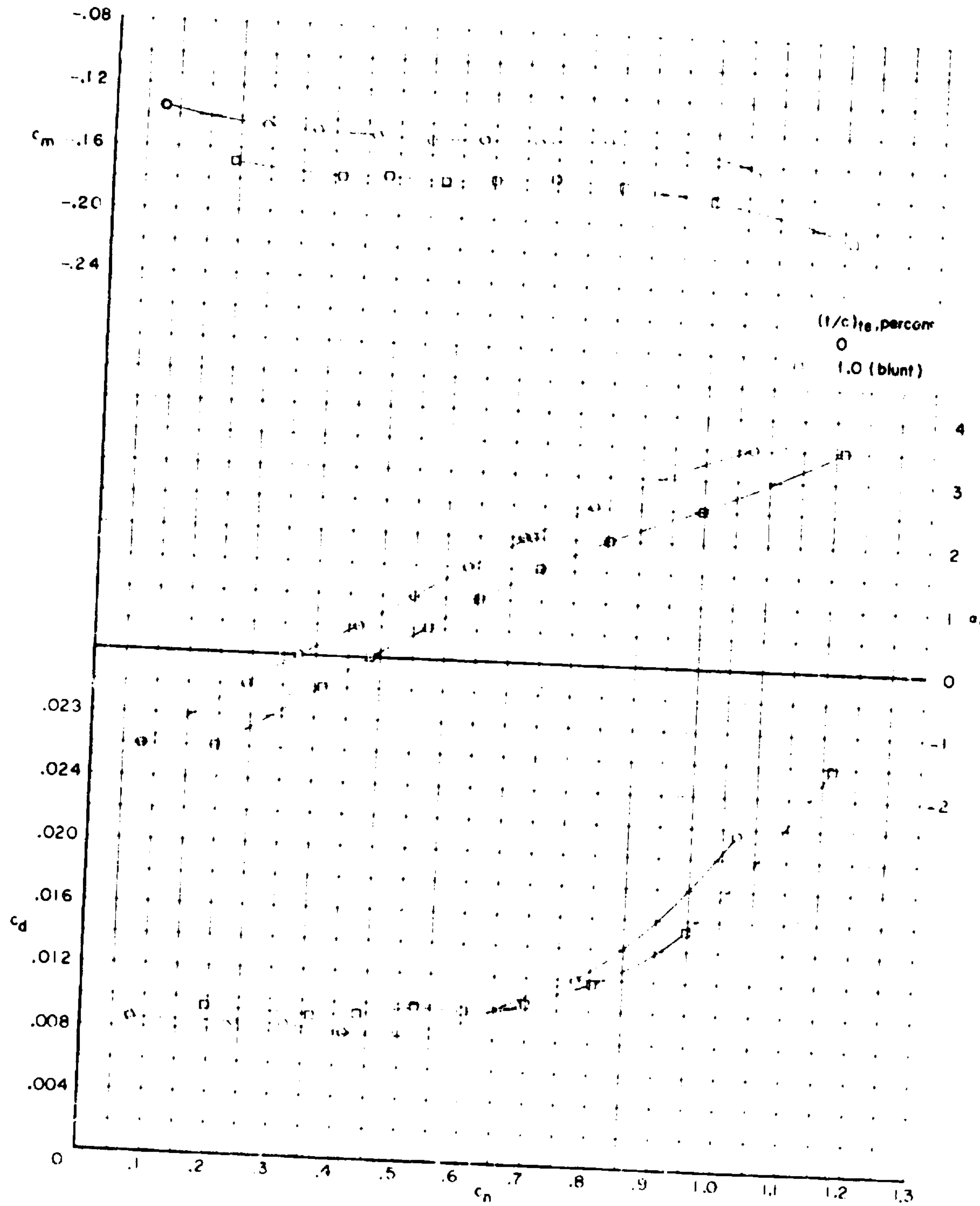

(d) M = 0.74.

Figure 6.- Continued.

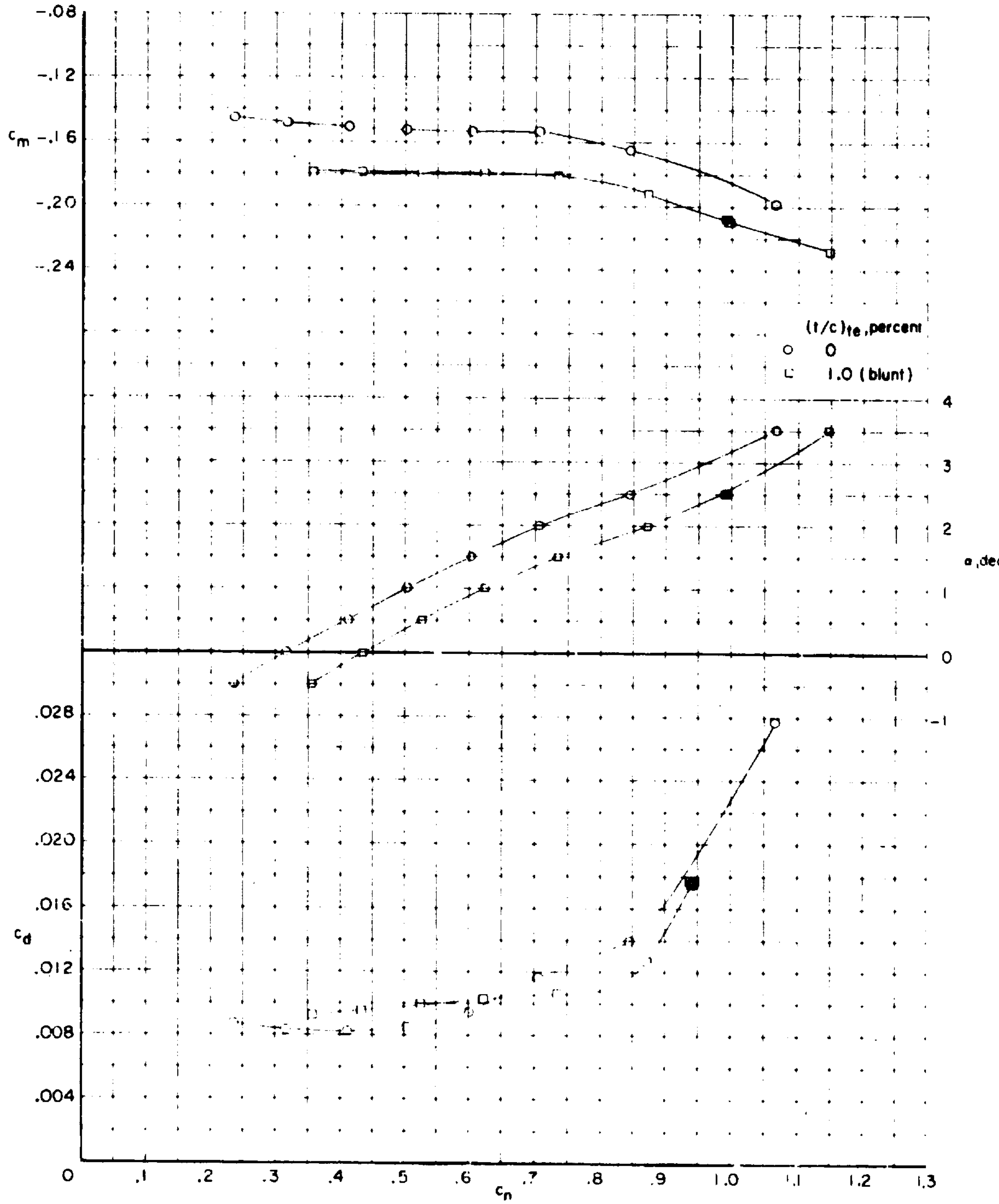

(e) M = 0.76.

Figure 6.- Continued.

ORIGINAL PAGE IS OF POOR QUALITY

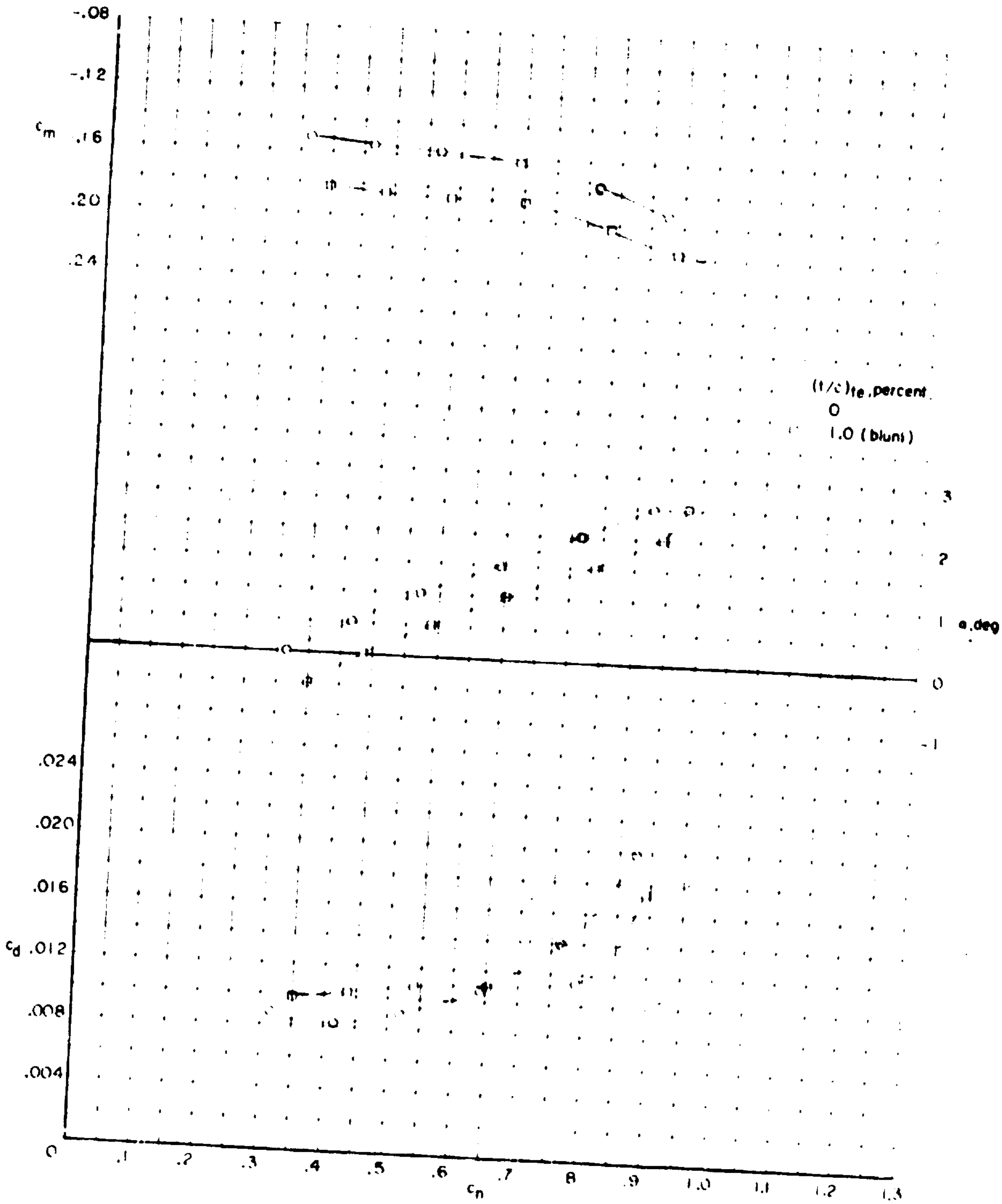

(f) M = 0.78.

Figure 6.- Continued.

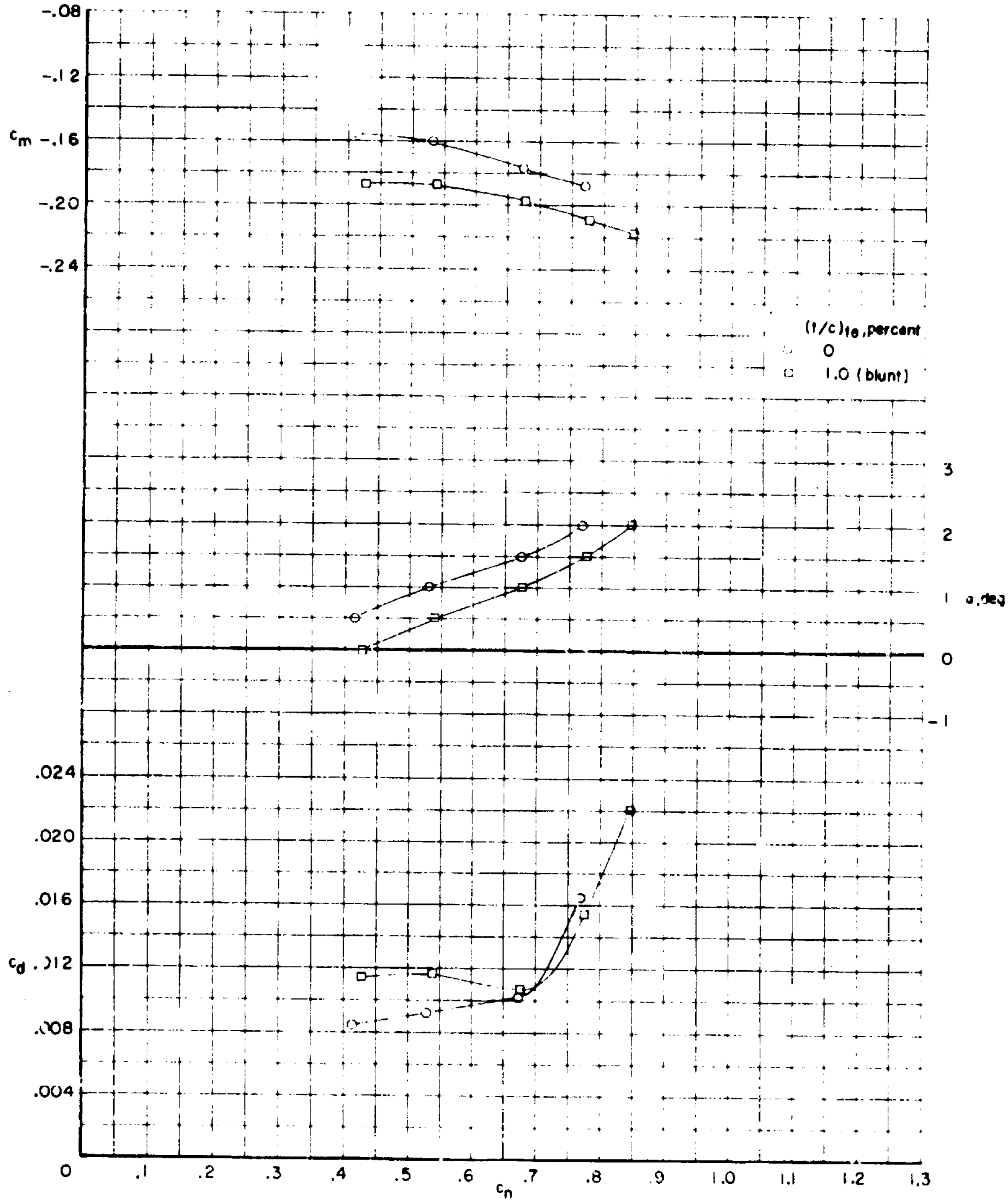

(g) M = 0.79.

Figure 6.- Continued.

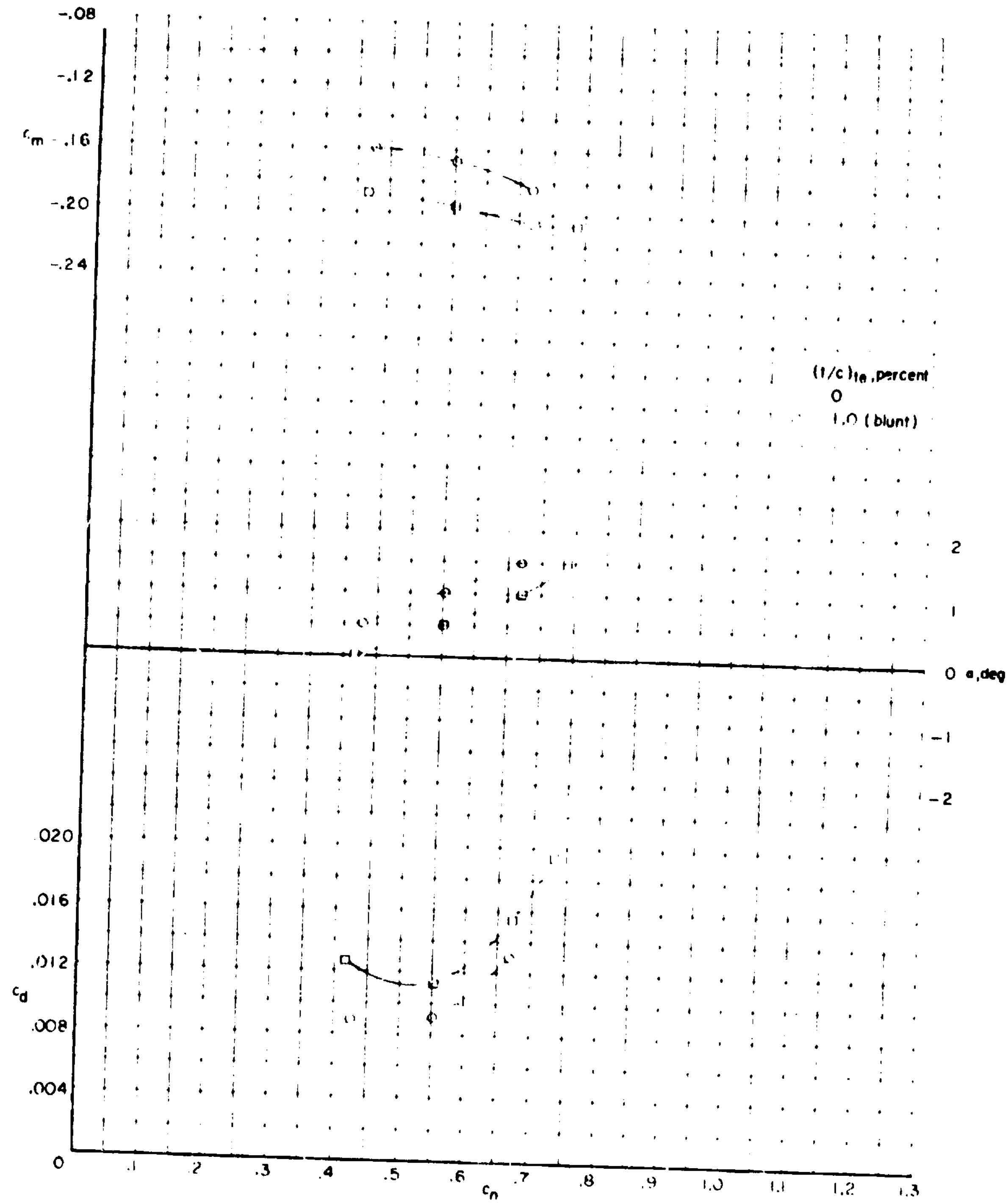

(h) M = 0.80.

Figure 6.- Continued.

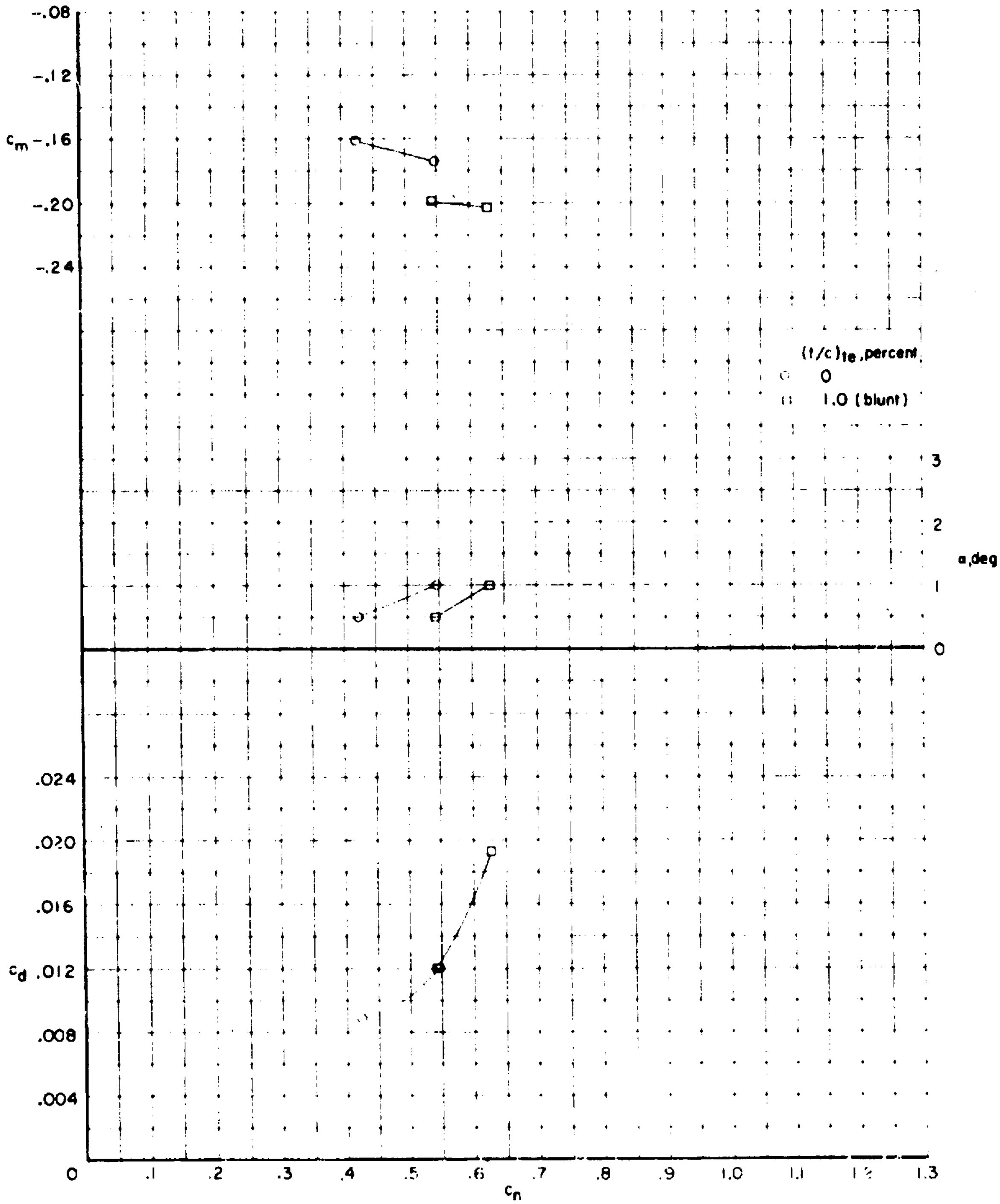

(i) M = 0.81.

Figure 6.- Concluded.

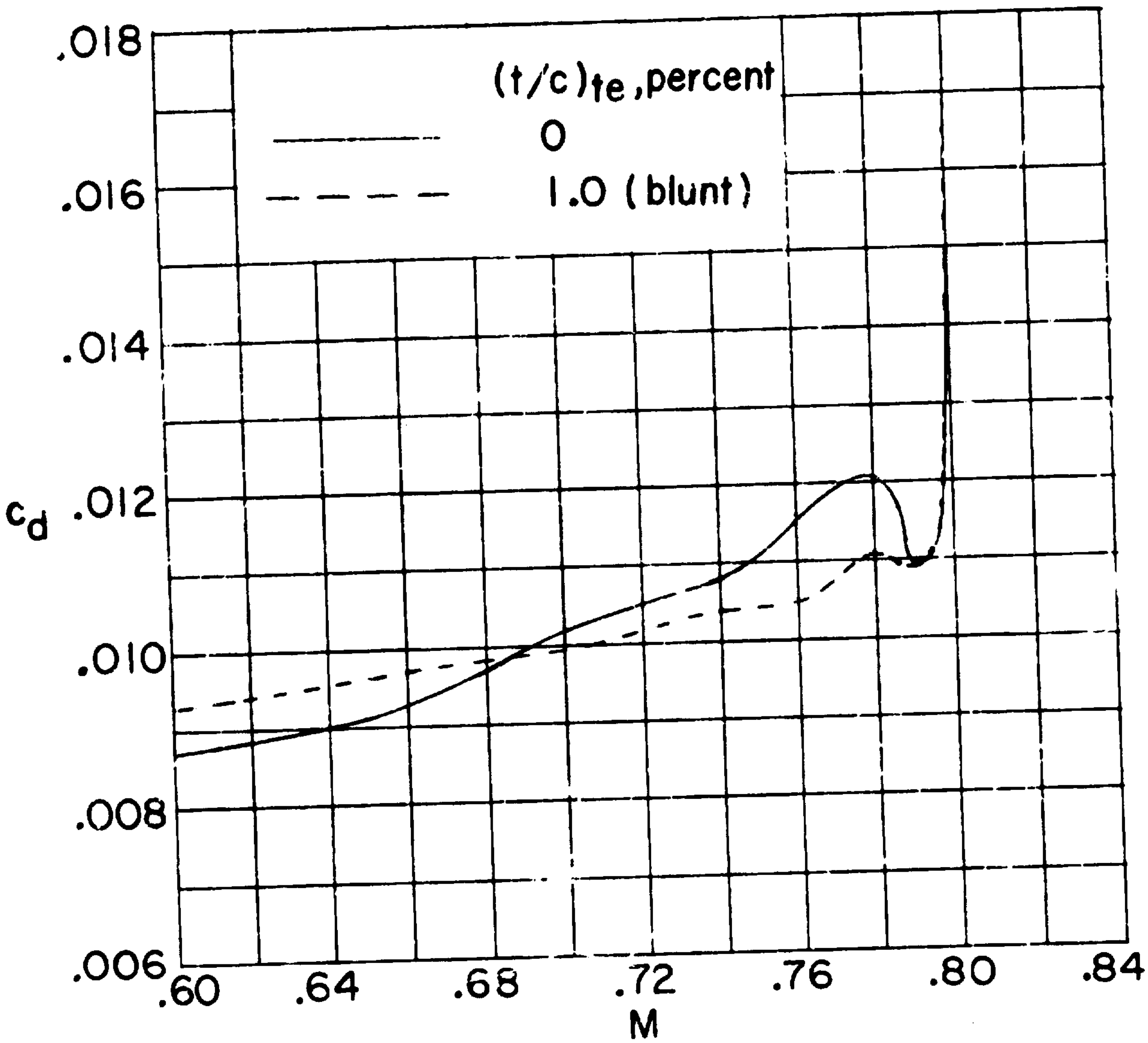

Figure 7.- Variation of section drag coefficient with Mach number at a normal-force coefficient of 0.7 for the 11-percent-thick interim supercritical airfoil with sharp and blunt trailing edge.

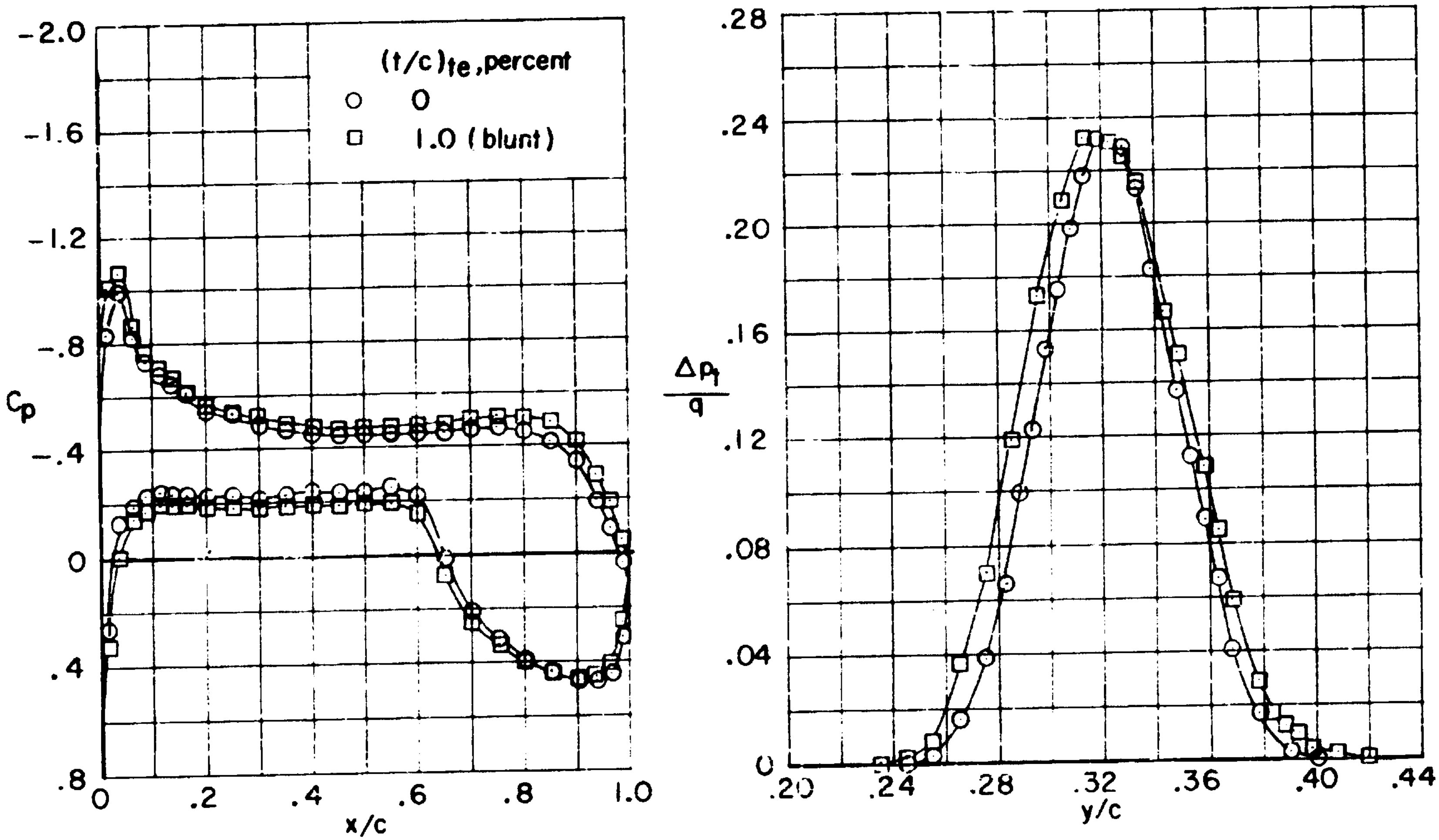

(c) M = 0.60; α = 1°.

Figure 8.- Representative effects of trailing-edge thickness on airfoil pressure distributions and wake profiles of an 11-percent-thick interim supercritical airfoil.

[redacted]

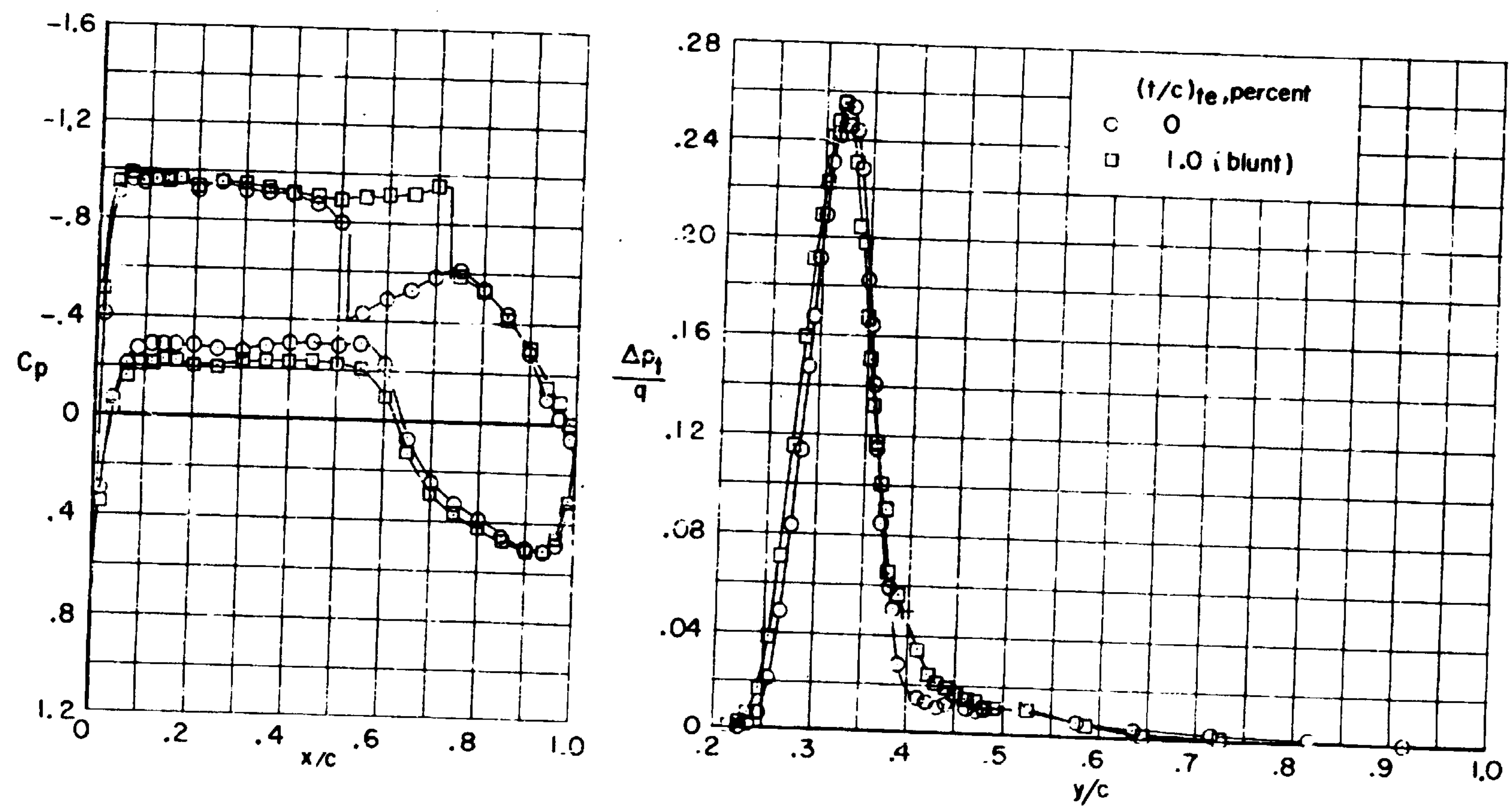

(b) $M = 0.78$; $\alpha = 1.5^{\circ}$.

Figure 8.- Concluded.

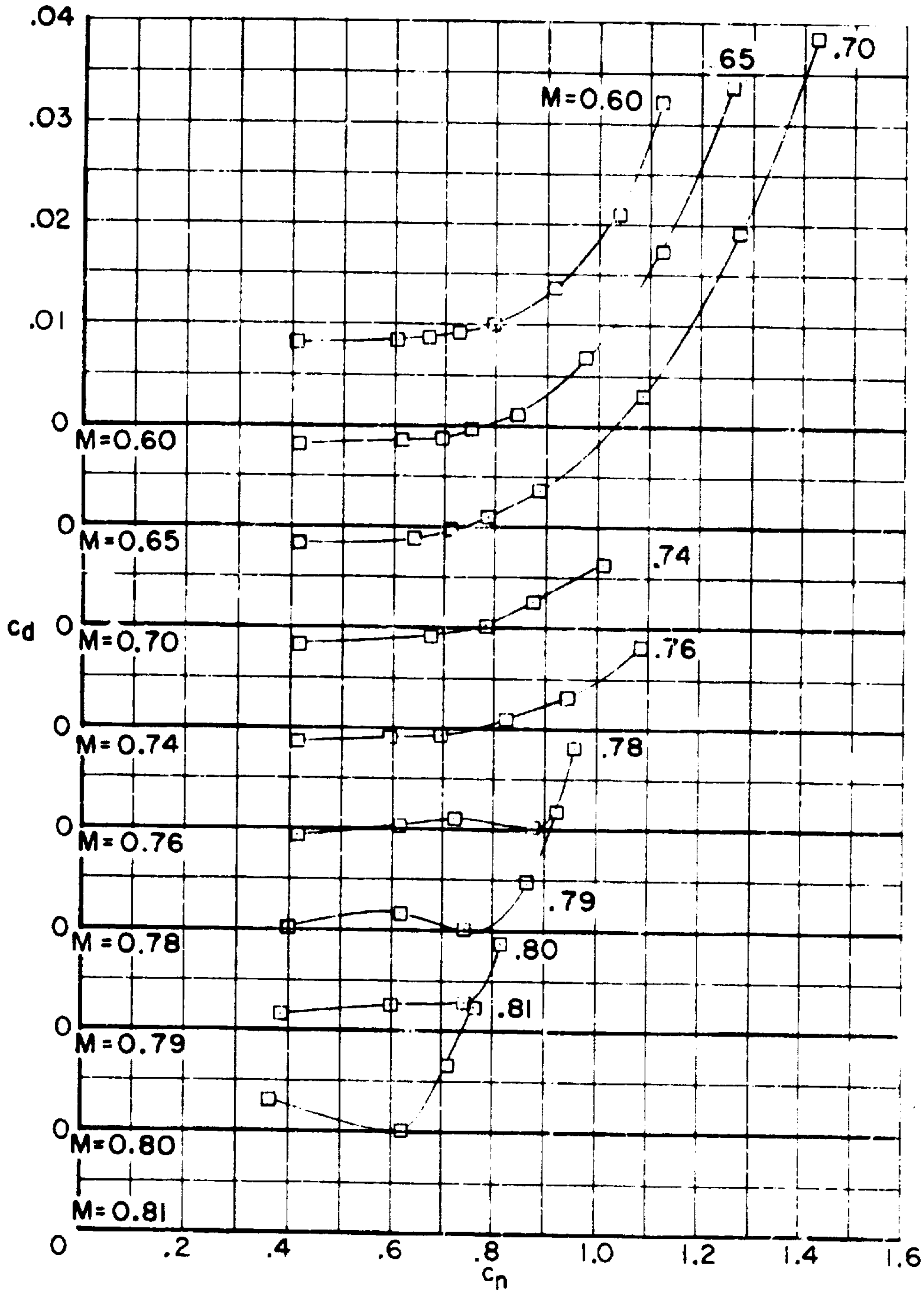

Figure 9.- Variation of section drag coefficient, angle of attack, and section pitching-moment coefficient at various Mach numbers for 10-percent-thick supercritical airfoil with 1.0-percent-thick trailing edge with cavity.

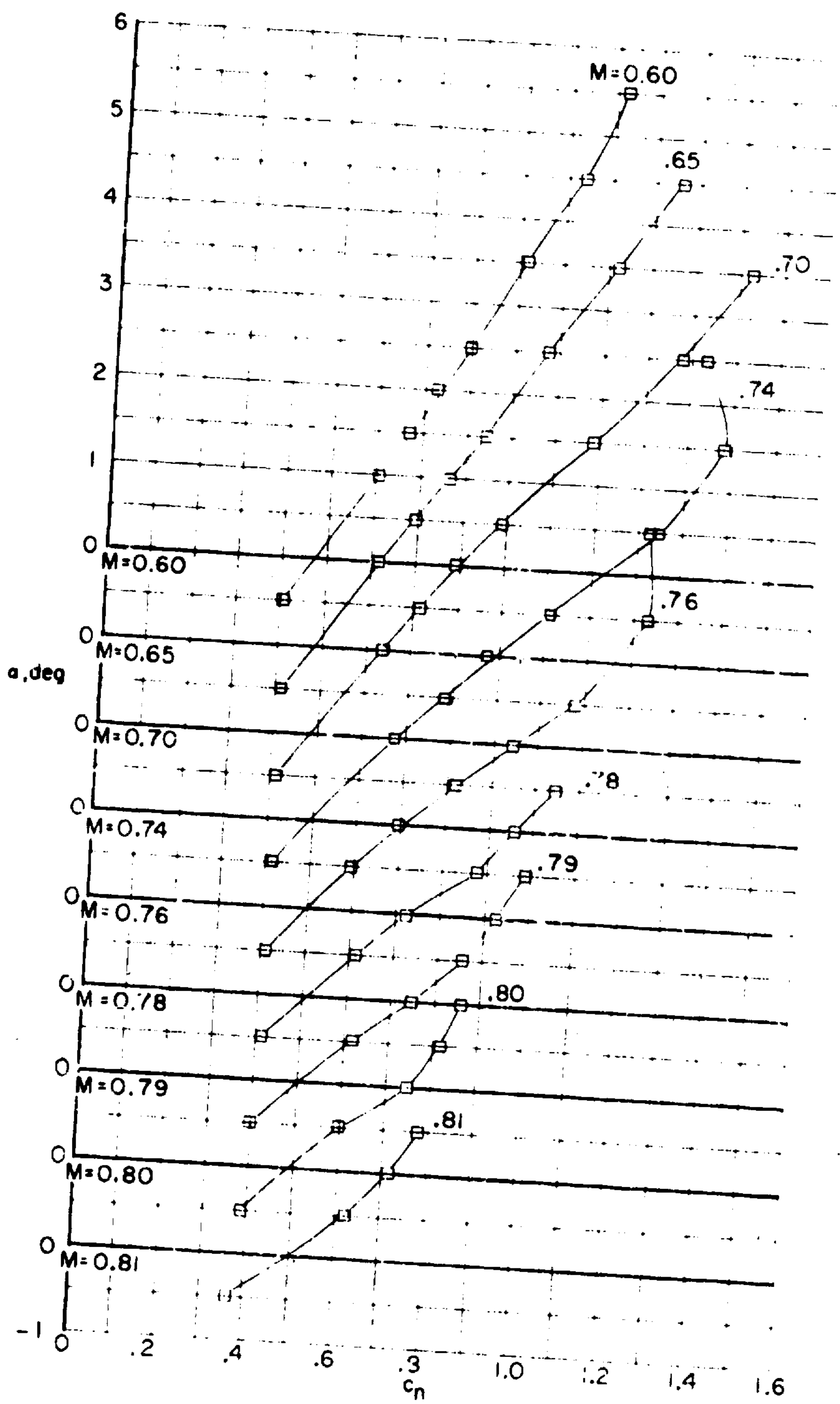

Figure 9.- Continued.

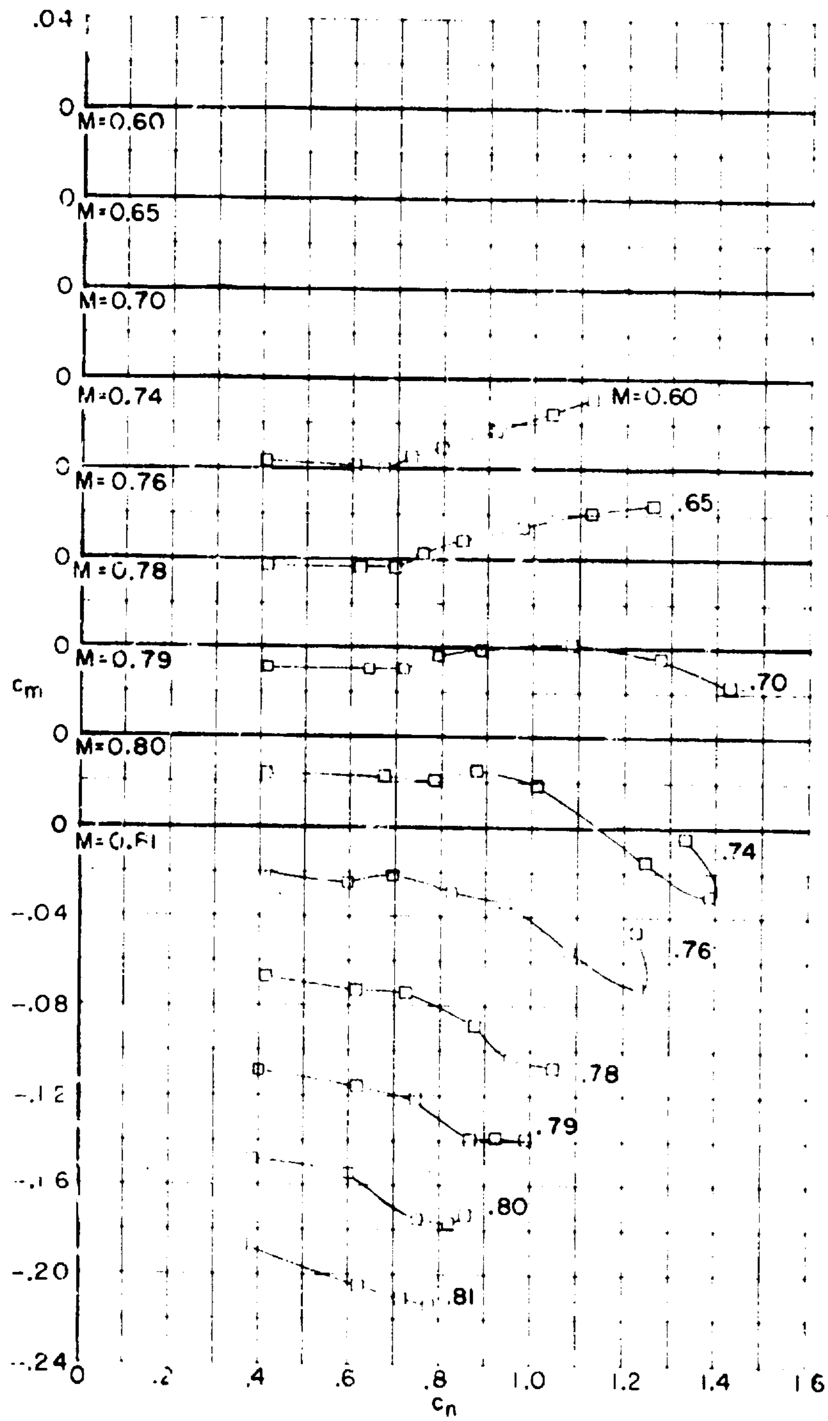

Figure 9.- Concluded.

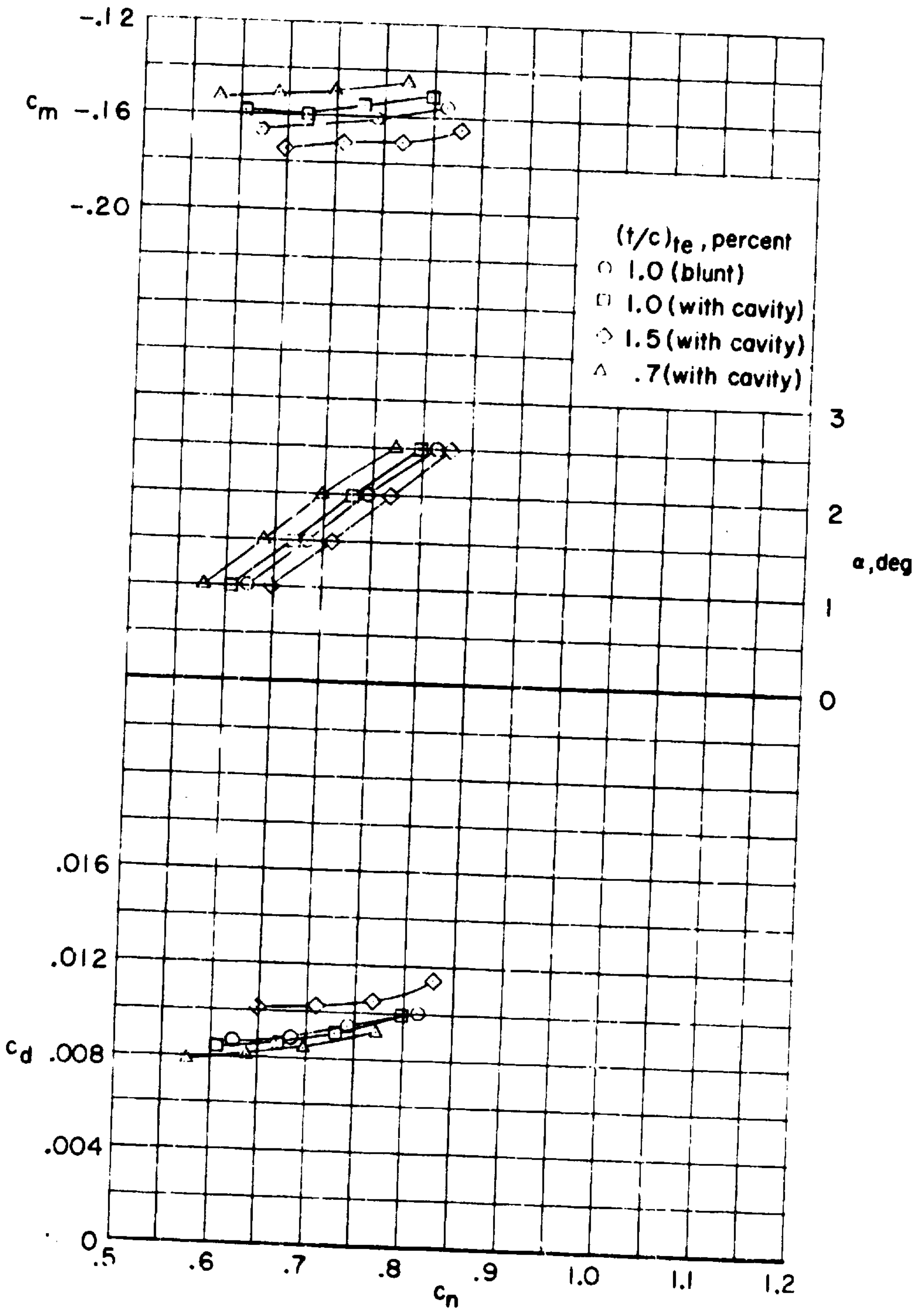

(a) M = 0.60.

Figure 10.- Effect of trailing-edge geometry on force and moment characteristics of 10-percent-thick supercritical airfoil.

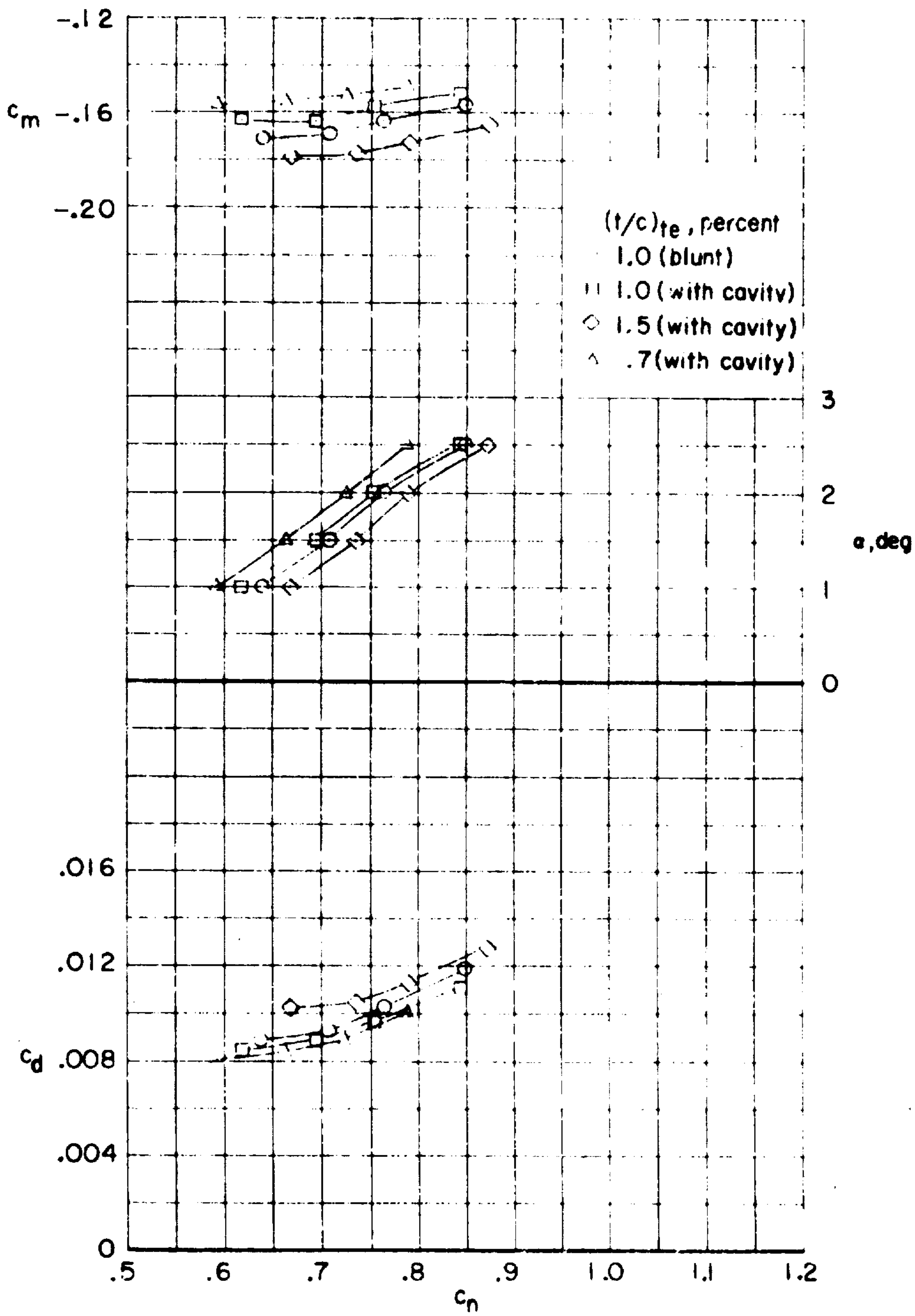

(b) M = 0.65.

Figure 10.- Continued.

ORIGINAL PAGE IS
OF POOR QUALITY

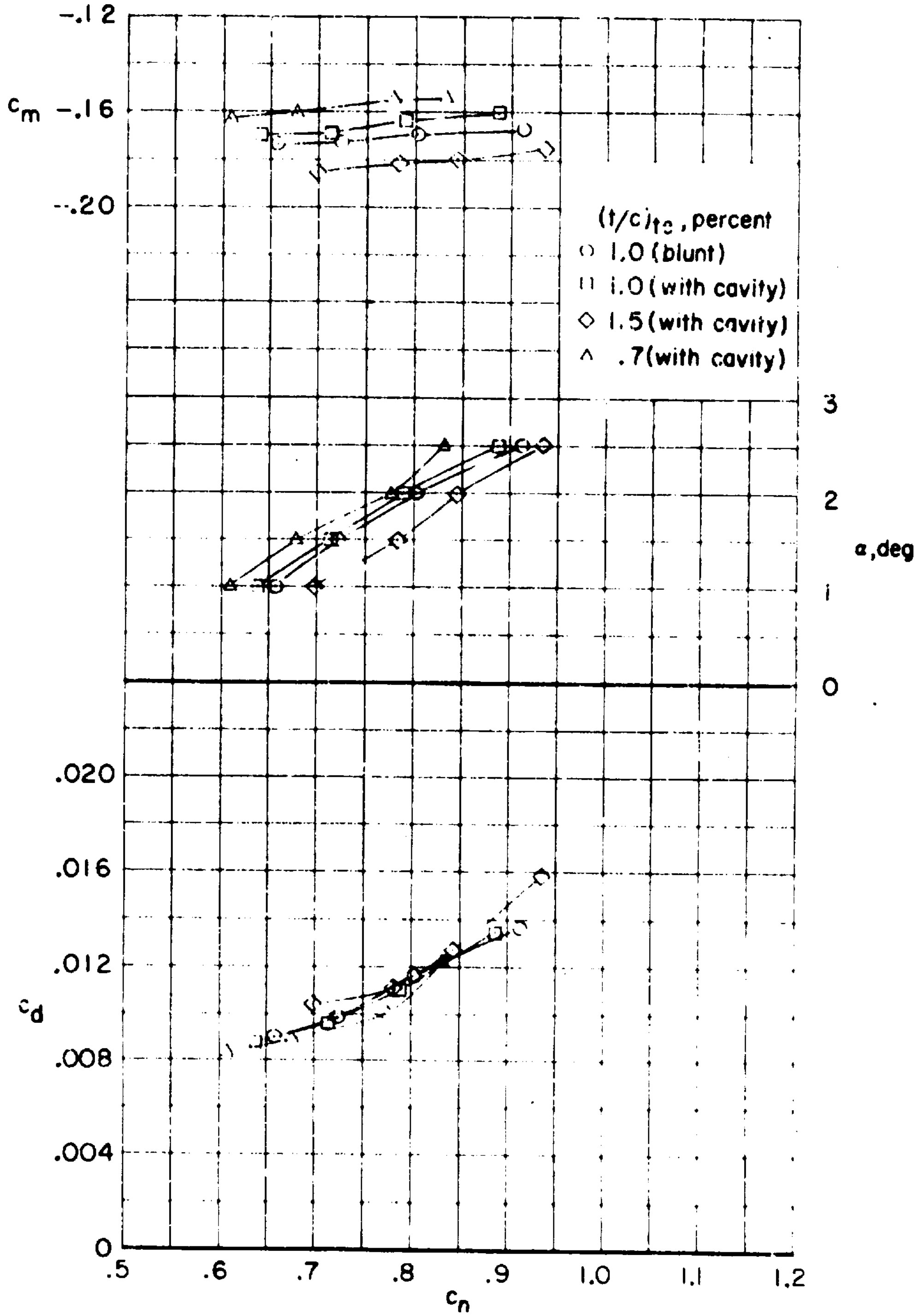

(c) M = 0.70.

Figure 10.- Continued.

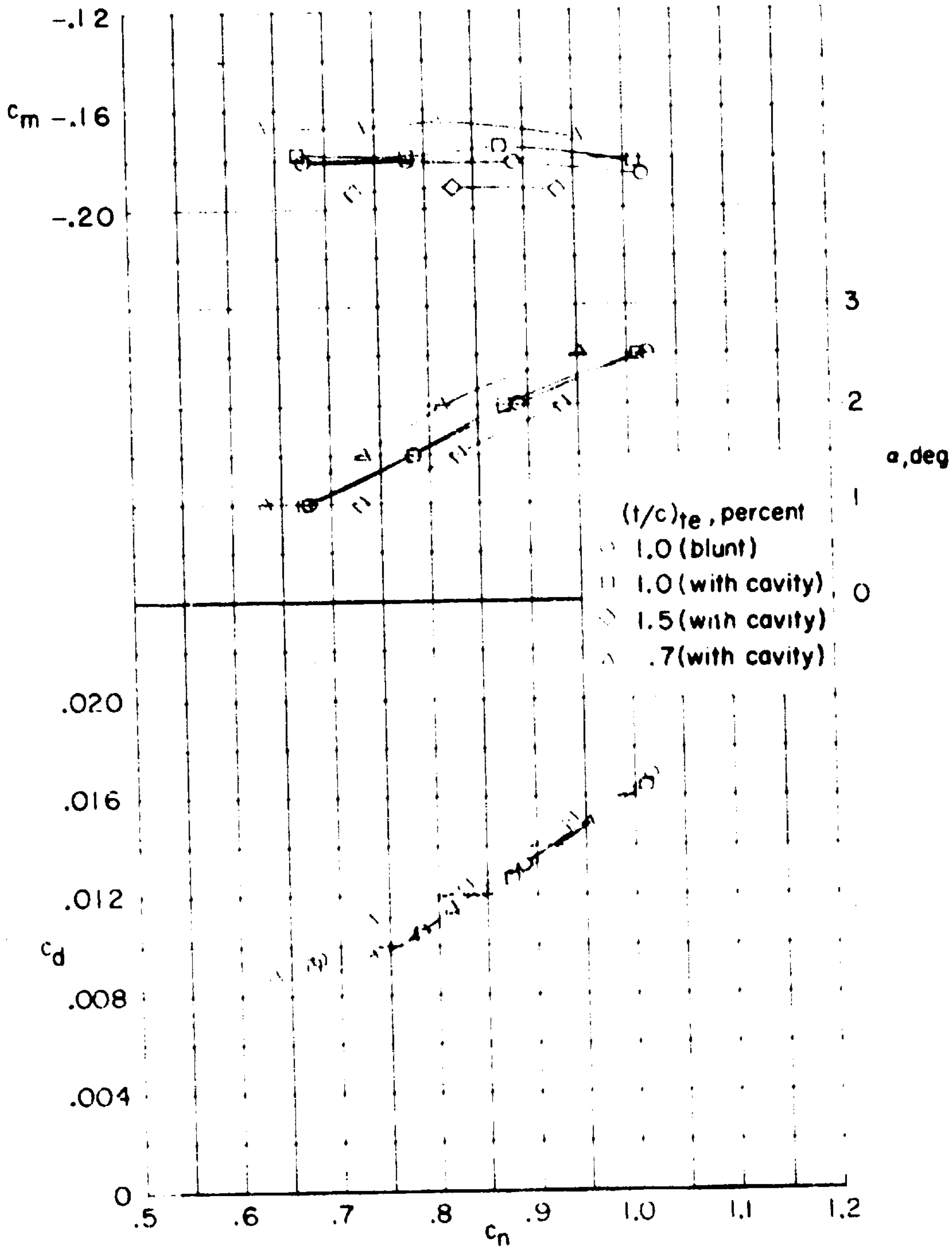

ORIGINAL PAGE IS
OF POOR QUALITY

(d) M = 0.75.

Figure 10.- Continued.

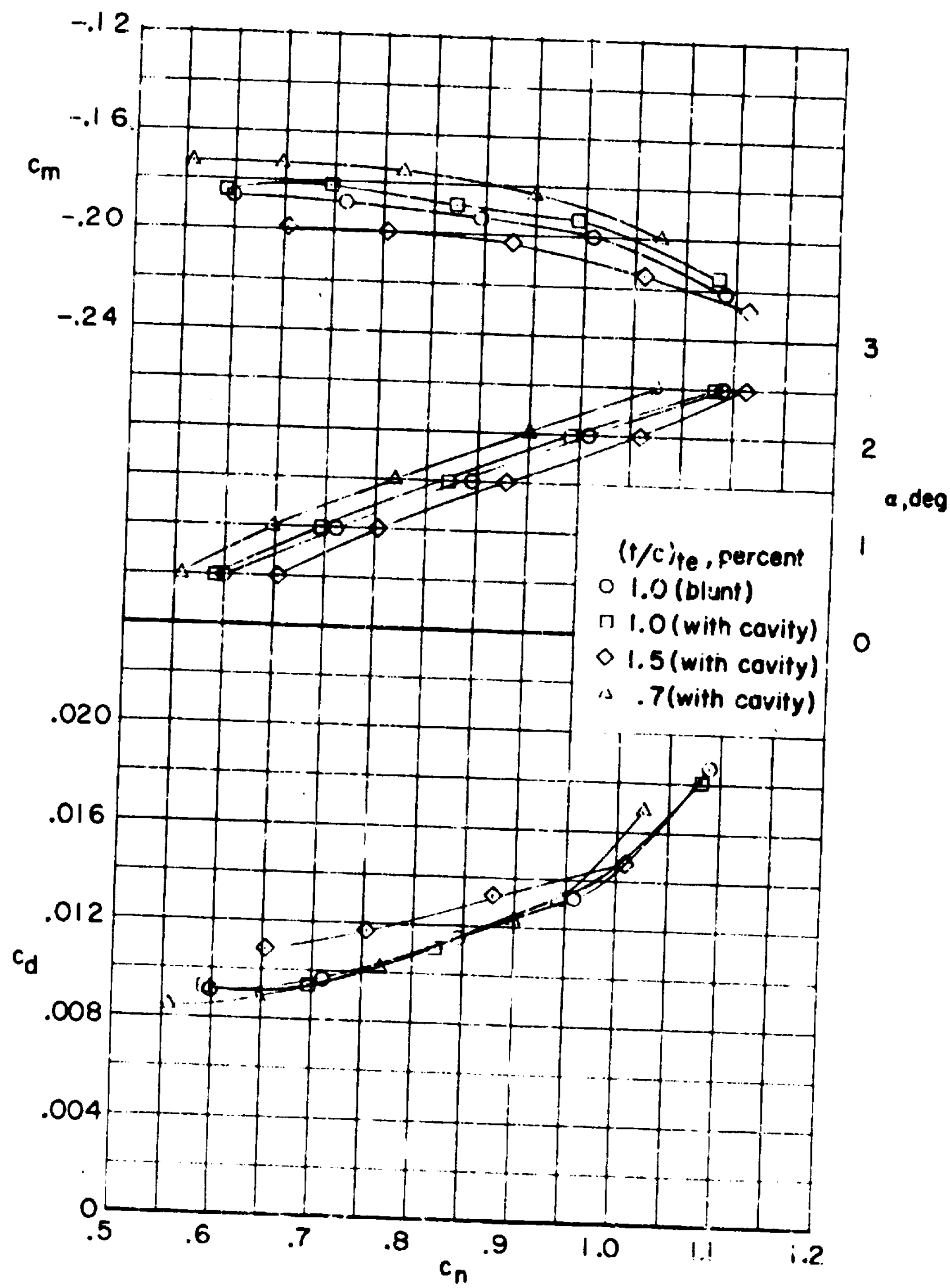

(e) M = 0.70.

Figure 10.- Continued.

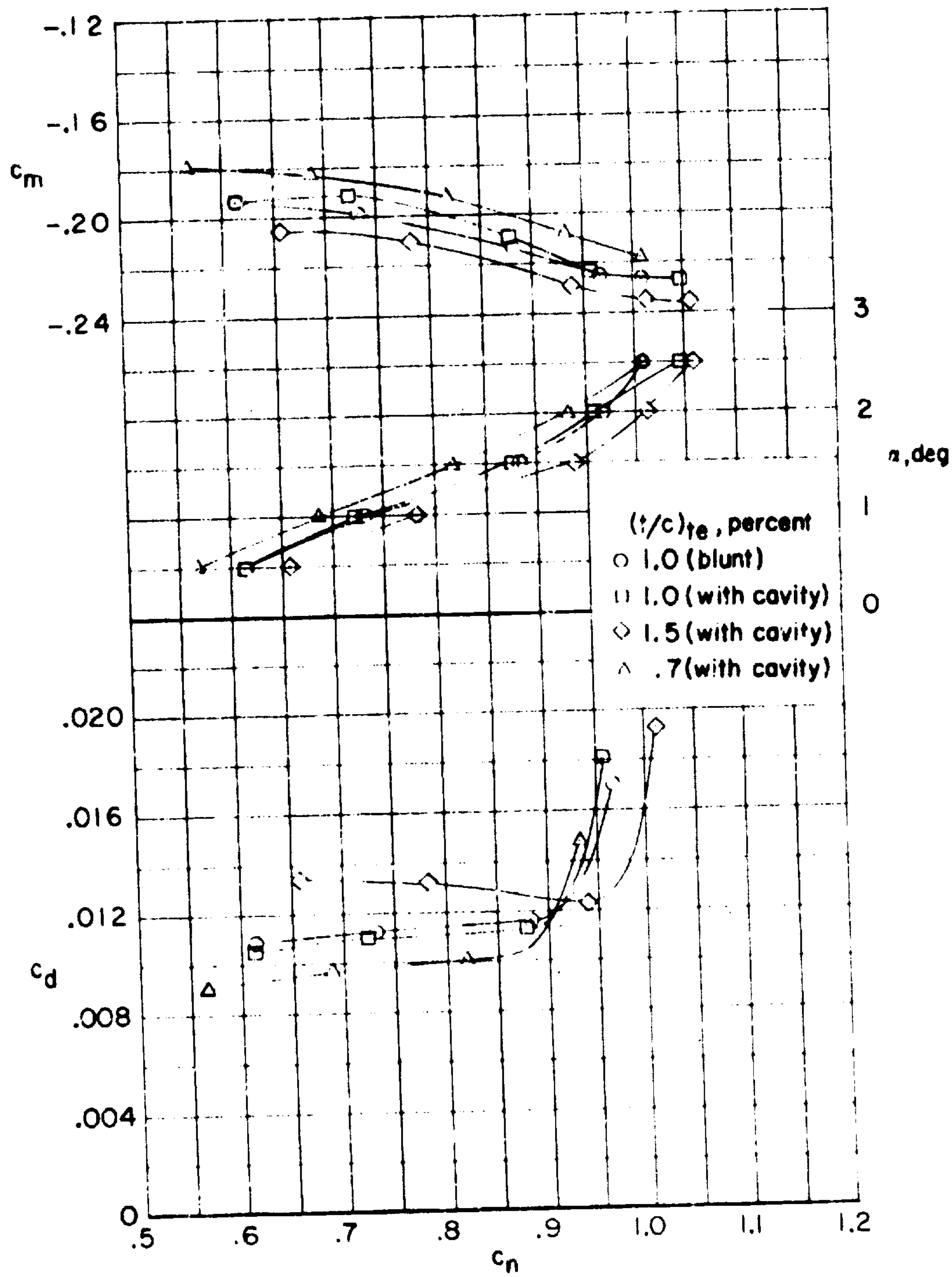

(f) M = 0.78.

Figure 10.- Continued.

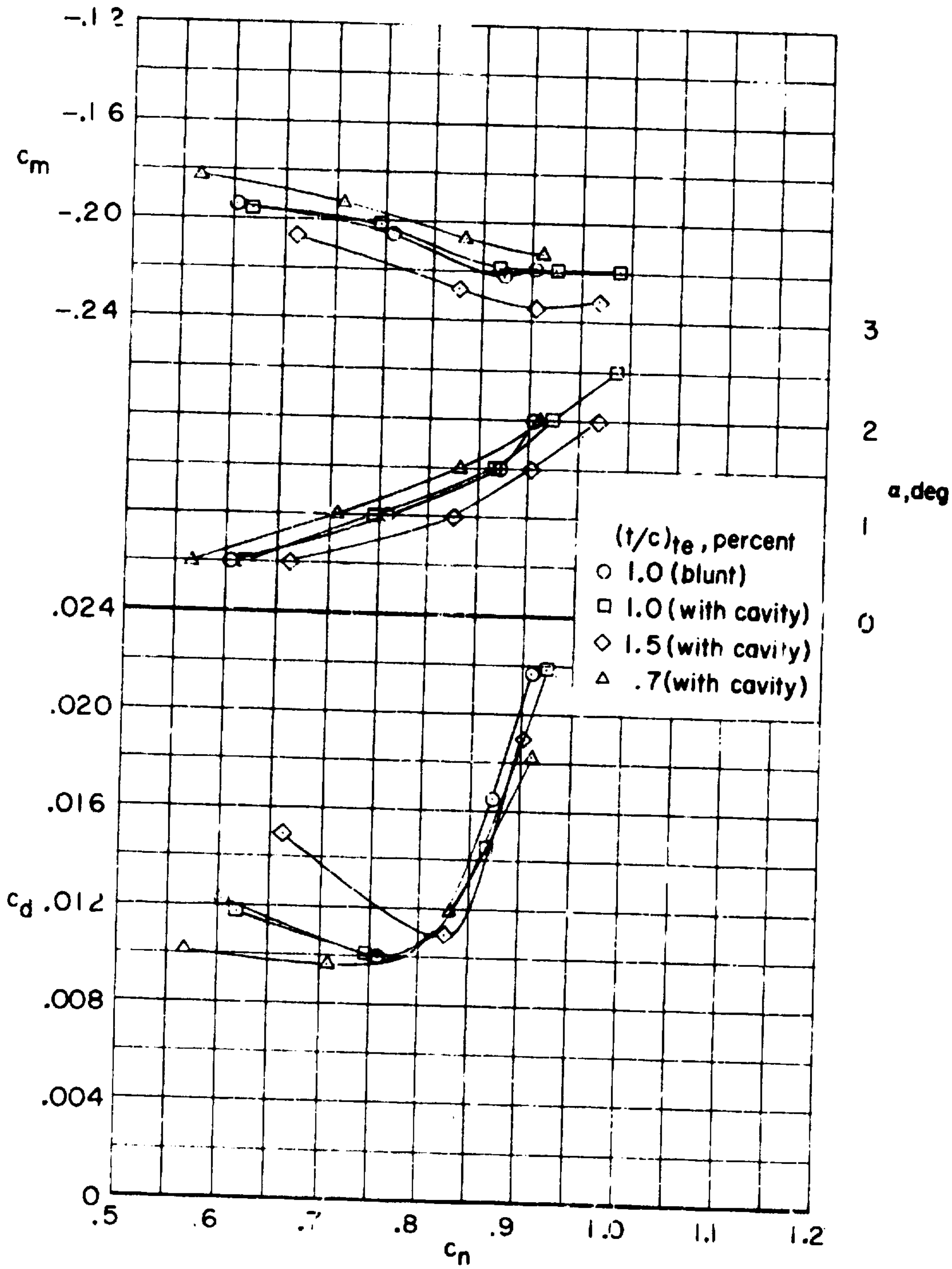

(g) M = 0.79.

Figure 10.- Continued.

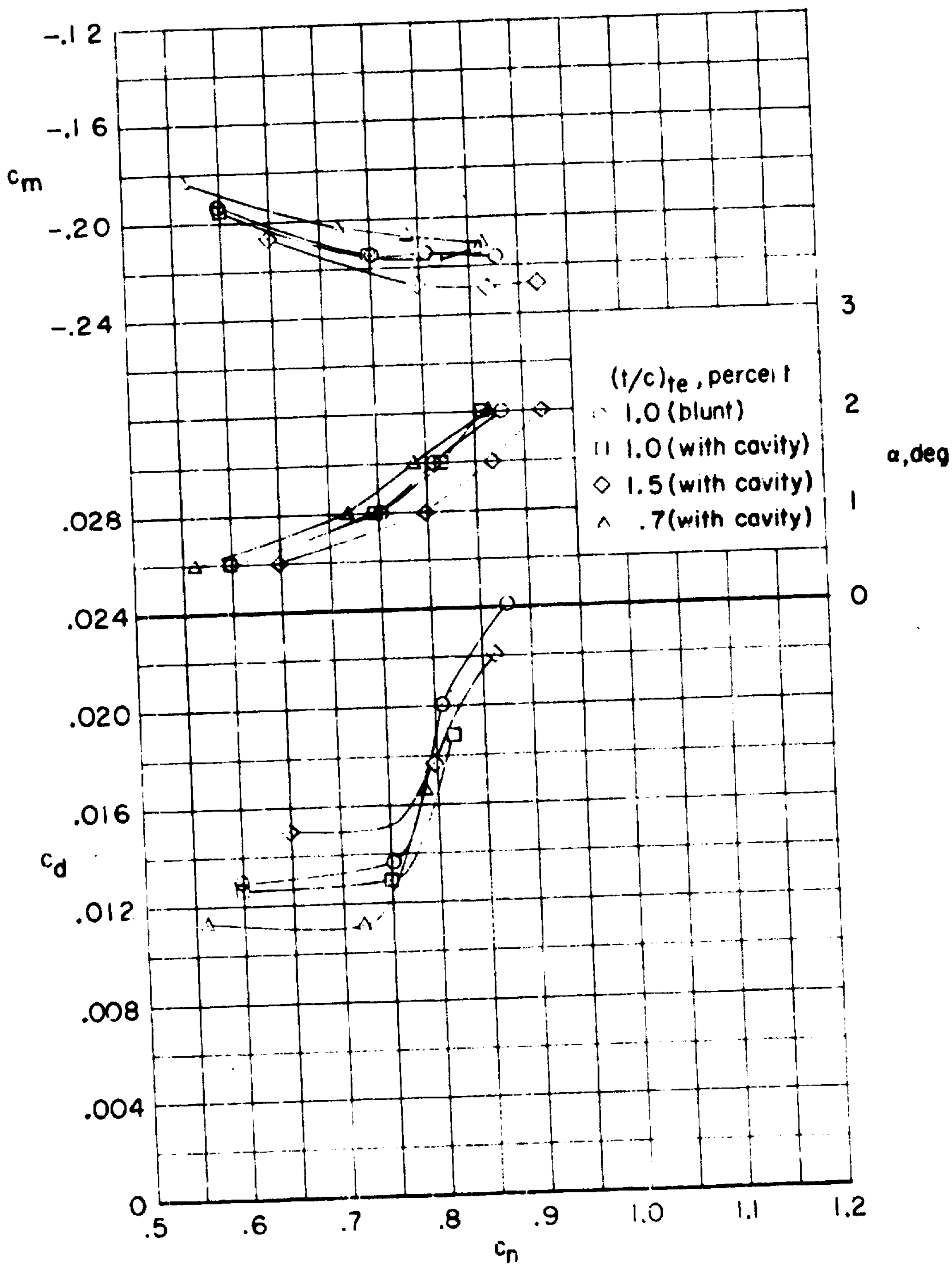

(h) M = 0.80.

Figure 10.- Continued.

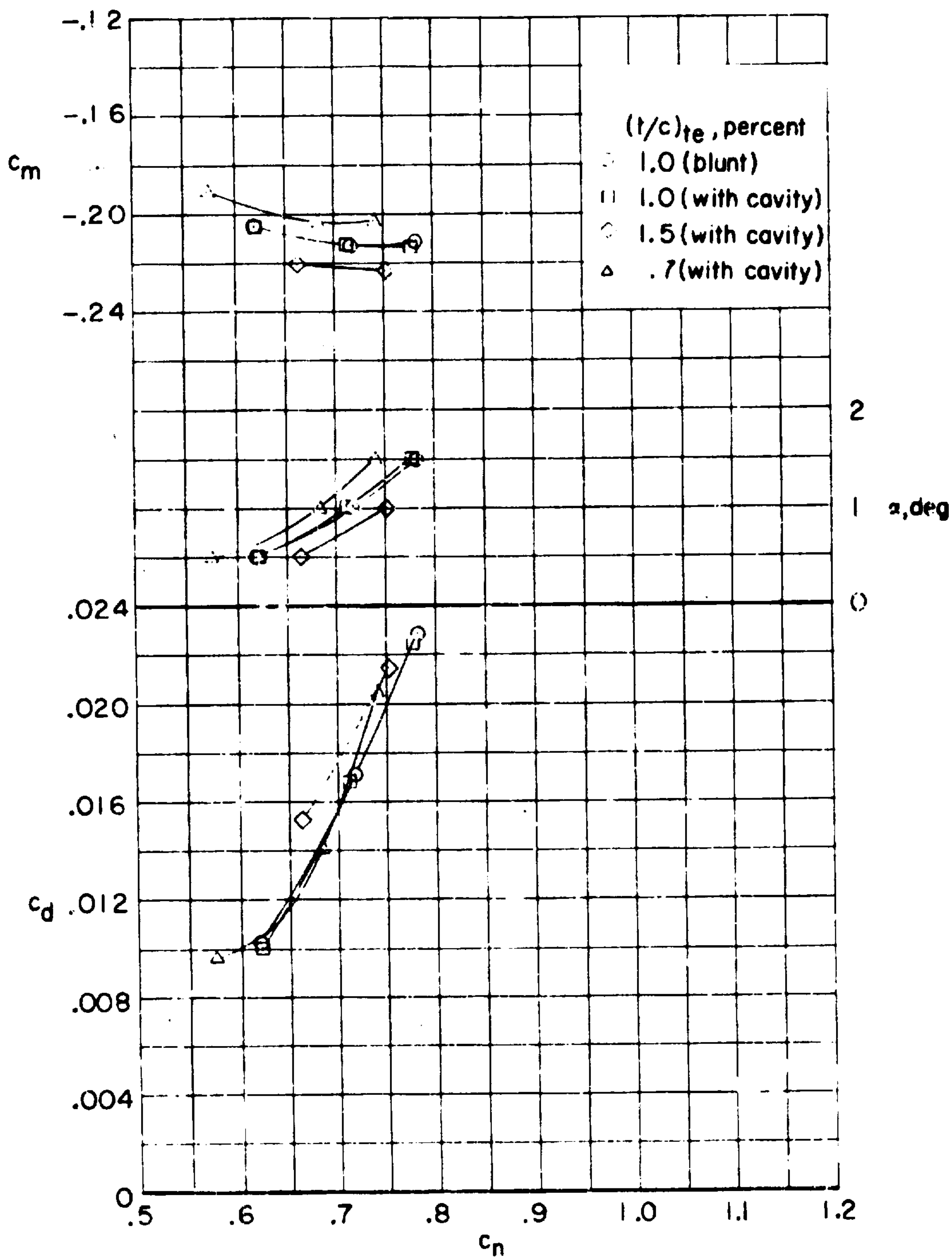

(i) M = 0.81.

Figure 10.- Concluded.

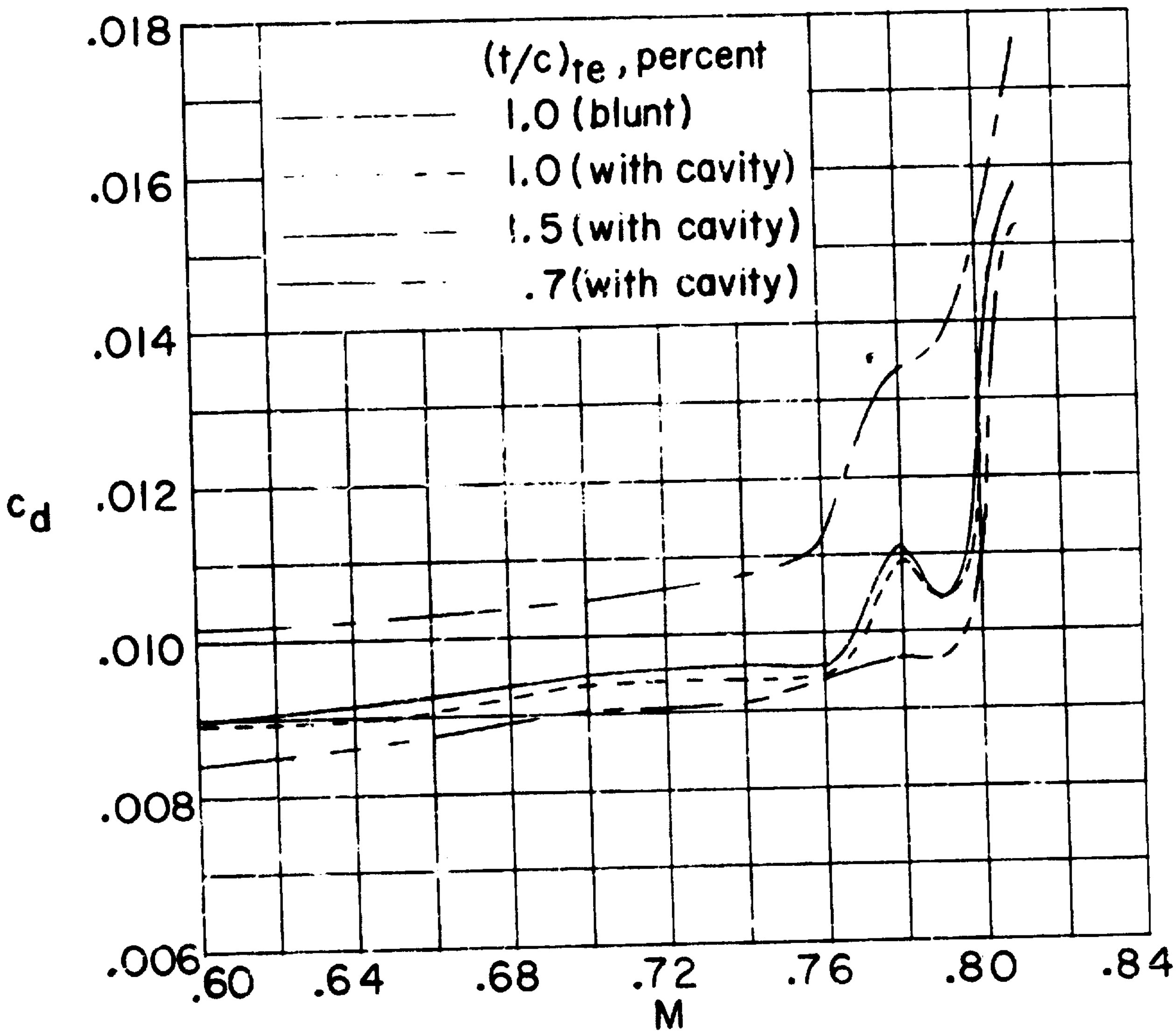

Figure 11.- Effect of trailing-edge geometry on variation of section drag coefficient with Mach number at a normal-force coefficient of 0.7 for the 10-percent-thick supercritical airfoil.

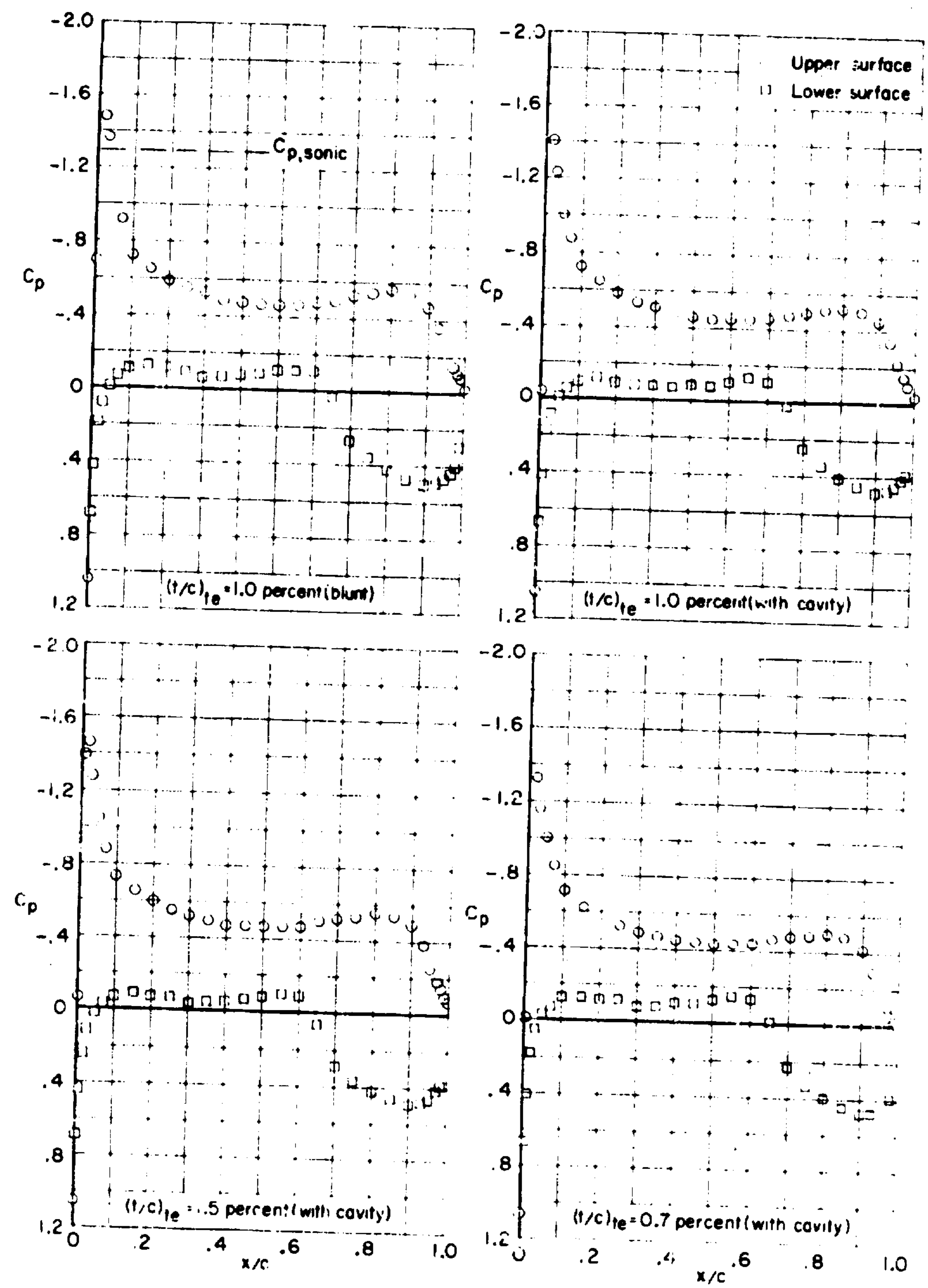

(a) M = 0.60; $\alpha = 1.0^{\circ}$.

Figure 12.- Chordwise pressure distribution for 10-percent-thick supercritical

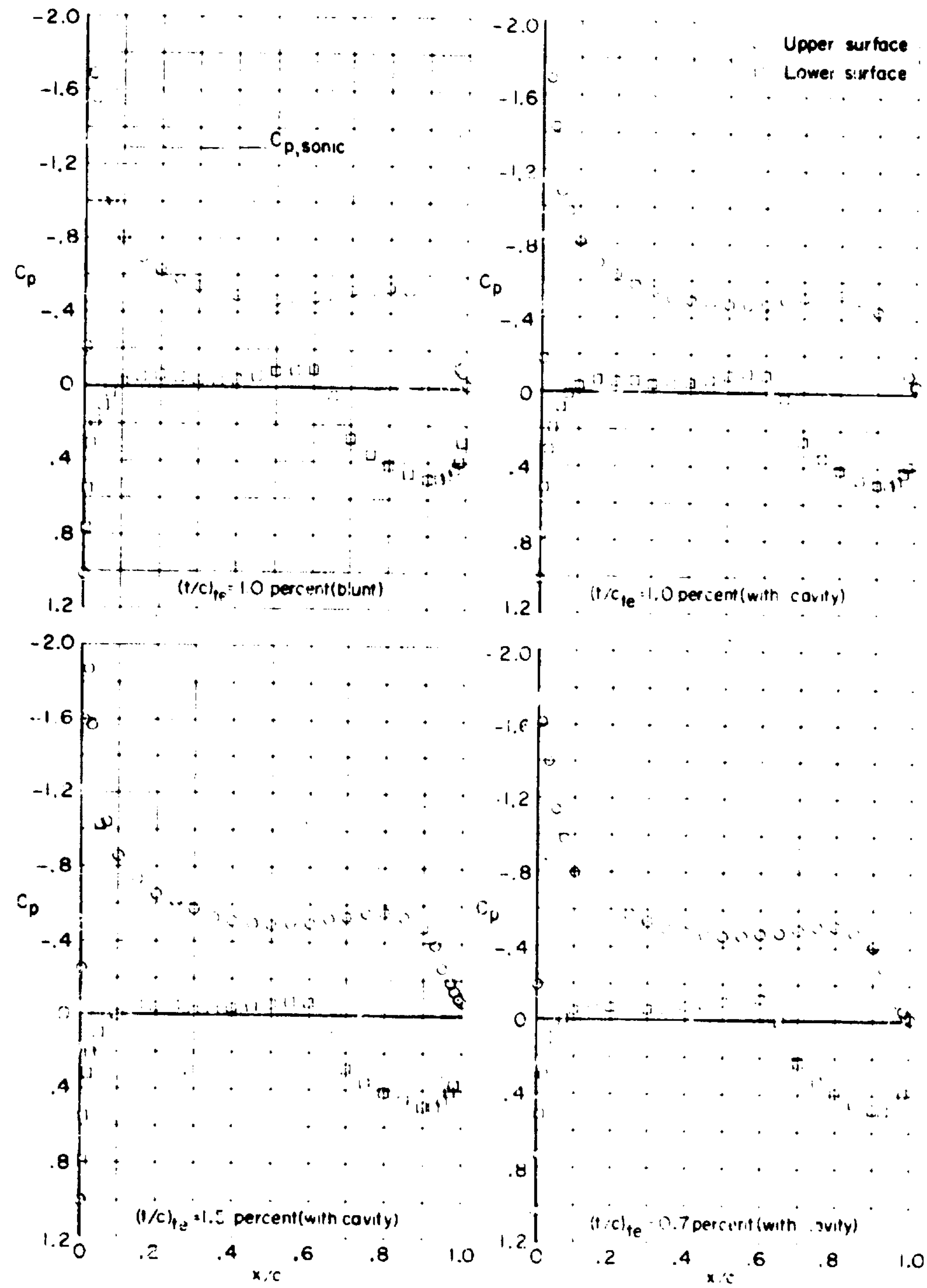

(b) M = 0.60; α = 1.5°.

Figure 1?.- Continued.

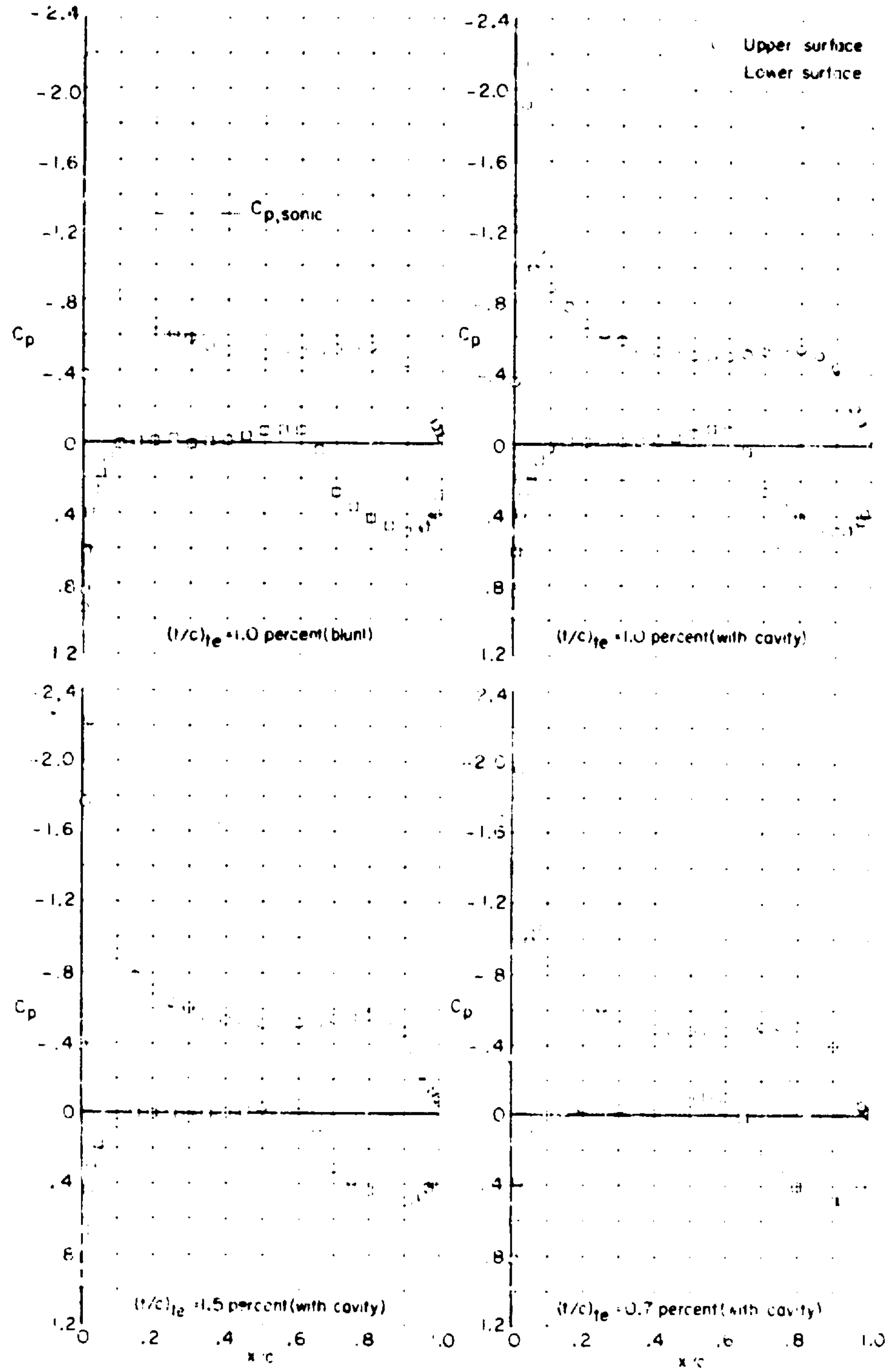

(c) M = 0.60; α = 2.0°.

Figure 12.- Continued.

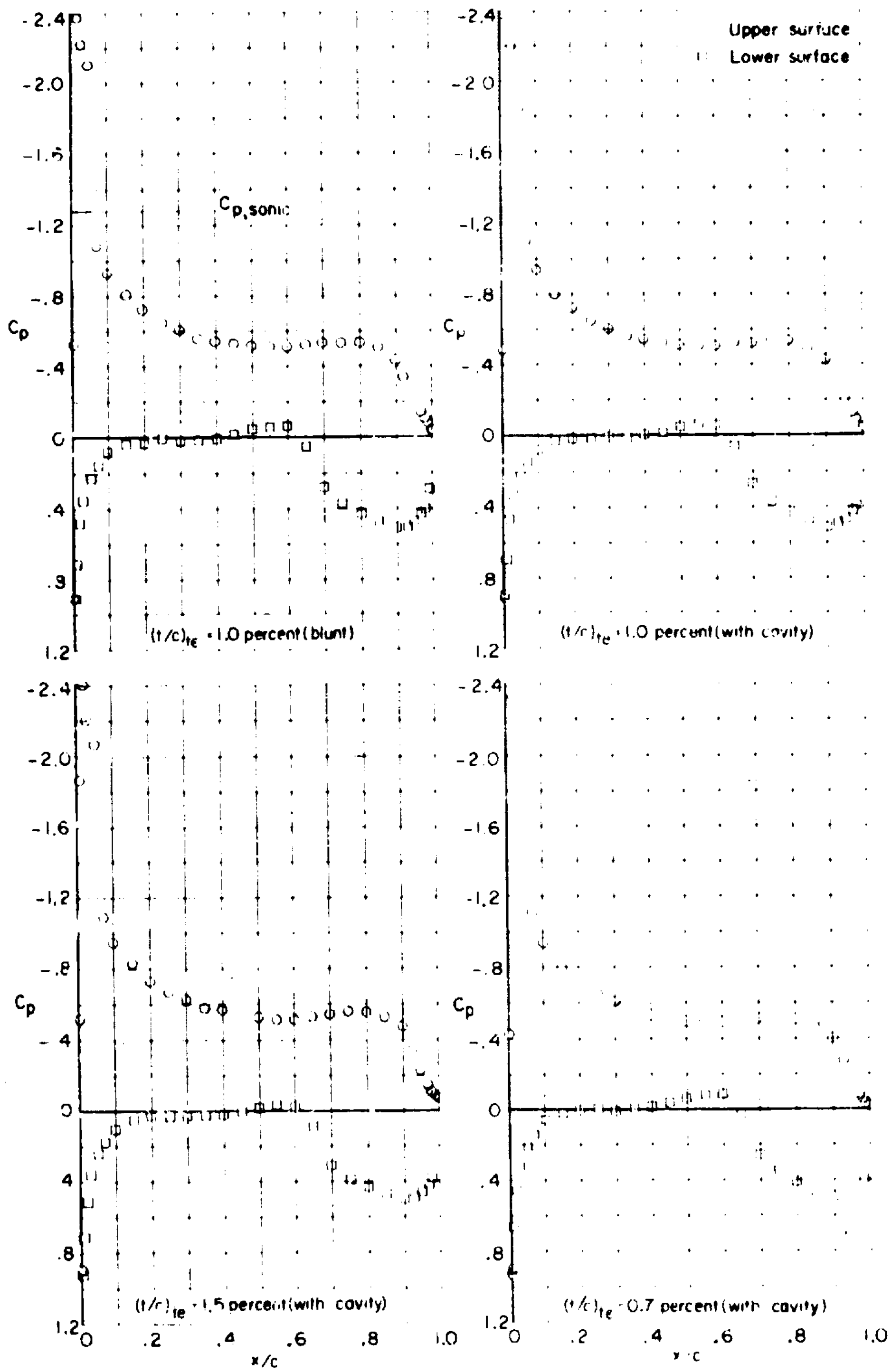

(d) M = 0.[illegible]0; α = [illegible].5°.

Figure 12.- Continued.

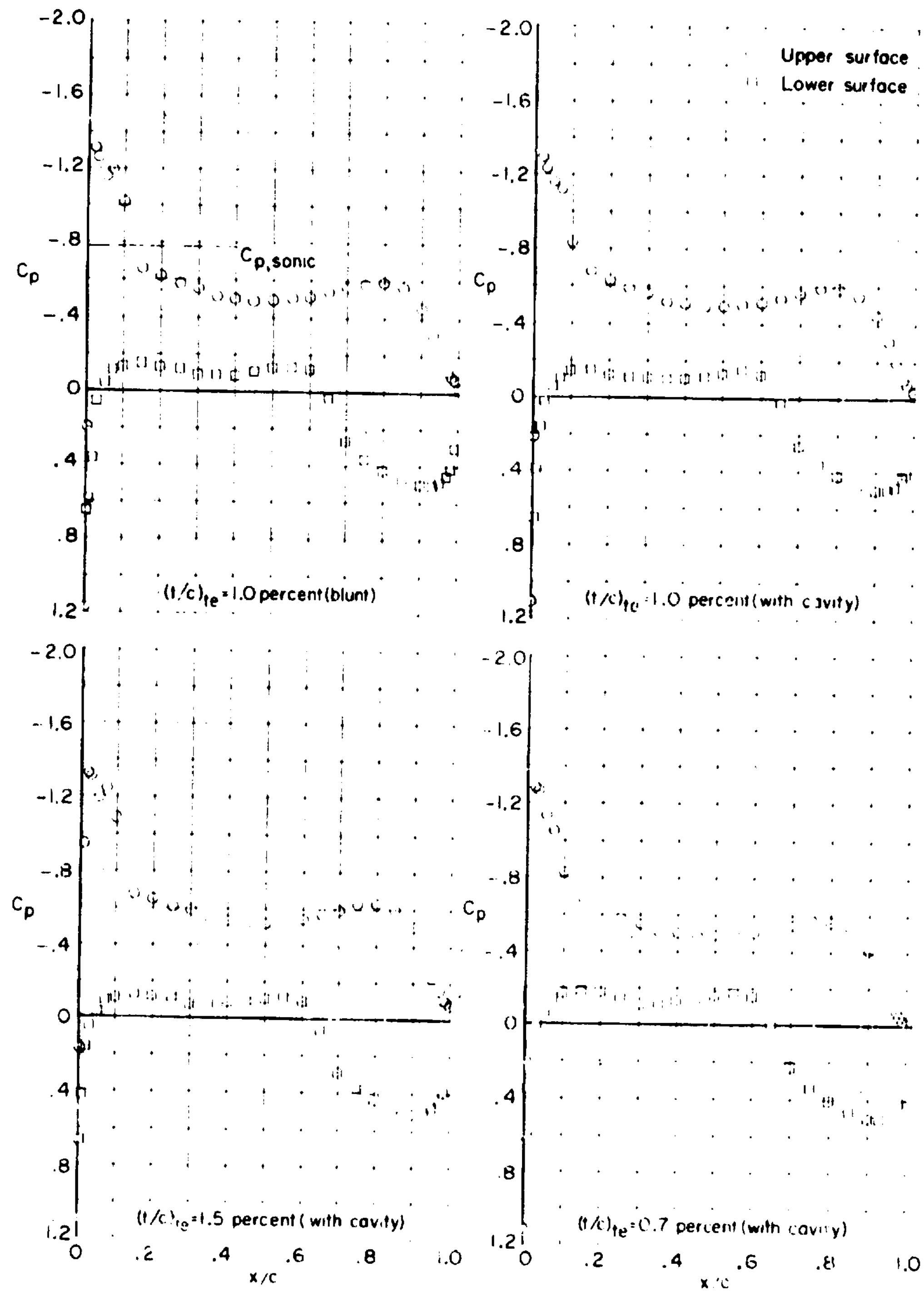

(e) M = 0.70; α = 1.0°.

Figure 1?.- Continued.

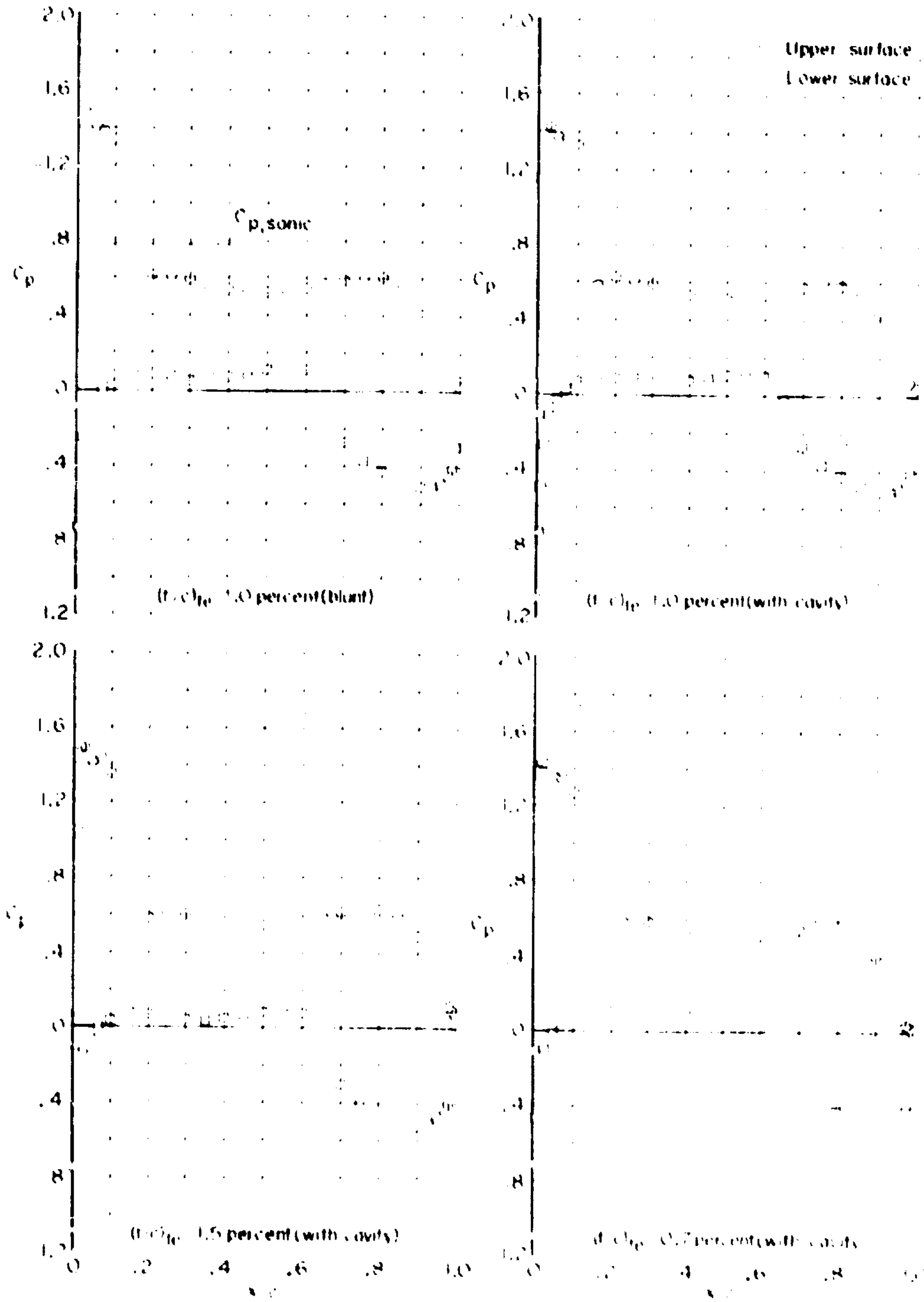

(c) M 0.70; α 1.5°.

Figure 19.- Continued.

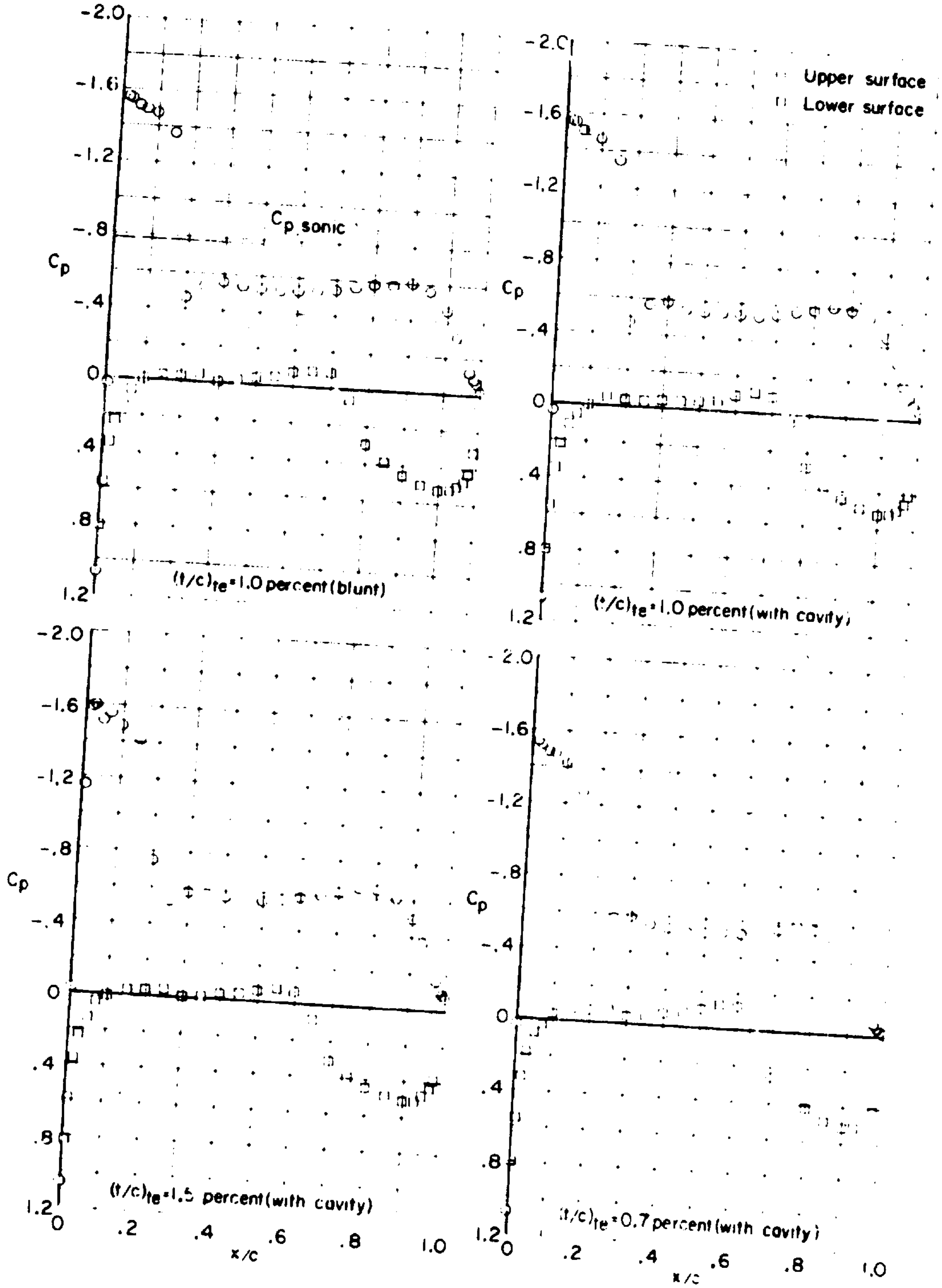

(g) M = 0.70; α = .̣.0°.

Figure 12.- Continued.

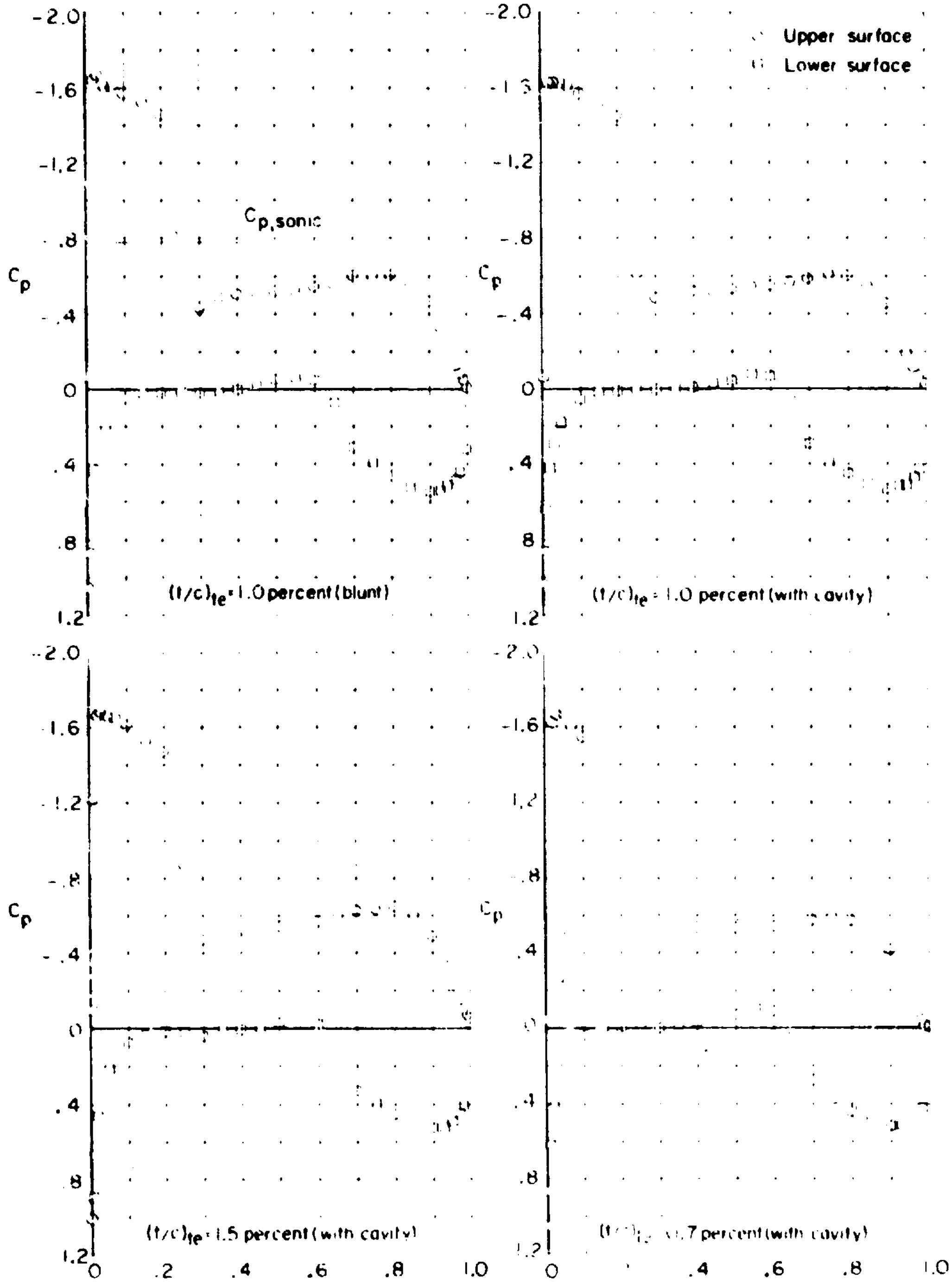

(h) M = 0.70; α = [illegible]°.

Figure 1[illegible].- Continued.

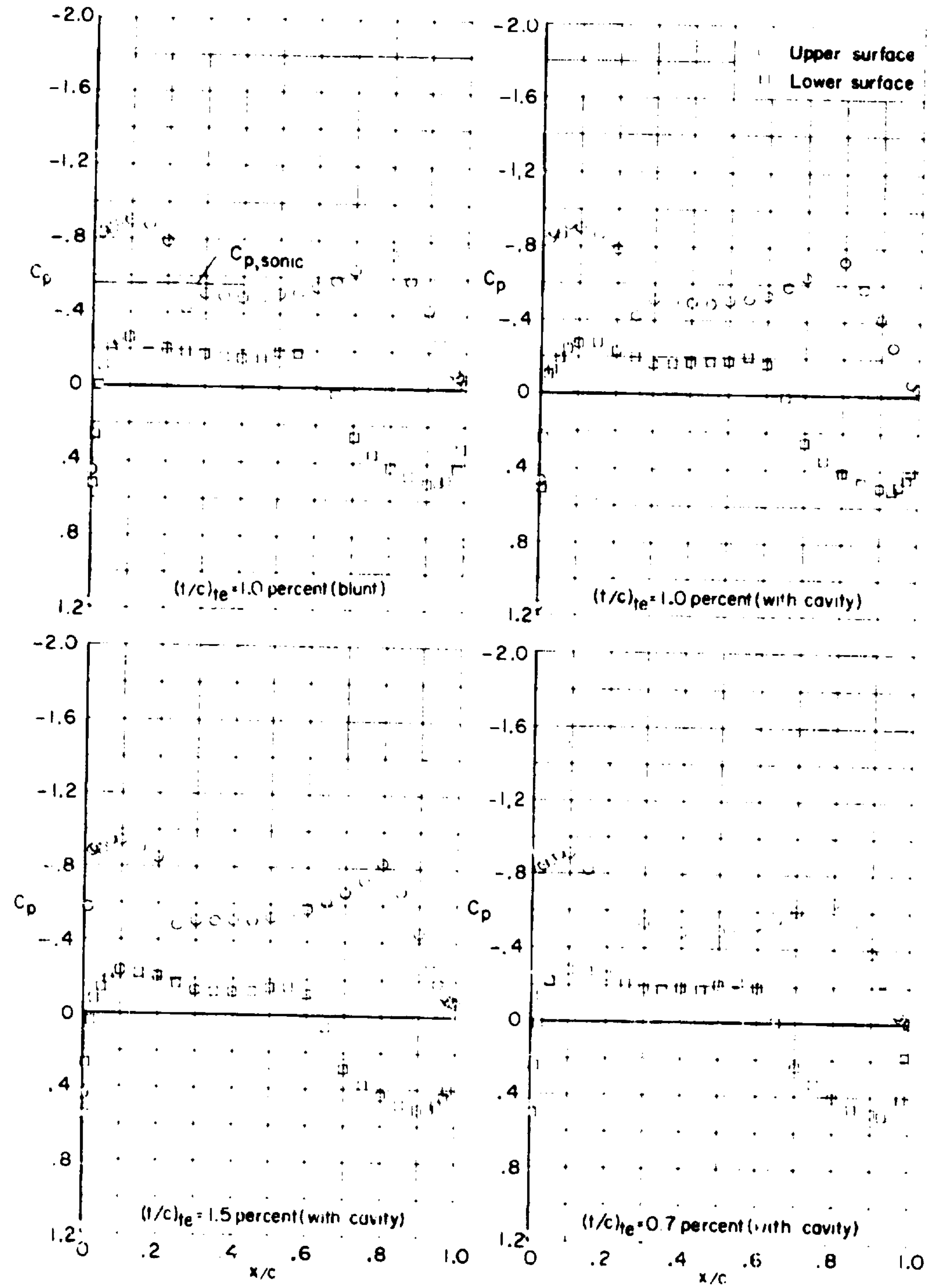

(l) M = 0.70; α = 0.5°.

Figure 2.- Continued.

ORIGINAL PAGE IS OF POOR QUALITY

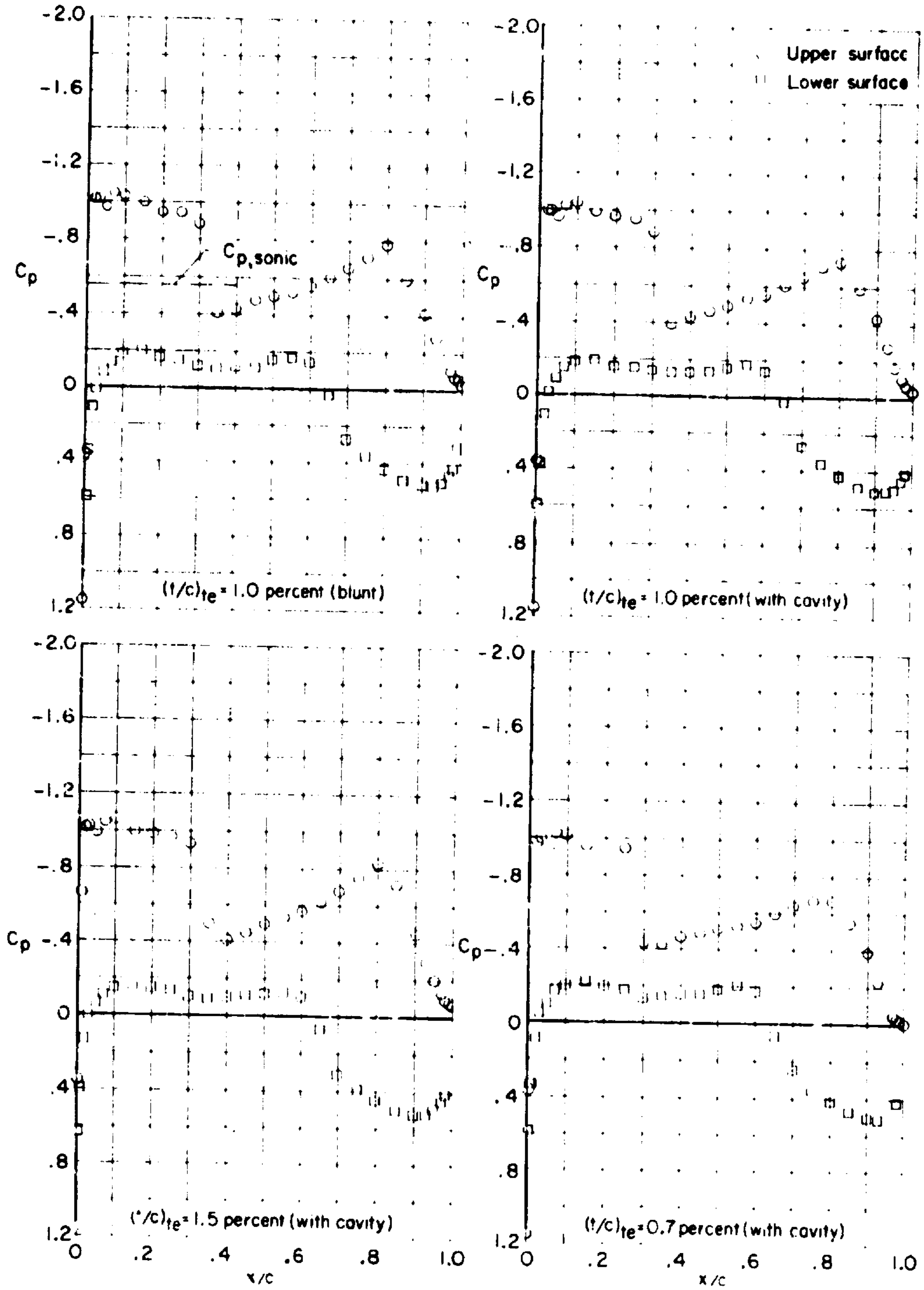

(j) M = 0.75; α = 1°.

Figure 12.- Continued.

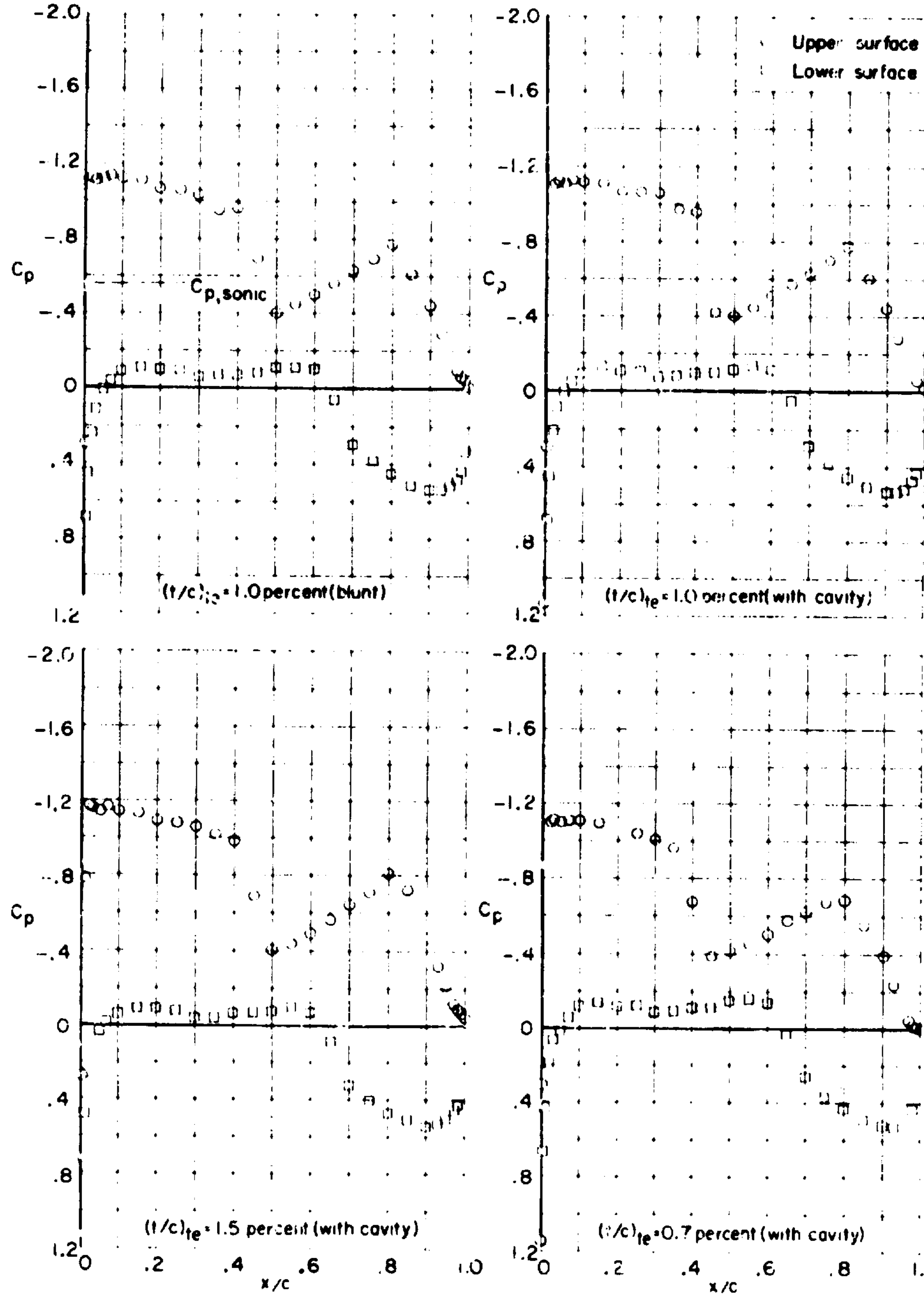

(k) M = 0.76; α = 1.5°.

Figure 12.- Continued.

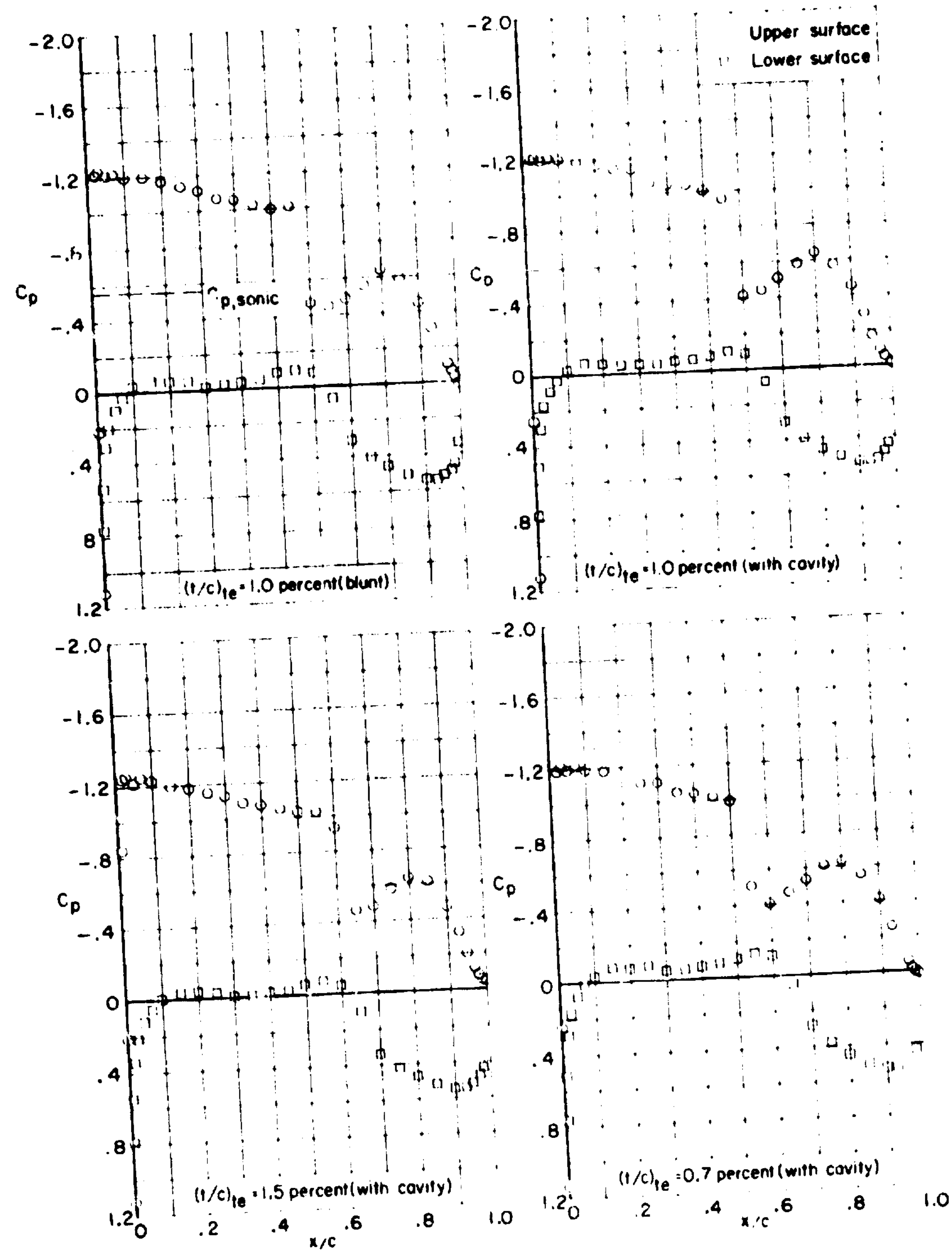

(7) M = 0.70; α = 2.0°.

Figure 12.- Continued.

ORIGINAL PAGE IS
OF POOR QUALITY

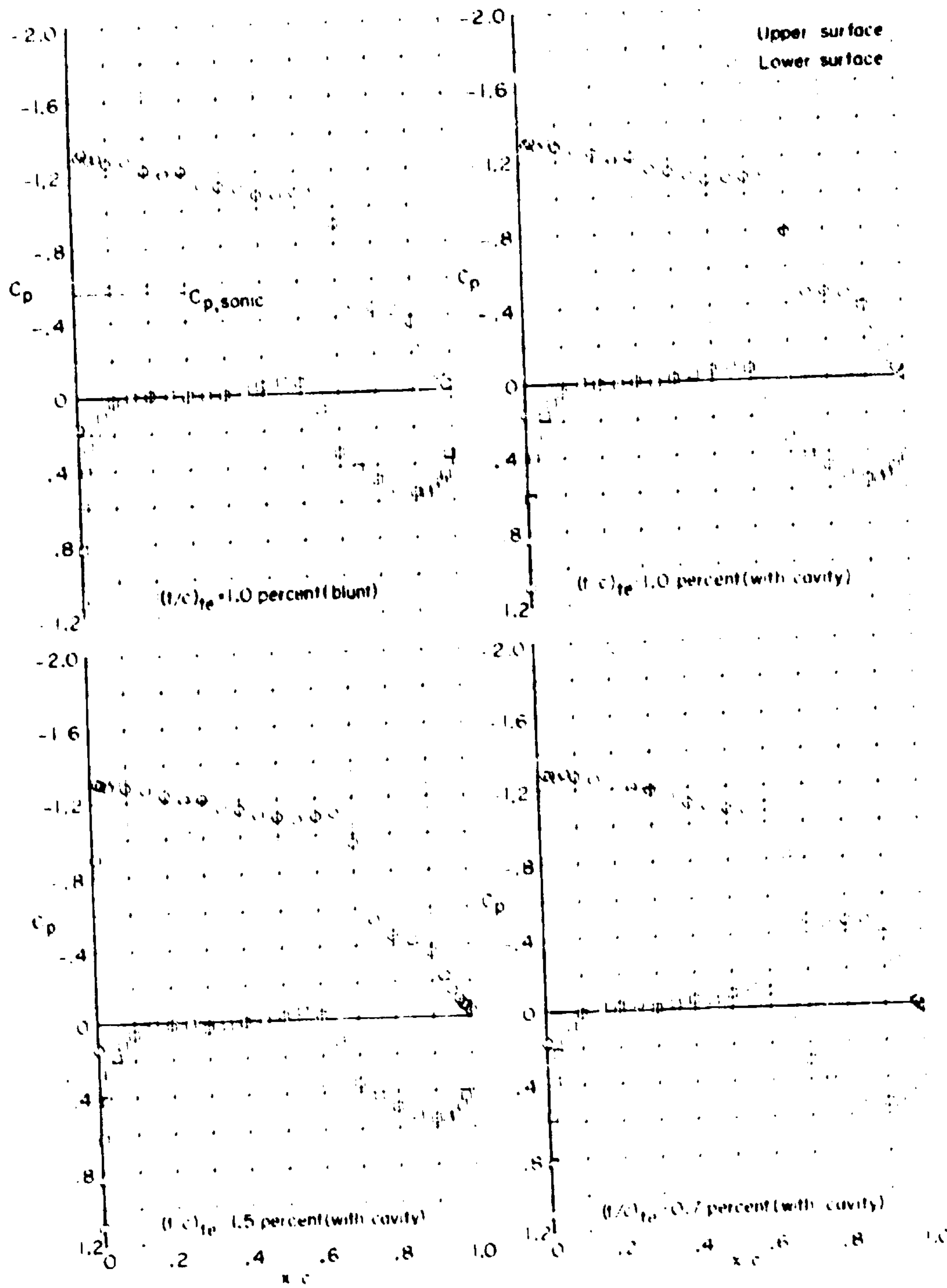

(m) M = 0.70; α = [illegible].

Figure 12.- Continued.

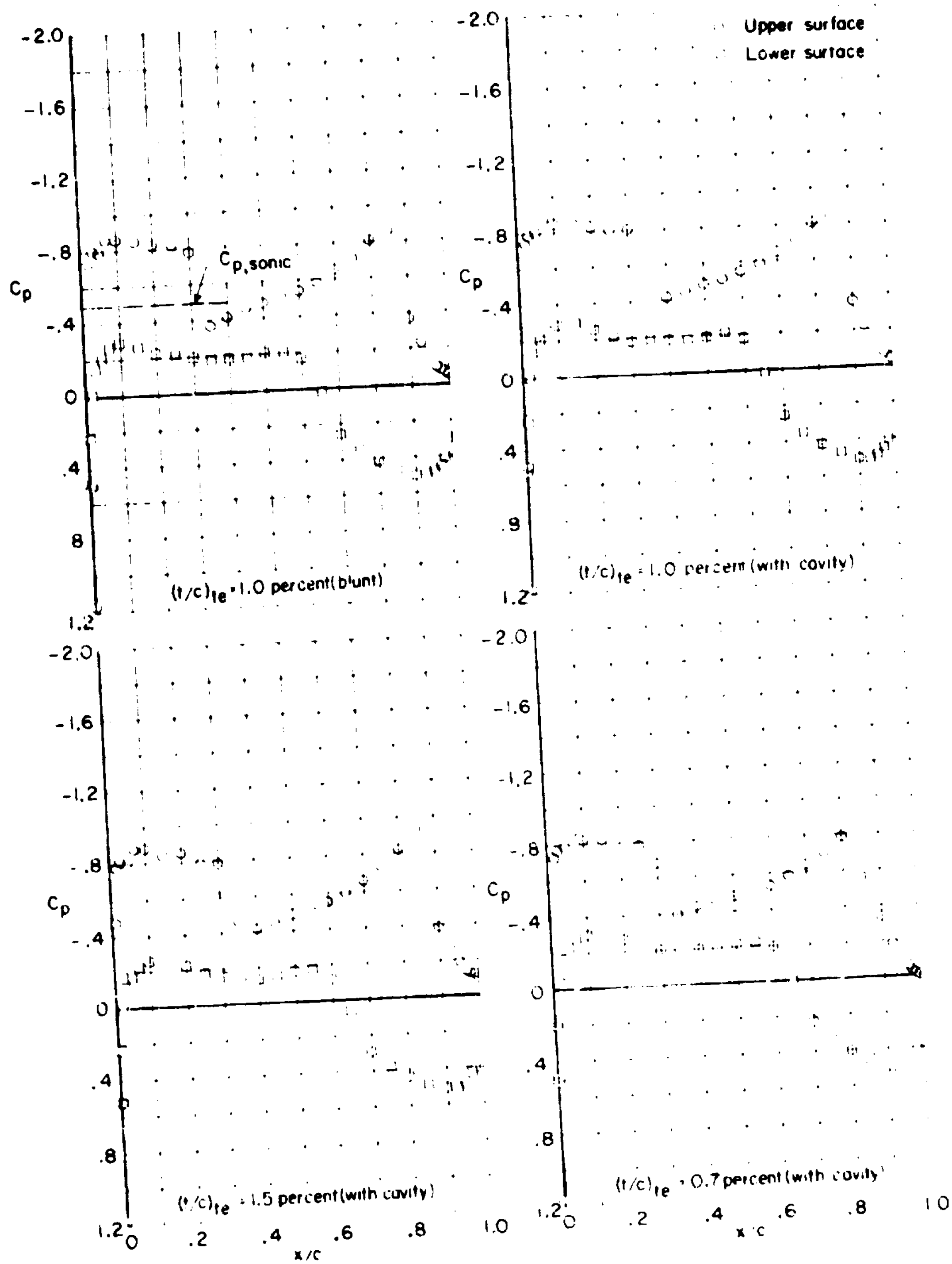

ORIGINAL PAGE IS
OF POOR QUALITY

(n) $M = 0.78$; $\alpha = 0.5°$.

Figure 1?.- Continued.

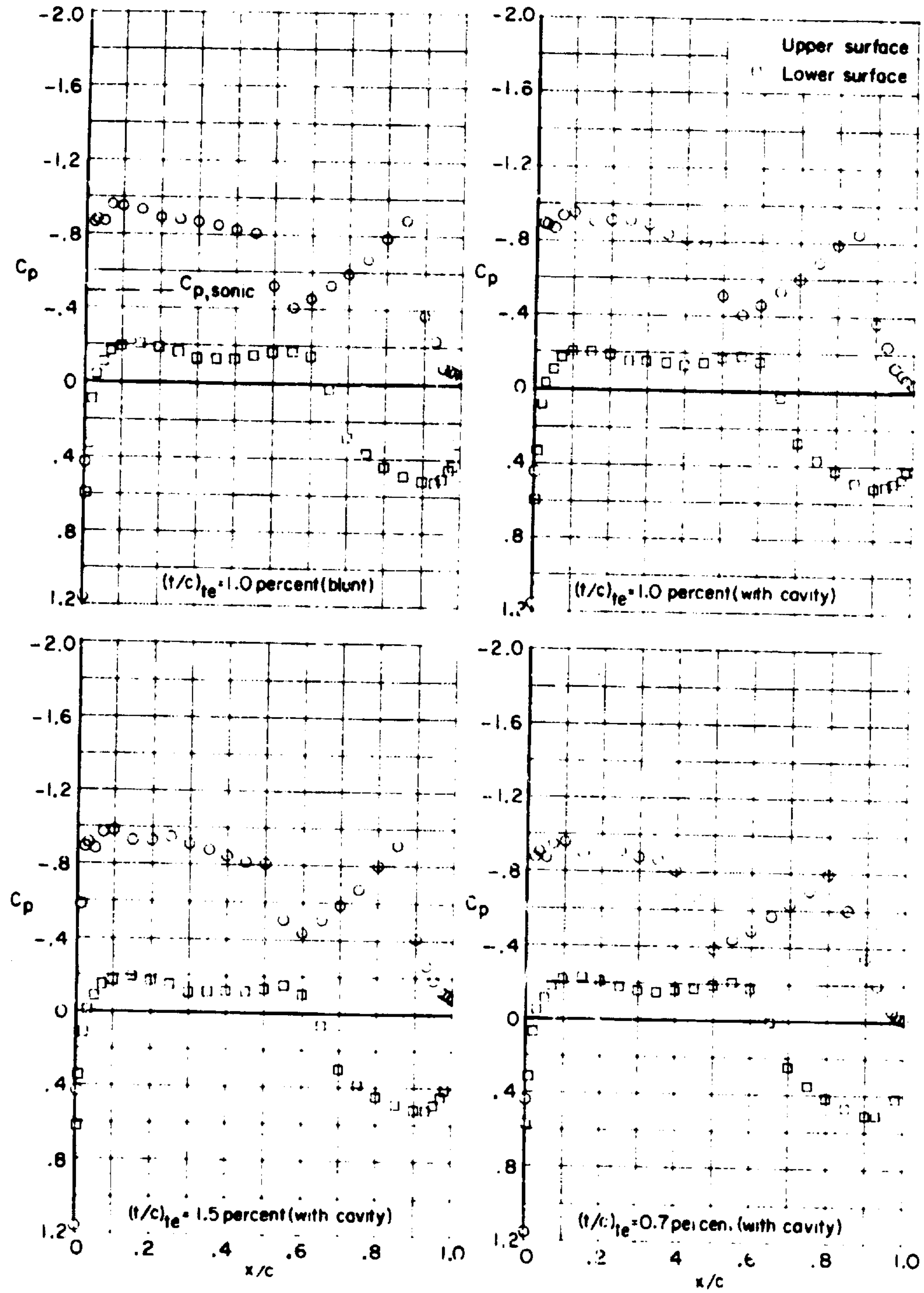

(o) $M = 0.78$; $\alpha = 1.0^{\circ}$.

Figure 12.- Continued.

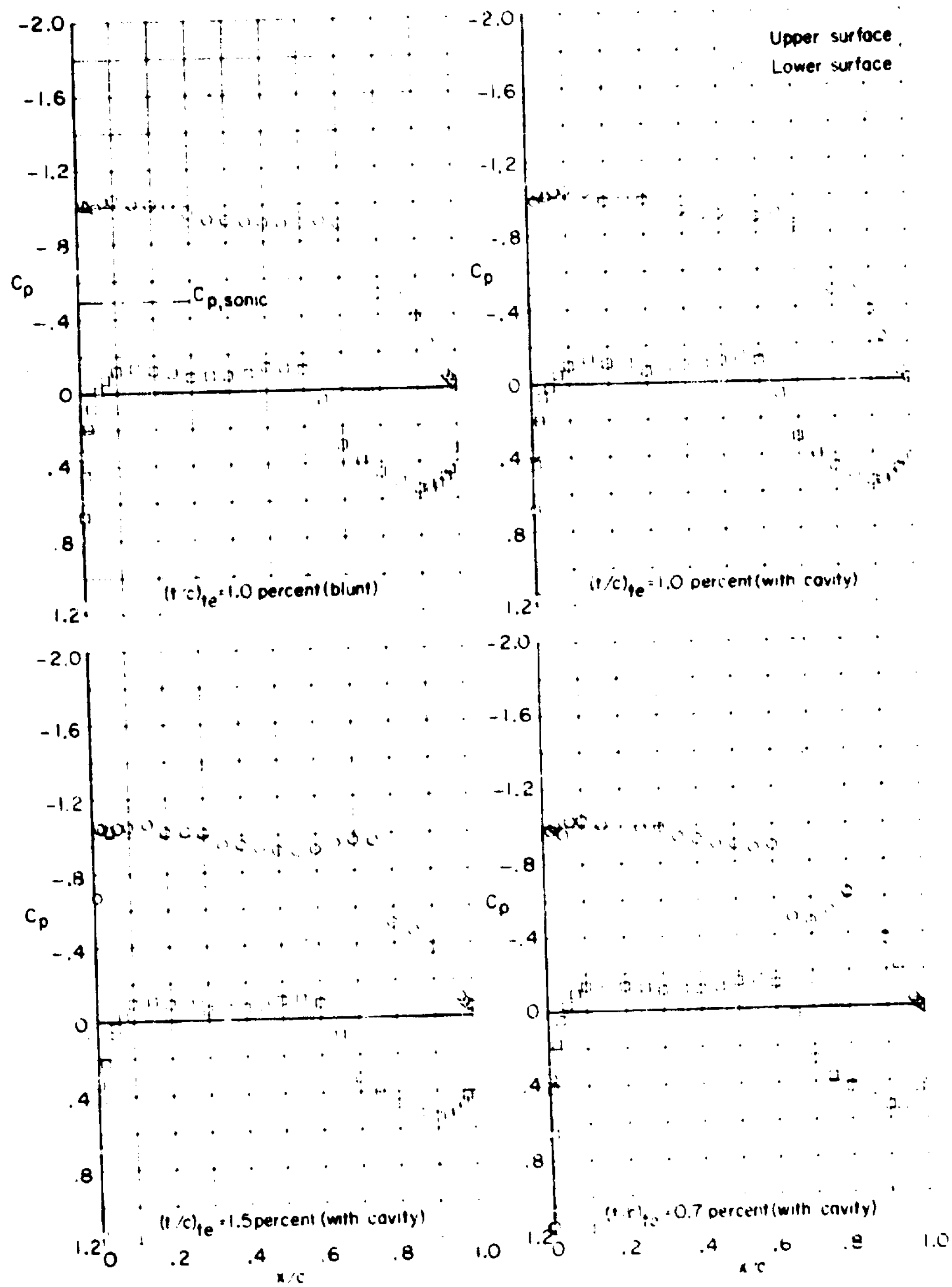

(p) M = 0.78; α = 1.5°.

Figure 12.- Continued.

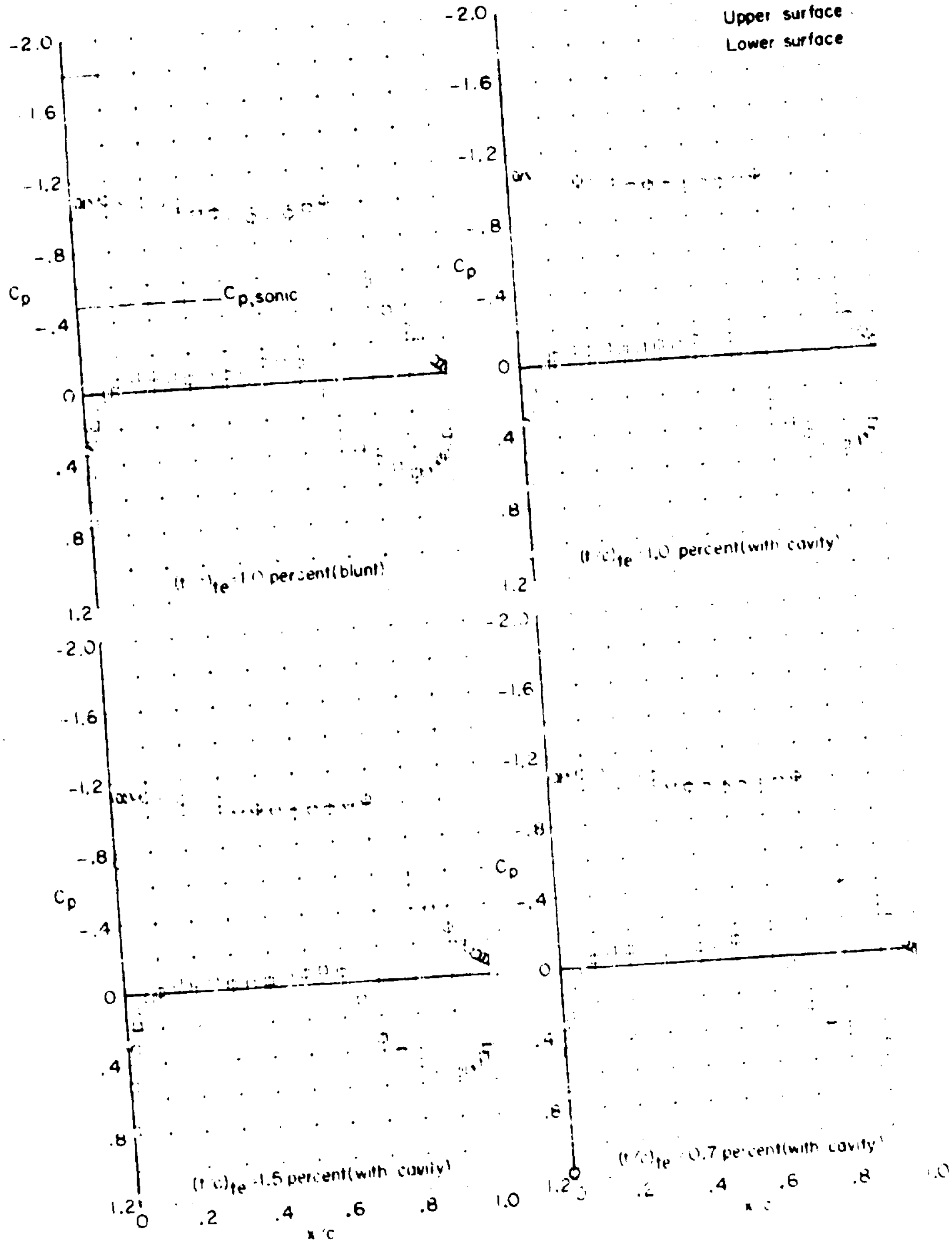

(q) $M = 0.7$; $\alpha = .0^{\circ}$.

Figure 1 .- Continued.

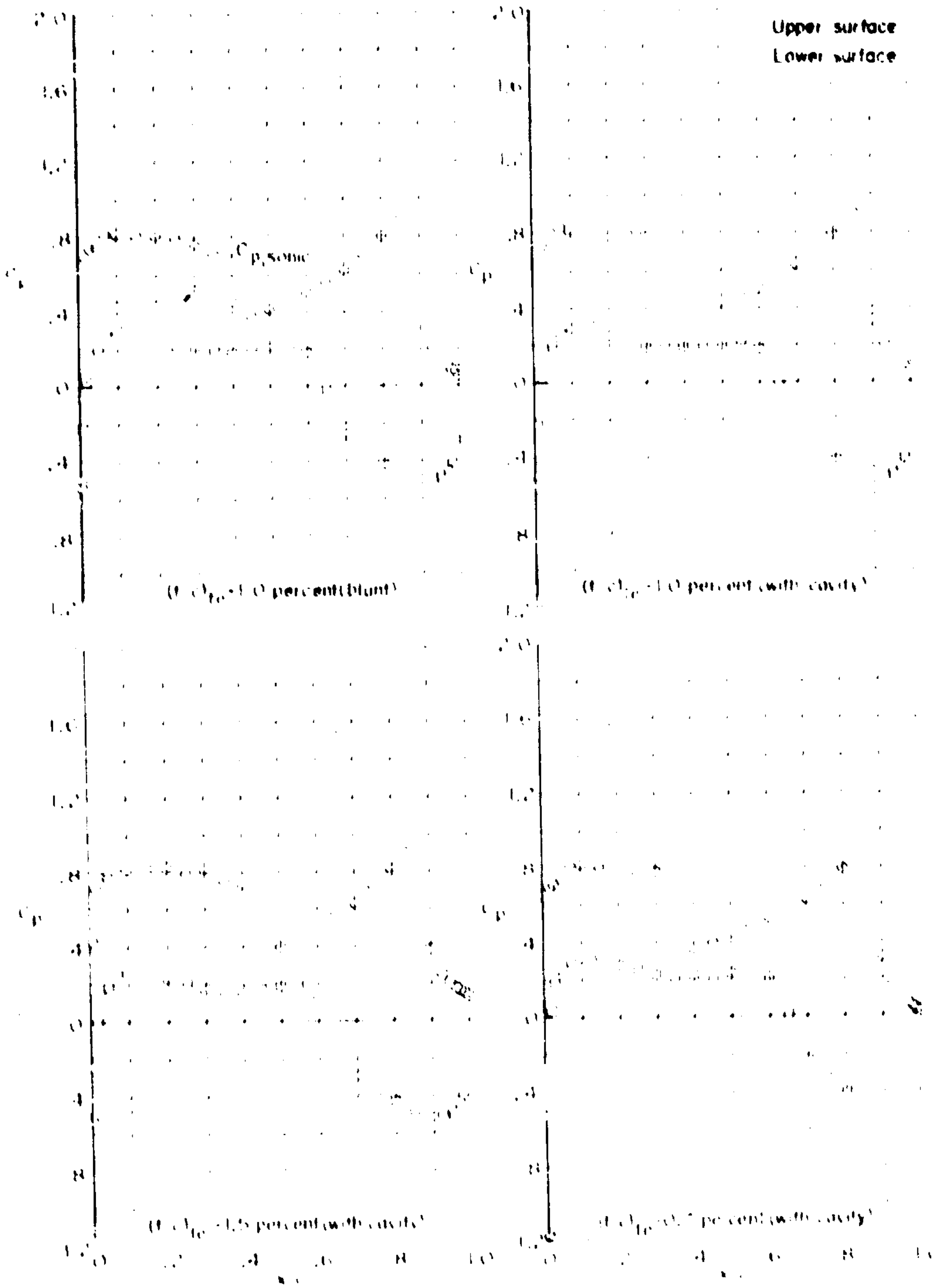

(r) M [illegible]; α [illegible]

Figure [illegible].- Continued.

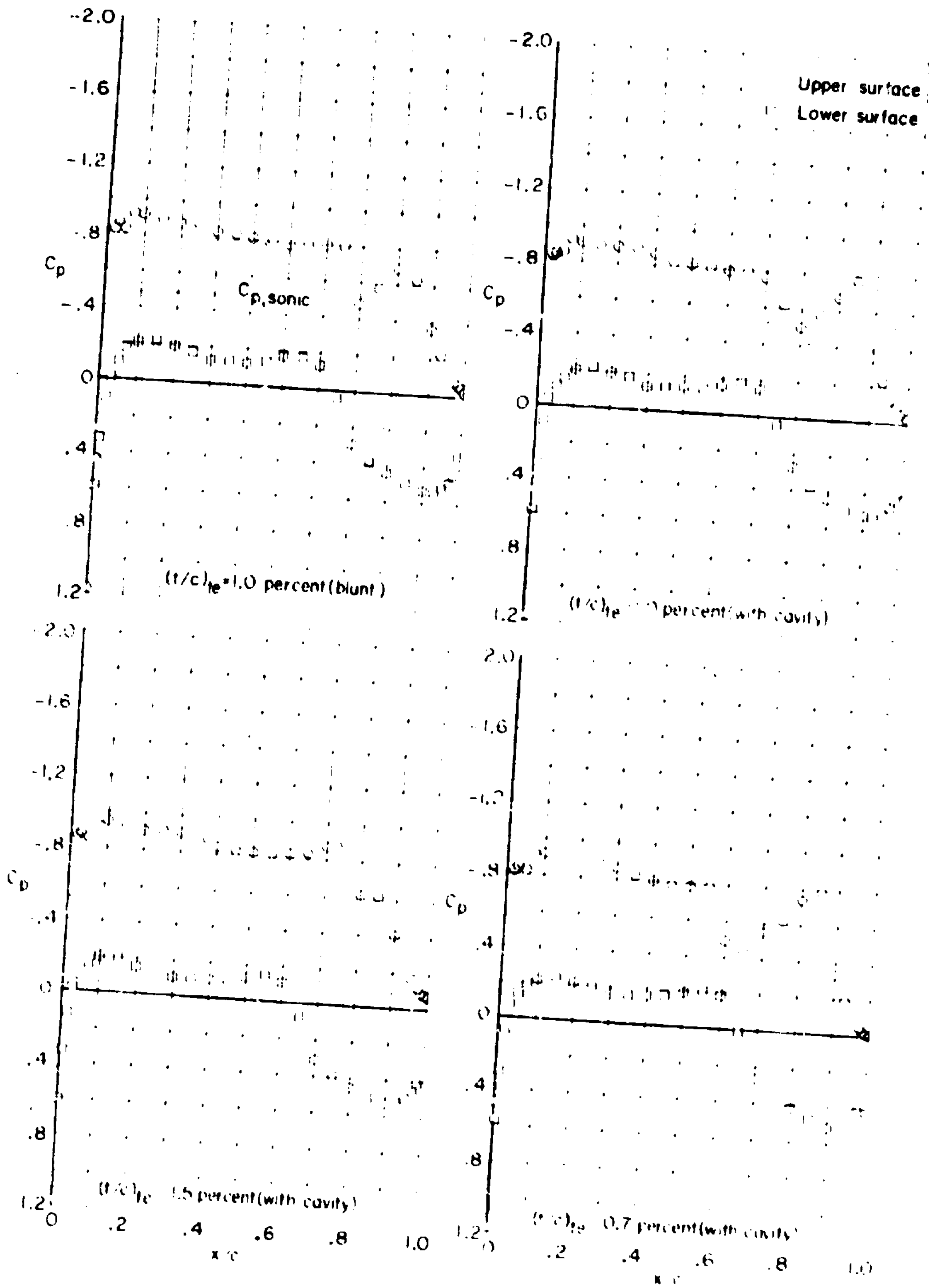

(a) M = 0.7; α = 1.0°.

Figure 1?.- Continued.

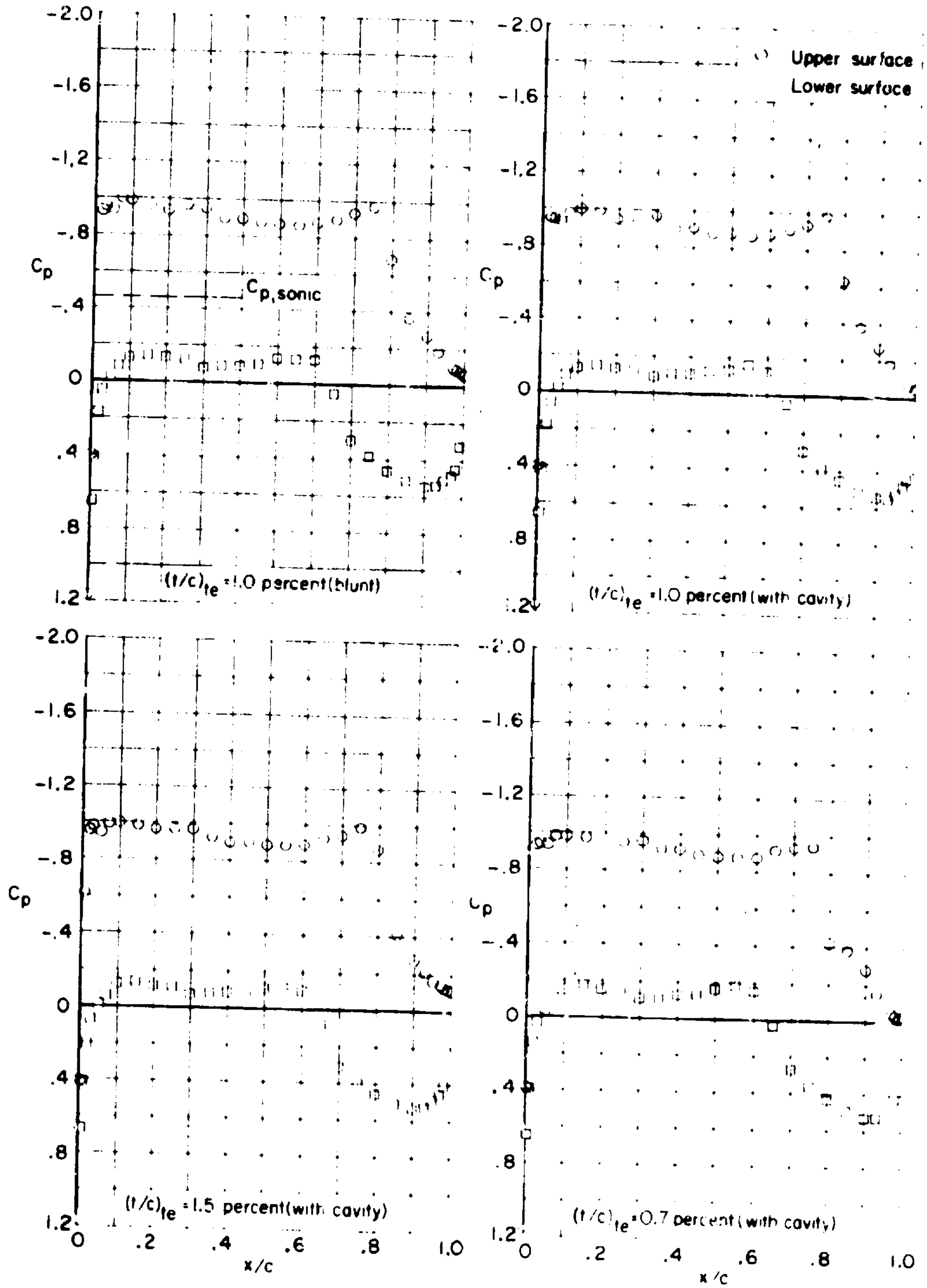

(t) $M = 0.79$; $\alpha = 1.5°$.

Figure 12.- Continued.

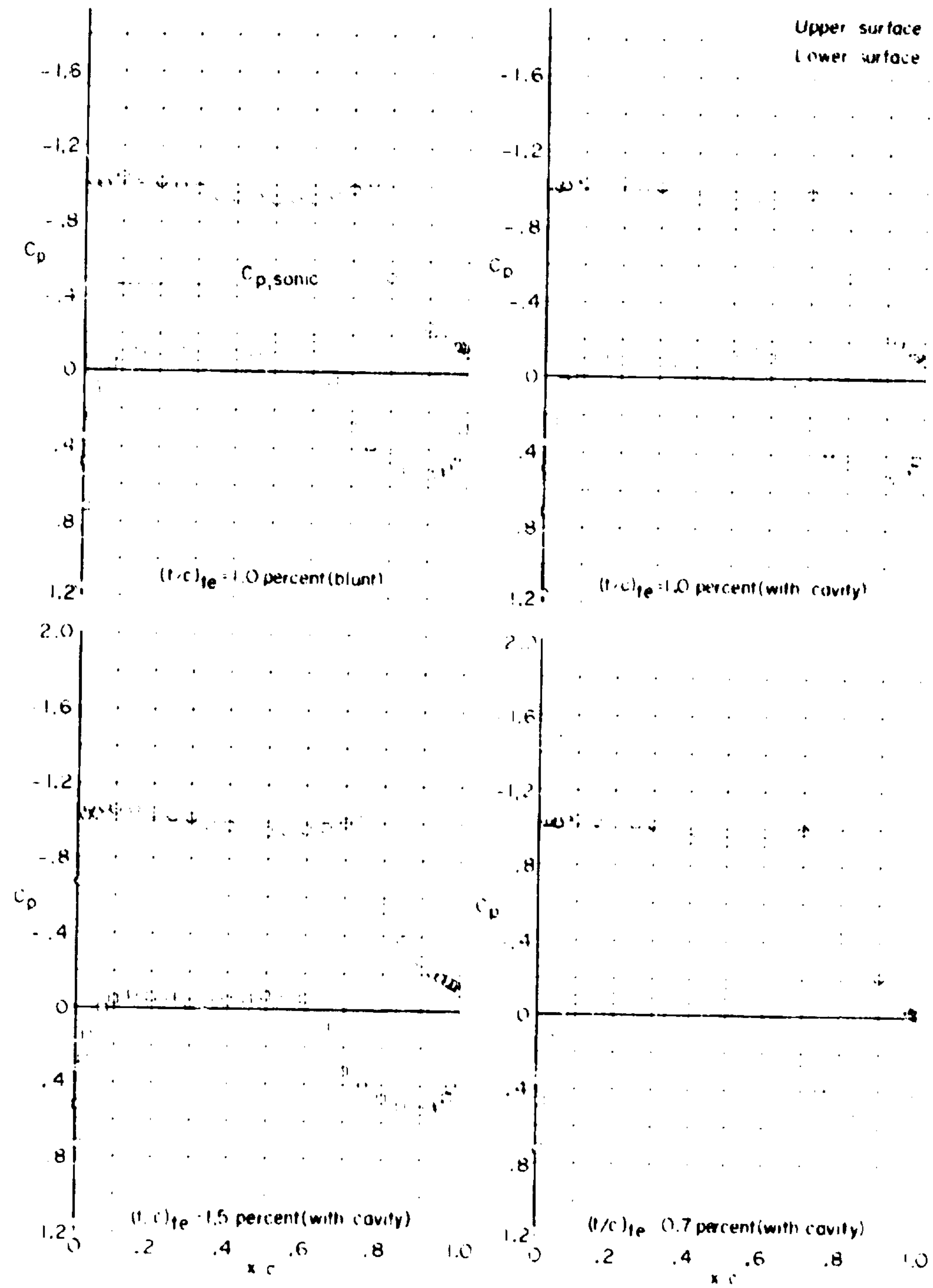

(u) M = 0.7?; α = .0°.

Figure 1?.- Continued.

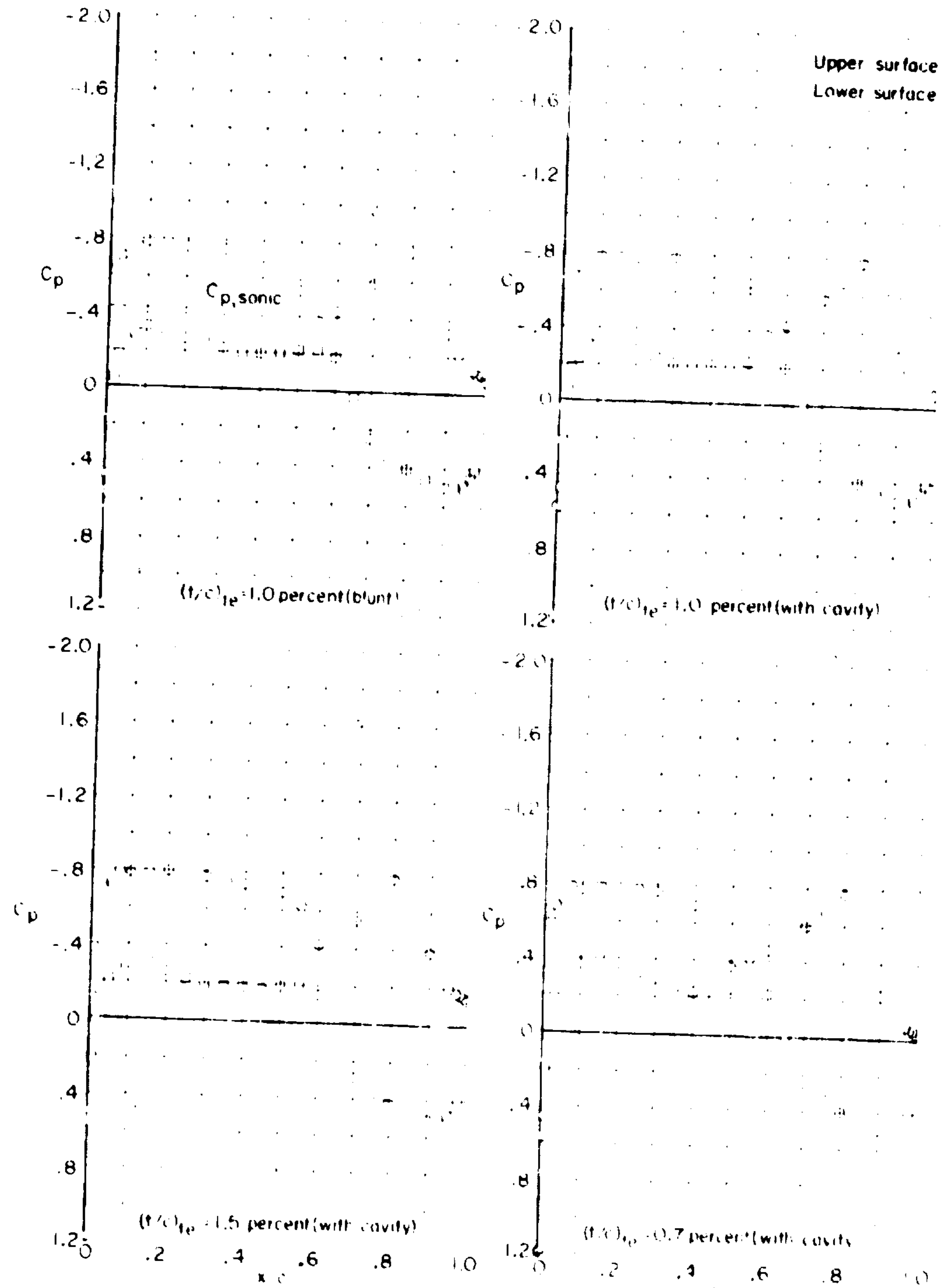

(v) M = 0.80; α = 0.5°.

Figure 2... Continued.

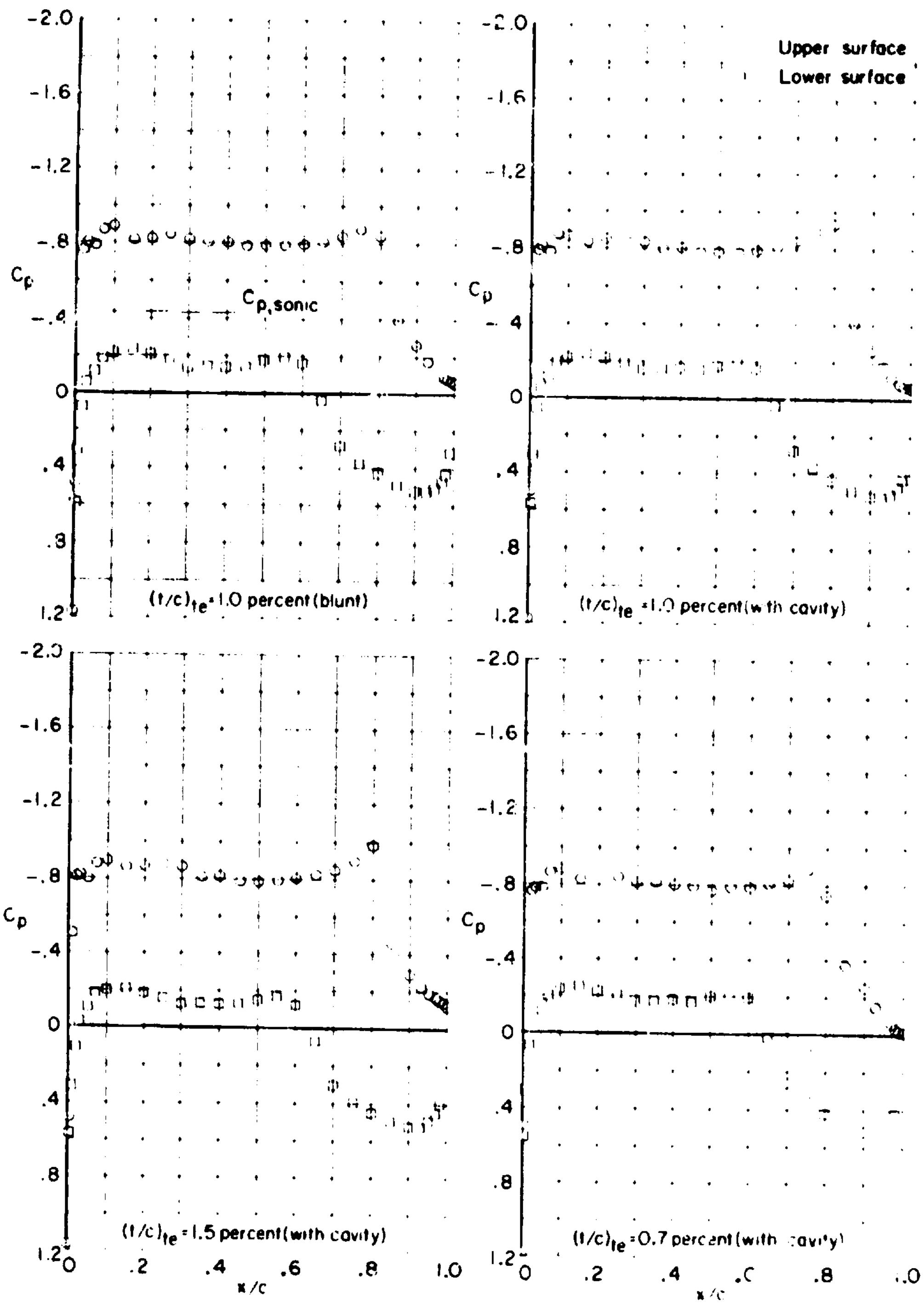

(w) $M = 0.80$; $\alpha = 1.0^{\circ}$.

Figure 1[illegible].- Continued.

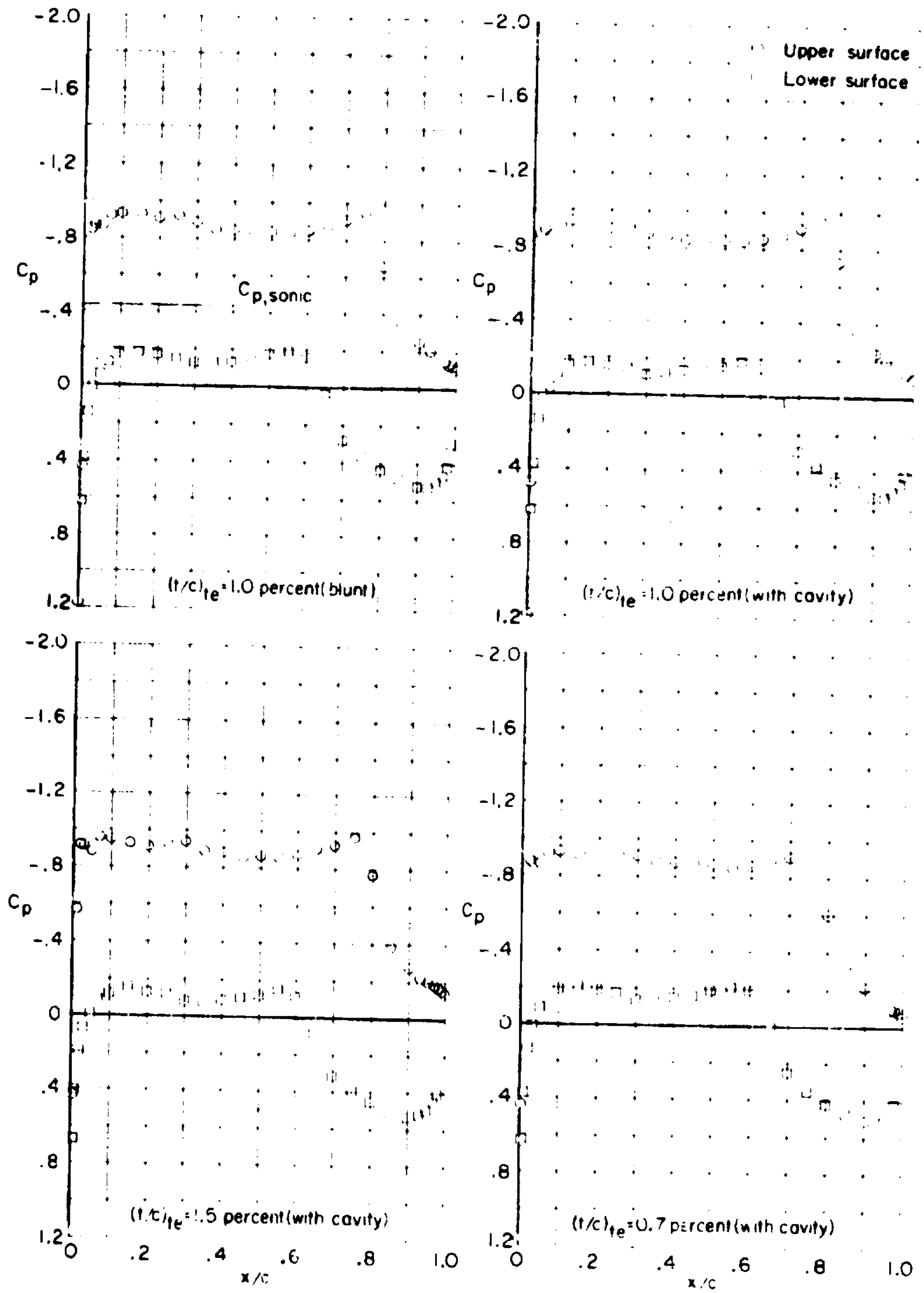

(x) M = 0.80; α = 1.5°.

Figure 12.- Concluded.

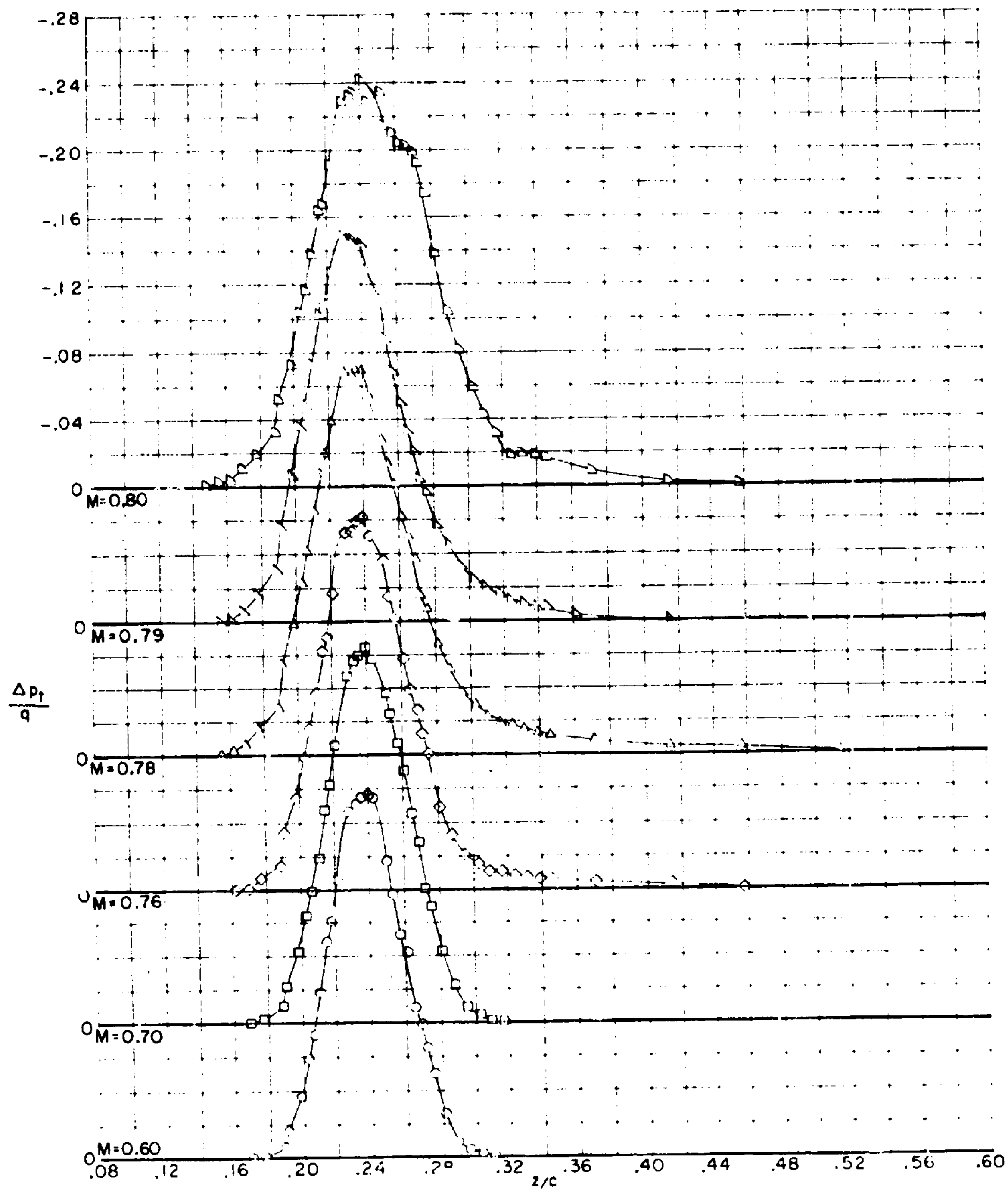

Figure 13.- Representative wake profiles for 10-percent-thick supercritical airfoil with 1.0-percent-thick trailing edge with cavity. $\alpha = 1^{\circ}$.

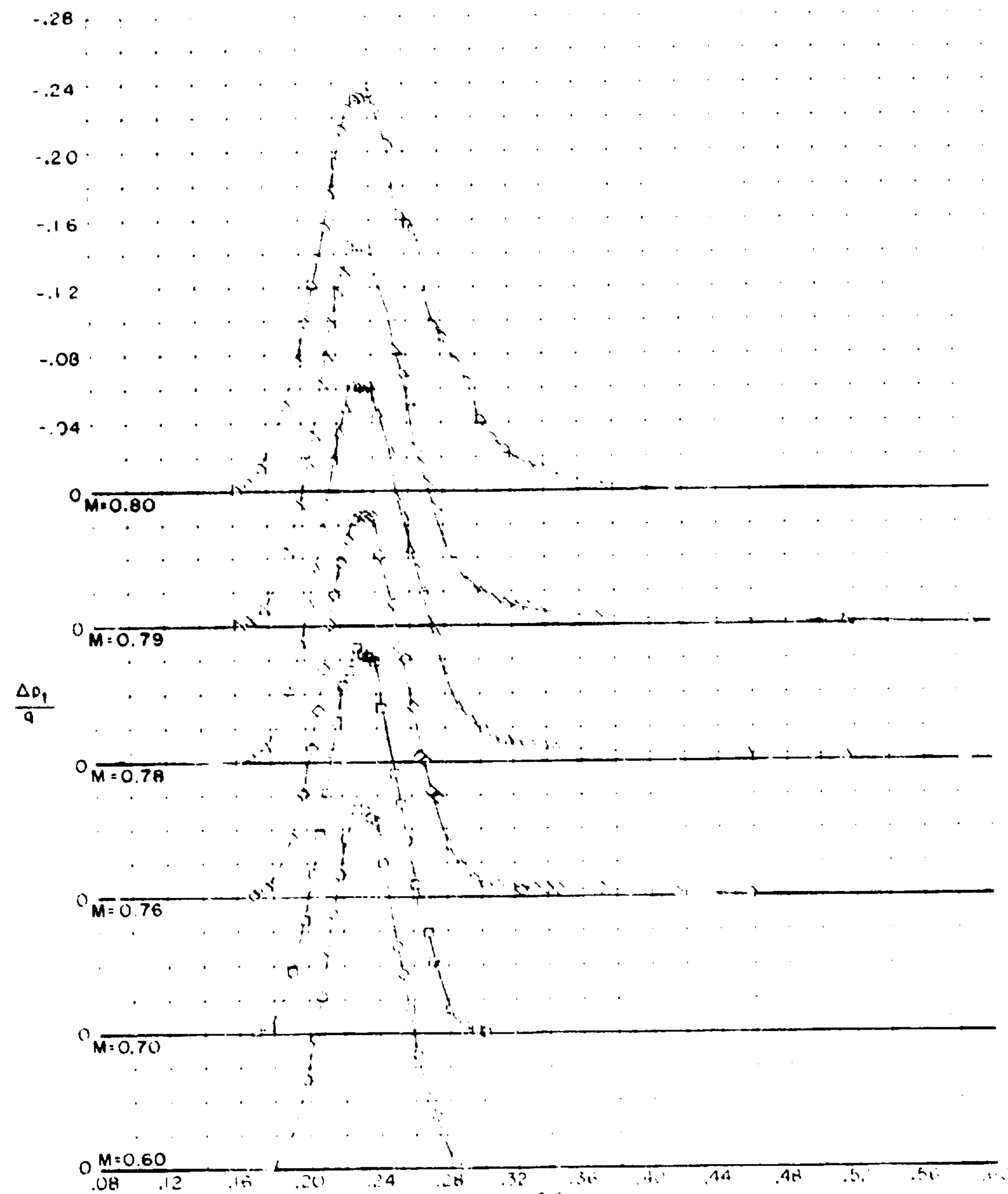

Figure 34.- Representative wake profiles for 10-percent-thick supercritical airfoil with 0.7-percent-thick trailing edge with cavity. α = 1°.